International Journal of Alzheimer's Disease

γ-Secretase Pharmacology: What Pharmacology Will Work for Alzheimer's Disease?

Guest Editors: Jeremy H. Toyn, Adele Rowley, Yasuji Matsuoka, Taisuke Tomita, and Bruno P. Imbimbo

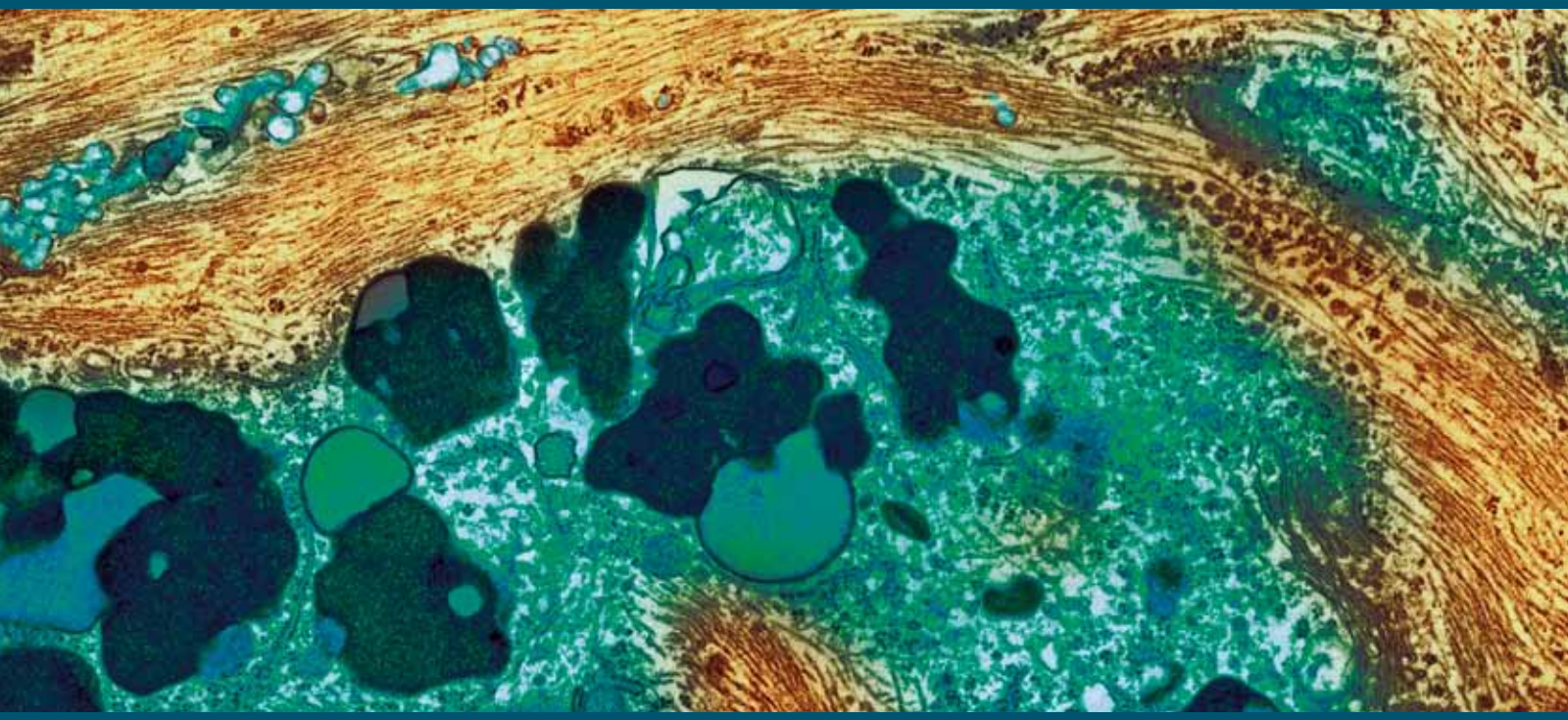

γ-Secretase Pharmacology: What Pharmacology Will Work for Alzheimer's Disease?

International Journal of Alzheimer's Disease

γ-Secretase Pharmacology: What Pharmacology Will Work for Alzheimer's Disease?

Guest Editors: Jeremy H. Toyn, Adele Rowley, Yasuji Matsuoka, Taisuke Tomita, and Bruno P. Imbimbo

Editorial Board

Contents

Hindawi Publishing Corporation
International Journal of Alzheimer's Disease
Volume 2013, Article ID 849128, 2 pages
http://dx.doi.org/10.1155/2013/849128

Editorial

γ-Secretase Pharmacology: What Pharmacology Will Work for Alzheimer's Disease?

Jeremy H. Toyn,[1] Adele Rowley,[2] Yasuji Matsuoka,[3] Taisuke Tomita,[4] and Bruno P. Imbimbo[5]

[1] *Neuroscience Biology, Bristol-Myers Squibb Research and Development, 5 Research Parkway, Wallingford, CT 06492, USA*
[2] *TopiVert Pharma Ltd., Imperial College Incubator, Bessemer Building Level 1, Imperial College, London SW7 2AZ, UK*
[3] *Neural Pathways Discovery, GlaxoSmithKline, Singapore Research Center, Singapore 138667*
[4] *Department of Neuropathology and Neuroscience, Graduate School of Pharmaceutical Sciences, The University of Tokyo, Tokyo 113-0033, Japan*
[5] *Research & Development, Chiesi Farmaceutici, Largo Francesco Belloli, 11/a, 43122 Parma, Italy*

Correspondence should be addressed to Jeremy H. Toyn; jeremy.toyn@bms.com

Received 19 March 2013; Accepted 19 March 2013

This special issue focuses on γ-secretase modulators (GSMs) and inhibitors (GSIs), two classes of small molecules with the potential to test the amyloid hypothesis of Alzheimer's disease. Recent clinical trials of GSI and GSM, including semagacestat, avagacestat, and R-flurbiprofen, have been discontinued for lack of efficacy and/or side effects, the mechanisms of which have not been elucidated. Detrimental effects of GSIs on cognition observed in AD patients may be linked to the accumulation of C-terminal fragment of APP (C99 or CTFβ). The stimulating effects of GSIs on skin cancer in AD patients have been linked to their inhibition of Notch processing. The lack of efficacy of the GSM R-flurbiprofen in AD patients has been explained with its low potency and poor ability to cross the blood-brain barrier. The two review articles and three research articles address key issues for GSI and GSM, namely, Notch-related side effects and drug-like properties, respectively. Although other amyloid-related approaches are continuing in clinical trials, including anti-Aβ antibodies and β-site amyloid precursor protein cleaving enzyme (BACE) inhibitors, it still remains to be seen whether or not they can decrease amyloid or Aβ for a sufficient period of time at tolerable doses in patients. Therefore, renewed efforts toward GSIs and GSMs appear justified.

The review by M. Takami and S. Funamoto provides a succinct but comprehensive introduction to the stepwise proteolytic mechanism of γ-secretase. They describe the experimental evidence for the multiple cleavages of the amyloid precursor protein (APP) and provide some particularly useful illustrations showing how the enzyme processes its substrates to make a series of Aβ peptides and tripeptides. They further propose that γ-secretase cleavage of Notch may be mechanistically different from the cleavage of APP, implying an untapped potential to discover APP-selective or Notch-selective inhibitors.

H. J. M. Gijsen and M. Mercken review the current status of GSM drug discovery, identify the limitations of current molecules, and present an approach to the future optimization of GSMs. The benchmark GSMs are succinctly reviewed and common trends are evaluated. They give a thoughtful and accessible explanation of the "conflict between the physicochemical properties required for highly efficacious GSM and those (properties) required for drug-likeness." This contrasts with GSI, where high potency and optimal physical properties have been achieved for some molecules, but the biological mechanism imposes inbuilt Notch-related side effects. Thus, benchmark GSMs suffer from low quality physical properties, whereas benchmark GSIs are of high drug-like quality but suffer from a limitation of the biological mechanism. The quantitative use of biological and physical properties in drug optimization is reviewed in a straightforward way, and illustrations are used to show where the current GSM and GSI molecules stand in this quantitative analysis.

Also included is new data relating to a novel GSM illustrating recent progress.

B. Tate et al. review the benchmark GSIs and GSMs while providing data describing the novel natural product-derived GSMs discovered by Satori. GSMs typically decrease Aβ42 and increase Aβ38 production; however, the Satori compounds decrease both Aβ42 and Aβ38, while increasing Aβ37 and Aβ39. These different effects on Aβ peptides are well illustrated by straightforward MALDI-TOF scans. An expanded definition of GSM is therefore given as compounds that cause "a shift of the Aβ pool to shorter, but variable length, Aβ peptides." In contrast to GSI, for which potency is sensitive to APP expression level, GSMs exhibit a relatively constant level of potency. Nevertheless, GSMs require high plasma concentrations for associated brain Aβ lowering, an observation that cannot be fully explained by properties such as nonspecific protein binding and brain penetrance.

The original research article by L. A. Hyde et al. describes approaches to mitigate the risk of Notch-related toxicity in rodents given the GSI SCH697466. Notch-related side effects were evaluated in the intestine and thymus, and Notch-related biomarkers were monitored in white blood cells. Either decreased frequency of dosing, or lower doses which caused a partial lowering of Aβ, were shown to decrease Notch inhibition. The results show that appropriate choices of the extent and duration of dosing can facilitate significant Aβ lowering without evidence of Notch-related side effects.

In the original research article by M. C. de Vera Mudry et al., the GSI RO4929097 was given to rats and mice to explore the effect on immune responses. One of the most characteristic Notch-related side effects of GSI is spleen marginal zone atrophy, which raises the possibility of a consequence for immune responses. Remarkably, despite the atrophy and decreased B cell numbers caused by chronic dosing of the GSI, the effect on immune responses was mild and reversible.

In summary, the main theme of this special issue is about recent approaches to address the limitations of the two main classes of γ-secretase-targeted small molecules. For GSIs, the focus is on the mitigation of side effects related to Notch and other non-APP substrates. Extent and duration of GSI dosing could be varied to decrease effects on Notch, and the consequences of decreased B cell numbers on immune responses were shown to be mild, thereby diminishing a perceived risk. Furthermore, the mechanisms of the γ-secretase cleavages of APP and Notch, while not well understood, may be sufficiently different to facilitate improved APP- or Notch-selectivity of GSIs in the future. For GSMs, the focus is on improving the drug-like physicochemical properties while maintaining high potency. The future of GSMs therefore appears to be a continuation of a challenging multiparameter drug optimization. We hope readers will derive intellectual benefit from these papers and enjoy them as much as we did.

Jeremy H. Toyn
Adele Rowley
Yasuji Matsuoka
Taisuke Tomita
Bruno P. Imbimbo

Hindawi Publishing Corporation
International Journal of Alzheimer's Disease
Volume 2013, Article ID 823528, 14 pages
http://dx.doi.org/10.1155/2013/823528

Research Article

In Vivo Characterization of a Novel γ-Secretase Inhibitor SCH 697466 in Rodents and Investigation of Strategies for Managing Notch-Related Side Effects

Lynn A. Hyde,[1] Qi Zhang,[1] Robert A. Del Vecchio,[1] Prescott T. Leach,[1] Mary E. Cohen-Williams,[1] Lei Chen,[2] Gwendolyn T. Wong,[1] Nansie A. McHugh,[1] Joseph Chen,[1] Guy A. Higgins,[1] Theodros Asberom,[3] Wei Li,[3] Dmitri Pissarnitski,[3] Diane Levitan,[2] Amin A. Nomeir,[4] John W. Clader,[3] Lili Zhang,[1] and Eric M. Parker[1]

[1] *Department of Neuroscience, Merck Research Laboratories, Kenilworth, NJ 07033, USA*
[2] *Department of Molecular Biomarkers, Merck Research Laboratories, Kenilworth, NJ 07033, USA*
[3] *Department of Medicinal Chemistry, Merck Research Laboratories, Kenilworth, NJ 07033, USA*
[4] *Department of Drug Metabolism and Pharmoackinetics, Merck Research Laboratories, Kenilworth, NJ 07033, USA*

Correspondence should be addressed to Lynn A. Hyde; lynn.hyde@merck.com

Received 29 August 2012; Accepted 27 November 2012

Academic Editor: Jeremy Toyn

Substantial evidence implicates β-amyloid (Aβ) peptides in the etiology of Alzheimer's disease (AD). Aβ is produced by the proteolytic cleavage of the amyloid precursor protein by β- and γ-secretase suggesting that γ-secretase inhibition may provide therapeutic benefit for AD. Although many γ-secretase inhibitors have been shown to be potent at lowering Aβ, some have also been shown to have side effects following repeated administration. All of these side effects can be attributed to altered Notch signaling, another γ-secretase substrate. Here we describe the in vivo characterization of the novel γ-secretase inhibitor SCH 697466 in rodents. Although SCH 697466 was effective at lowering Aβ, Notch-related side effects in the intestine and thymus were observed following subchronic administration at doses that provided sustained and complete lowering of Aβ. However, additional studies revealed that both partial but sustained lowering of Aβ and complete but less sustained lowering of Aβ were successful approaches for managing Notch-related side effects. Further, changes in several Notch-related biomarkers paralleled the side effect observations. Taken together, these studies demonstrated that, by carefully varying the extent and duration of Aβ lowering by γ-secretase inhibitors, it is possible to obtain robust and sustained lowering of Aβ without evidence of Notch-related side effects.

1. Introduction

Alzheimer's disease (AD) is a progressive age-related neurodegenerative disease characterized clinically by memory loss and cognitive dysfunction followed by a disruption of normal daily functions, organ system failure, and, ultimately, death. However, a diagnosis of AD can only be confirmed postmortem by the presence of distinct neuroanatomical hallmarks including senile plaques consisting primarily of β-amyloid (Aβ) peptides, neurofibrillary tangles consisting of hyperphosphorylated tau, and substantial neuronal loss, particularly in the hippocampus, an area of the brain which plays a key role in memory.

Substantial genetic and neuroanatomical evidence implicates Aβ peptides in the etiology of Alzheimer's disease (e.g., [1–3]). Therefore, it is thought that a reduction in Aβ production or an increase in Aβ clearance will have a beneficial, and potentially disease modifying, effect on the disease.

Aβ is produced by sequential cleavage of amyloid precursor protein (APP) by β-site APP cleaving enzyme 1 (BACE1) followed by γ-secretase. Thus, inhibiting γ-secretase should

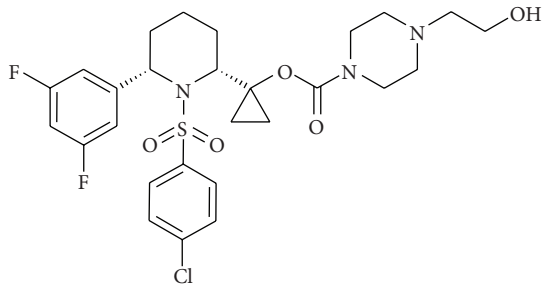

Figure 1: SCH 697466: 1-[cis-1-[(4-chlorophenyl)sulfonyl]-6-(3,5-difluorophenyl)-2-piperidinyl]cyclopropyl 4-(2-hydroxyethyl)-1-piperazinecarboxylate [34].

decrease Aβ production. Indeed, acute and chronic administration of small molecule γ-secretase inhibitors reduced Aβ in the plasma, brain and cerebrospinal fluid (CSF) of animals [4–12] and humans [8, 13–15], including AD patients [16, 17]. More importantly, γ-secretase inhibition has also been reported to slow and even halt the progression of amyloid plaque deposition in mouse models of amyloid production and deposition [18, 19].

However, the C-terminal fragment of APP (the product of BACE1 cleavage) is not the only substrate for γ-secretase [20, 21]. Additional physiologically relevant substrates include Notch [22], which has been shown to play a critical role in cell fate pathways [23]. Thus, γ-secretase inhibitors also disrupt Notch signaling. Although some "Notch sparing" (e.g., [8, 24–26]) and "APP selective" [10] γ-secretase inhibitors have been identified and characterized, other γ-secretase inhibitors have been shown to produce mechanism-based, Notch-related side effects following chronic administration in vivo including a reduction in thymus weight and intestinal goblet cell hyperplasia [5, 27–29]. These effects are usually observed at doses that provide sustained and near complete lowering of Aβ, in particular in the periphery (i.e., plasma Aβ).

Since there is a risk of Notch-related side effects with chronic administration of γ-secretase inhibitors, methods of minimizing or completely avoiding these side effects are highly desirable. Identifying relevant Notch-related biomarkers could be a useful means of managing Notch-related side effects in clinical trials involving γ-secretase inhibitors. HES-1 is a direct target of the Notch signaling pathway, while KLF4, mATH-1, and adipsin are downstream targets of HES-1 expression [30–33]. It would be of interest to determine to what extent changes in gene expression of these downstream targets of Notch correlate with Notch-related pathology in vivo following subchronic inhibition of γ-secretase. In addition, it has been shown that partial inhibition of γ-secretase is an effective way to reduce Aβ with no evidence of Notch-related side effects in rodents [5, 18]. However, it is not clear if partial Aβ lowering and/or complete Aβ lowering for a part of the day are effective methods for minimizing Notch-related side effects.

Here we describe the in vivo characterization of a novel γ-secretase inhibitor, SCH 697466 [34]. We have assessed Aβ lowering in rats, transgenic CRND8 mice (TgCRND8, mouse model of amyloid production and deposition [35]) and nontransgenic mice following acute and subchronic administration. Using SCH 697466 as a tool, we have also attempted to identify strategies to maintain Aβ lowering while managing Notch-related side effects in vivo by varying the extent and duration of Aβ lowering. Further, we measured gene expression of several downstream targets of Notch in the intestine and blood as potential safety biomarkers for Notch disruption.

2. Materials and Methods

2.1. Animals. Male CD rats (115–175 g; Crl:CD(SD); Charles River Laboratories, Kingston, NY) were group housed, and female nontransgenic B6C3F1 mice (6 weeks; Charles River Laboratories, Raleigh, NC; the background strain on which TgCRND8 mice are maintained) were single housed; all groups were acclimated to the vivarium for one week prior to use in a study.

The transgenic (Tg) CRND8 male and female (counterbalanced across groups) mice (carrying the Swedish and Indiana familial Alzheimer's disease APP mutations under the control of the Syrian hamster prion protein [35]) used in these studies were bred at Merck Research Laboratories in Kenilworth, NJ, or Taconic in Germantown, NY, as described previously [36]. Before dosing began and for the duration of the study, mice were singly housed with a plastic igloo and nesting material. TgCRND8 mice were 5–7 weeks old (preplaque) because at this age total cortical Aβ is primarily in a soluble form [36] and thus is more amenable to reduction following relatively short-term γ-secretase inhibition [37, 38] (unpublished observations show better survival if TgCRND8 mice are single housed versus group housed).

Table 1 describes the various studies conducted in rats, TgCRND8 mice, and nontransgenic mice. Body weight was assessed prior to drug administration. All in vivo procedures adhered to the NIH Guide for the Care and Use of Laboratory Animals and were approved by the Institutional Animal Care and Use Committee of Merck Research Laboratories in Kenilworth, an AAALAC accredited institution.

2.2. SCH 697466. SCH 697466 (Figure 1) is a novel sulfonamide γ-secretase inhibitor [34]. It was synthesized by the Medicinal Chemistry group at Merck Research Laboratories in Kenilworth, NJ, and formulated in 20% hydroxypropyl-β-cyclodextrin for all studies, except for the 6-day TgCRND8 study where the vehicle was diluted 1 : 10 with 0.4% methylcellulose. SCH 697466 was administered orally to both mice and rats, and the dosing volume was 10 mL/kg for mice and 5 mL/kg for rats.

2.3. β-Amyloid Quantification. In vitro procedures for measuring γ-secretase activity in membranes prepared from HEK293 cells expressing APP and procedures for collecting tissues and assessing Aβ40 levels in plasma and cortex (following guanidine extraction; biotin-4G8 and S-tag G2-10 antibodies for transgenic and nontransgenic mice and

Table 1: Summary of in vivo studies conducted with SCH 697466.

Group	Species	Duration of dosing	Total # of doses	Post-treatment time*	*n*/group
Acute Rat	Rat	single dose	1	3 hr	7–8
Acute TgCRND8	Mouse	single dose	1	3 or 6 hr	4–6
Acute Non-transgenic	Mouse	single dose	1	3 hr	7
Time course TgCRND8	Mouse	single dose	1	2, 4, 6, 12, 18 or 24 hr	4-5
6 days *b.i.d.* TgCRND8	Mouse	6 days *b.i.d*†	11	3 hr	4–9
11 days *q.d.* Non-transgenic	Mouse	11 days *q.d.*	11	3 hr	4-5
6 days *b.i.d.* Non-transgenic	Mouse	6 days *b.i.d*†	11	3 hr	4–7

*Time in between administration of the last (or only) dose and collecting tissues following euthanasia.
†Five full days of dosing with the final dose given the morning of day 6.

antibody 585 and S-tag G2-10 for rats) have been previously described [28, 39]. Plasma and cortex Aβ42 were quantified in select TgCRND8 studies using biotin-4G8 and S-tag G2-11 and 4G8 antibodies.

Cerebrospinal fluid (CSF) was collected from the cisterna magna immediately following euthanasia with excess CO_2 and quickly frozen on dry ice and stored at −70°C until Aβ quantification using procedures identical to those used to quantify plasma Aβ. Only visibly clear CSF samples were analyzed. CSF was not collected in some studies because the studies were performed before technique was developed and optimized.

2.4. Histology. The thymus was weighed as previously described [5]. The ileum (harvested just proximal to the ileocecal junction) was processed, sectioned (3 μm), and stained as previously described [28], and intestinal goblet cell hyperplasia was quantified as percent villi area covered by Periodic Acid-Schiff (PAS) stain as previously described [5].

2.5. Notch Pathway Biomarker Analyses. The jejunum was harvested, rinsed, and flash frozen in liquid nitrogen until later analyses. RNA was isolated from tissues using the Trizol reagent (Molecular Research Center, Inc.) followed by purification over an RNAeasy column (Qiagen).

White blood cells were isolated after collection in heparin tubes. Tubes were centrifuged for 10 minutes at 5000 rpm, and the interphase cells were removed to a tube containing Trizol reagent. RNA was purified over an RNAeasy column. Quantitative, real-time PCR was performed on an ABI7900 machine (Applied Biosystems, Foster City, CA), using the Bio-Rad iScript Custom one-step RT-PCR Kit for Probes with ROX (Hercules, CA). Primer and probe were designed using the Universal Probe Library Assay Design Center (Roche Applied Sciences, Basel, Switzerland). The probes and primers used are as follows:

KLF4: Forward primer CGGGAGGGAGAAGACACT; Reverse primer CGTTGGCGTGAGGGAAC PROBE#62 from Roche Universal Probe Library;

HES1: Forward primer ATCCCGGTCTACACCAGCAA; Reverse primer AAGGTCACCGAGGAG PROBE#20 from Roche Universal Probe Library;

Adipsin: Forward primer CTGGGAGCGGCTGTATGT; Reverse primer TCCTACATGGCTTCCGTG PROBE#79 from Roche Universal Probe Library;

mATH1: Forward primer TCCCCTTCCTCCTACCTTCT; Reverse primer TGTACCTTTACGTGGCATCG PROBE#34 from Roche Universal Probe Library.

2.6. Quantification of Drug Levels. Plasma and brain concentrations of SCH 697466 were quantified by liquid chromatography tandem mass spectrometry (LC-MS/MS) using an Acquity UPLC HSS T3 C18 column (2.1 × 50 mm, 1.7 μ), operated at 50°C. The flow rate was 0.75 mL/min, and the instrument used was a Sciex API 4000/5500 mass spectrometer equipped with a Turbo Ion Spray source and operated at unit mass resolution. Plasma and brain samples were quantified against standard curves generated in the corresponding matrix. Standard curves for mouse plasma were generated from frozen heparinized plasma spiked with SCH 697466 to give final concentrations in the range of 1 ng/mL—5000 ng/mL. In the case of the mouse brains, control and sample brains were placed in a 48-well plate and 3 mL of water was added for each gram of tissue. Glass beads were added into each well, and samples were homogenized using an SPEX SamplePrep 2010 apparatus for 2.5 min at 1450 rpm. The calibration standards for brain were prepared from 1 ng/g to 10,000 ng/g. Brain homogenate and plasma samples and standards were prepared for analysis in the same manner, by subjecting them to protein precipitation with acetonitrile containing internal standard. The samples were vortexed and centrifuged and the supernatants were transferred to a 96-well plate for LC-MS/MS analysis.

2.7. Data Analyses. Analyses of variance (ANOVA) with dose group as the between-subject factor followed by Dunnett post hoc tests comparing the vehicle-treated group to all others were used to analyze most data.

During subchronic administration of 100 mg/kg of SCH 697466 to TgCRND8 mice, all mice showed signs of poor health (e.g., hypothermic, hypoactive, poorly groomed, and hunched posture) and some died. If a mouse died prior to the tissue collection day, no tissues were used. If an animal died on the tissue collection day, thymus and ileum were isolated. If an animal was in very poor health on the collection

Table 2: Concentration of SCH 697466 (μM) in plasma and brain for various acute studies in rats, TgCRND8 mice and non-transgenic mice.

Dose (mg/kg)	Rat		TgCRND8 mouse				Nontransgenic mouse	
	3 hr post-Treatment time		3 hr post-Treatment time		6 hr post-treatment time		3 hr post-Treatment time	
	Plasma	Brain	Plasma	Brain	Plasma	Brain	Plasma	Brain
3	nd	nd	nd	nd	0.05 ± 0.01	0.008 ± 0.002	0.03 ± 0.003	BLOQ
10	0.60 ± 0.07	0.13 ± 0.01	0.68 ± 0.09	0.04 ± 0.004	0.36 ± 0.02	0.06 ± 0.01	0.35 ± 0.05	0.01 ± 0.002
30	2.34 ± 0.16	1.33 ± 0.08	3.13 ± 0.26	0.96 ± 0.22	4.22 ± 1.27	0.36 ± 0.05	1.91 ± 0.12	0.18 ± 0.02
100	4.60 ± 0.39	4.49 ± 0.50	7.79 ± 1.33	9.71 ± 2.95	3.76 ± 1.19	1.99 ± 0.26	6.90 ± 0.81	3.04 ± 0.36

nd: Not done; BLOQ: below the limit of quantification (0.003 μM).

day, it was not possible to obtain enough blood for Aβ quantification or exposure, but all other tissues were used.

3. Results

3.1. SCH 697466 Is a Potent γ-Secretase Inhibitor In Vitro. SCH 697466 is a potent γ-secretase inhibitor when assessed in a variety of assay formats. The IC_{50} for Aβ40 inhibition in membranes prepared from human embryonic kidney 293 (HEK293) cells expressing human APP with the Swedish and London familial AD mutations ($APP^{Swe\text{-}Lon}$) is 2 nM. In intact HEK293 cells expressing human $APP^{Swe\text{-}Lon}$, SCH 697466 inhibits Aβ40 and Aβ42 production with IC_{50}s of 5 and 3 nM, respectively. SCH 697466 also inhibits Notch processing in intact HEK293 cells expressing a portion of the human Notch1 protein with an IC_{50} of 123 nM. Thus, in vitro, there is a 24-fold separation between Aβ40 inhibition and Notch.

3.2. SCH 697466 Dose-Dependently Reduced Aβ in Plasma, Cortex, and/or Cerebrospinal Fluid in Rats and TgCRND8 and Nontransgenic Mice following Acute Administration. In rats, 3 hr after administration of SCH 697466, plasma, cortex, and CSF Aβ40 levels were significantly reduced (Figure 2(a); main effect of dose: $F(3, 26) = 6.37$ and $F(3, 28) = 19.44$ and 64.86, $P < 0.003$, for plasma, cortex, and CSF, resp.) with significant Aβ lowering in each compartment at all doses ($P < 0.006$). The effect of SCH 697466 on Aβ seemed to plateau at about 60% reduction in both plasma and cortex, while near complete lowering of Aβ was observed in CSF at the 100 mg/kg dose. The inclusion of lower doses may have provided a better understanding of the dose-response relationship of this compound in rats.

In TgCRND8 mice, 3 hr after-drug administration, SCH 697466 dose-dependently reduced Aβ40 levels in the plasma, cortex, and CSF (Figure 2(b); $F(3, 13) = 36.35$ and 17.17 and $F(3, 10) = 12.97$, resp., $P < 0.0009$) with significant lowering at all doses in each compartment ($P < 0.006$, except 10 mg/kg in CSF). Similar to what was observed at 3 hr, six hr after administration, SCH 697466 continued to produce a dose-dependent reduction of plasma and cortex Aβ40 in TgCRND8 mice (Figure 2(b); main effect of dose: $F(4, 22) = 41.86$ and 12.52, resp., $P < 0.0001$) with near complete lowering of plasma Aβ40 at 100 mg/kg. Six hr after-administration, SCH 697466 was similarly effective at lowering Aβ42 in plasma and brain such that the 100 mg/kg dose reduced plasma and cortex Aβ42 by 84% and 47%, respectively (data not shown), compared to 93% and 55% for plasma and cortex Aβ40. SCH 697466 seemed to be more potent in plasma and cortex 3 hr following administration compared to 6 hr, although the 3 hr and 6 hr studies were not conducted or analyzed together.

In nontransgenic mice, 3 hr after administration, SCH 697466 increased plasma Aβ at lower doses while it decreased Aβ at higher doses (Figure 2(c); main effect of dose: $F(4, 30) = 30.79$, $P < 0.0001$); significant increase in Aβ was observed at 3 and 10 mg/kg and significant lowering of Aβ was observed at 100 mg/kg ($P < 0.005$). In the cortex, SCH 697466 dose-dependently reduced Aβ [main effect of dose: $F(4, 30) = 63.23$, $P < 0.0001$) with significant lowering for the 10, 30, and 100 mg/kg groups ($P < 0.005$). Near complete lowering of Aβ was observed in plasma and cortex at 100 mg/kg.

There was a dose related increase (although in some cases it was more than dose-proportional) in the concentration of SCH 697466 in plasma and brain (one time point per animal), and the concentrations were usually greater in plasma than brain in rats, TgCRND8 mice, and nontransgenic mice (Table 2). The T_{max} of SCH 697466 in rats is 2 hr (from a separate pharmacokinetic study) which basically agrees with our results in TgCRND8 mice showing that plasma concentrations were higher at 3 hr after administration than 6 hr. The concentration of SCH 697466 in plasma and brain tended to be higher in TgCRND8 mice compared to nontransgenic mice, but these studies were not conducted together. Nevertheless, there are no major species differences in the concentration of SCH 697466 in plasma and brain when comparing rats to TgCRND8 and nontransgenic mice.

3.3. Duration of Aβ Lowering in Plasma and Cortex following a Single Dose of SCH 697466 in TgCRND8 Mice. To determine the duration of action of SCH 697466 on lowering plasma and cortex Aβ over 24 hr, two time course studies were conducted.

Following a single dose of 30 mg/kg of SCH 697466 in TgCRND8 mice, plasma and cortex Aβ40 levels were significantly reduced at 2, 4, 8, and 12 hr (Figure 3(a); main effect of time point: $F(5, 23) = 85.76$ and 15.02, $P < 0.0001$; Dunnett test: $P < 0.02$); however, 24 hr after dosing, Aβ levels had returned to baseline and were not different from vehicle ($P > 0.20$). SCH 697466 was not quite as potent at lowering plasma and cortex Aβ42 compared to Aβ40 (data not show); for example, 8 hr after-dose, SCH 697466 lowered plasma and

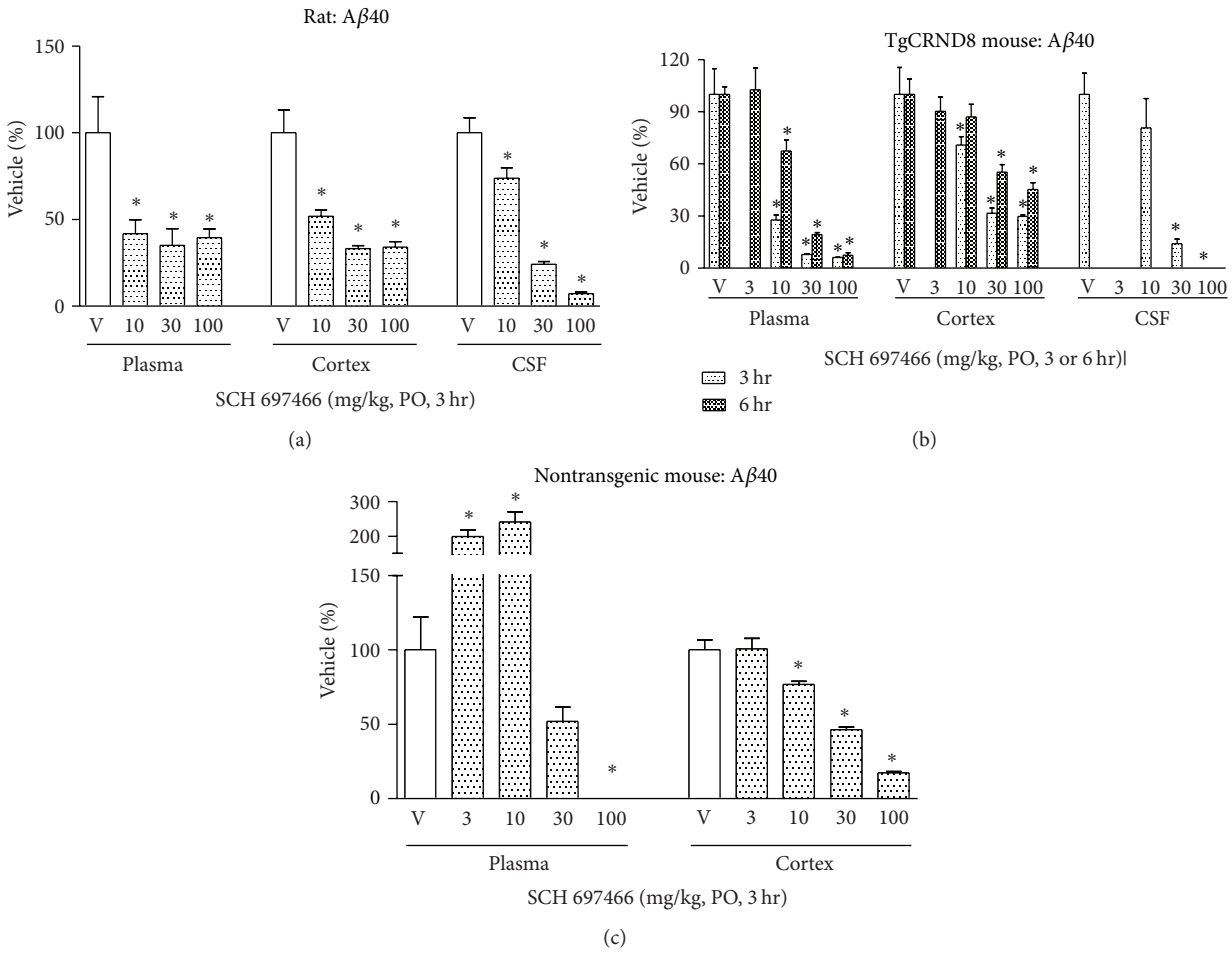

Figure 2: Aβ40 levels expressed as a percent of vehicle in plasma, cortex, and CSF following acute administration of SCH 697466 to (a) rats, (b) TgCRND8 mice, and (c) nontransgenic B6C3F1 mice. For the TgCRND8 studies (b) CSF was not collected in the 6 hr study and 3 mg/kg SCH 697466 was not included in the 3 hr study. $^{*}P < 0.02$ versus vehicle, Dunnett post hoc test.

cortex Aβ42 by 80% and 42%, respectively. compared to 89% and 82% for plasma and cortex Aβ40. There was a time-dependent reduction in the concentration of SCH 697466 in plasma and brain with very little remaining 24 hr later, respectively (Figure 3(b)).

A single dose of 100 mg/kg of SCH 697466 inhibited Aβ in the plasma and cortex 6, 12, 18, and 24 hr after administration (Figure 3(c); main effect of time point: $F(4, 20) = 46.95$ and 20.72, $P < 0.0001$; Dunnett test: $P < 0.0001$). There was a time-dependent reduction in the concentration of SCH 697466 in plasma and brain with 1.4 and 0.3 μM remaining 24 hr later (Figure 3(d)).

3.4. SCH 697466 Reduced Plasma and Cortex Aβ, but Produced Notch-Related Side Effects following Subchronic Administration in TgCRND8 Mice. As has been reported previously [5, 27–29], upon repeated administration some γ-secretase inhibitors produce mechanism-based Notch-related side effects including a reduction in thymus weight and an increase in goblet cell hyperplasia in the intestine. In an effort to determine the potential Notch-related side effect liability and the therapeutic window of SCH 697466 in rodents, we tested SCH 697466 in our TgCRND8 rapid 6-day therapeutic index assay [5]. In this assay, we include doses that provide continuous, near complete lowering Aβ in plasma. Since 30 mg/kg of SCH 697466 provided reasonable lowering (~80% reduction) of Aβ in plasma for 12 hr after administration, but not 24 hr, we decided to administer all doses of SCH 697466 *b.i.d.*

3.4.1. Aβ Lowering. Six days of *b.i.d.* dosing with SCH 697466 in TgCRND8 mice (5 full days with a final dose 3 hr prior to sacrifice on day 6) significantly reduced plasma and cortical Aβ40 levels (Figure 4(a); main effect of dose: $F(4, 29) = 49.76$ and $F(4, 30) = 106.92$, $P < 0.0001$, for plasma and cortex, resp.) with near complete lowering of in both compartments at 100 mg/kg. There was a significant increase of Aβ40 in plasma with the 3 mg/kg dose. SCH 697466 was not as potent at lowering Aβ42 in plasma and brain compared to Aβ40, such that the 100 mg/kg dose reduced plasma and cortex Aβ42 by 90% and 66%, respectively (data not shown), compared to 100% and 98% for plasma and cortex Aβ40.

Table 3: Concentration of SCH 697466 (μM) in plasma and brain for various sub-chronic studies in TgCRND8 and non-transgenic mice.

Dose (mg/kg)	TgCRND8 mouse		Nontransgenic mouse			
	6 days *b.i.d.*		11 days *q.d.*		6 days *b.i.d.*	
	Plasma	Brain	Plasma	Brain	Plasma	Brain
3	0.02 ± 0.003	0.003 ± 0.003	0.03 ± 0.01	BLOQ	0.06 ± 0.04	BLOQ
10	0.47 ± 0.06	0.05 ± 0.01	0.43 ± 0.06	0.01 ± 0.0002	0.35 ± 0.05	BLOQ
30	2.64 ± 0.29	0.32 ± 0.05	2.99 ± 0.22	0.20 ± 0.03	2.03 ± 0.56	0.10 ± 0.02
100	ns	14.96 ± 5.44	8.10 ± 0.84	2.63 ± 0.52	10.21 ± 0.68	3.15 ± 0.54

ns: No samples; BLOQ: below the limit of quantification (0.003 μM).

3.4.2. Notch-Related Side Effects. Six days of *b.i.d.* administration of SCH 697466 significantly reduced thymus weight (Figure 4(b); main effect of dose: $F(4, 19) = 15.59$, $P < 0.002$) with a significant reduction observed in the 100 mg/kg dose group ($P < 0.003$), but not the 30 mg/kg group.

This dosing regime also increased PAS staining in the ileum (Figure 4(c); main effect of dose: $F(4, 17) = 91.34$, $P < 0.0001$) such that there was almost a 6-fold increase in the 100 mg/kg group compared to vehicle treated mice (Figures 4(d) and 4(e); $P < 0.0001$), but not the 30 mg/kg group (just under a 2-fold increase).

Further, mice treated with 100 mg/kg of SCH 697466 steadily lost weight during the 6 days of drug administration; 100 mg/kg mice lost 4.3 g over 6 days while vehicle-treated mice lost only 1 g over the same time period and 66.6% of the mice in the 100 mg/kg group died before the study was completed (compared to 12.5% in the vehicle treated group), and the surviving mice appeared in poor health by the last day of the study (e.g., hypothermic, hunched posture, etc.).

3.4.3. Exposure. There was a dose-related increase (although in some cases it was more than dose proportional) in the concentration of SCH 697466 in plasma and brain (one time point per animal) (Table 3). Drug concentrations following 6 days of *b.i.d.* administration were similar to those observed following a single dose (3 hr) with the exception of the 100 mg/kg group where there was much greater brain exposure following 6 days of *b.i.d.* dosing than following a single dose (c.f., Tables 2 and 3). Due to the poor condition of the mice, there was insufficient plasma to obtain exposure data for mice in the 100 mg/kg group.

3.5. Two Different Dosing Paradigms of SCH 697466 in Nontransgenic Mice Provided Equivalent Lowering of Plasma and Cortex Aβ but Resulted in Different Observations of Notch-Related Side Effects and Biomarker Changes. The time course study suggested that both *q.d.* and *b.i.d.* administration of SCH 697466 at 100 mg/kg would provide sustained and near complete lowering of Aβ, and the subchronic study suggested that Notch-related side effects would be observed under conditions of sustained and near complete lowering of Aβ. In an effort to determine whether Notch-related side effects could be managed by giving SCH 697466 *q.d.* instead of *b.i.d.*, mice were orally administered SCH 697466 either once a day for 11 days (11 days *q.d.*) or twice a day for 5 days with the final dose on the 6th day (6 days *b.i.d.*) with both groups being given a total of 11 doses. All tissues were collected 3-4 hr after the last dose. In addition, we assessed changes in expression of genes downstream of Notch in the intestine and blood to assess the potential of these measures to be useful biomarkers for Notch-related pathology. This study was conducted in nontransgenic B6C3F1 mice since as noted above TgCRND8 mice did not tolerate high doses of SCH 697466.

3.5.1. Aβ Lowering. For each dosing paradigm, the effects of SCH 697466 on Aβ in the plasma of nontransgenic mice were nonlinear such that lower doses increased Aβ40 levels while higher doses decreased Aβ40 levels (Figure 5(a); main effect of dose: $F(4, 19) = 11.02$ and $F(4, 21) = 38.43$, $P < 0.0001$ for 11 days *q.d.* and 6 days *b.i.d.* groups, resp.). The effects of SCH 697466 on Aβ in the plasma were similar between the dosing paradigms with 50% lowering of Aβ occurring at a dose between 10 and 30 mg/kg and complete lowering of Aβ at 100 mg/kg. Plasma Aβ lowering was similar to what was observed in TgCRND8 mice following a single dose and following 6 days of *b.i.d.* drug administration. The increase in plasma Aβ observed at lower doses was more substantial in nontransgenic mice than what was observed in TgCRND8 mice following 6 days of *b.i.d.* administration which has been alluded to elsewhere [40].

In the cortex of nontransgenic mice, SCH 697466 dose-dependently lowered Aβ40 in a more linear fashion following 11 days of *q.d.* and 6 days of *b.i.d.* administration (Figure 5(a), main effect of dose: $F(4, 19) = 105.53$ and $F(4, 21) = 101.04$, resp., $P < 0.0001$). Cortical Aβ lowering was strikingly similar between the dosing paradigms with 50% lowering occurring around 30 mg/kg. The dose-responsive nature of cortical Aβ lowering observed here was similar to what was observed in TgCRND8 mice but did not plateau like what was observed in acutely rats. There was no evidence of an increase in Aβ in the cortex.

3.5.2. Notch-Related Side Effects. Eleven days of *q.d.* administration of SCH 697466 at 30 and 100 mg/kg did not affect thymus weight, while 6 days of *b.i.d.* administration significantly decreased thymus weight by about 60% (Figure 5(b); main effect of dose: $F(2, 14) = 32.40$, $P < 0.0001$) with significant weight reduction in the 100 mg/kg group, but not the 30 mg/kg group, compared to vehicle-treated mice ($P < 0.0001$). This is similar to what was observed in TgCRND8 mice treated for 6 days *b.i.d.* with 100 mg/kg SCH 697466.

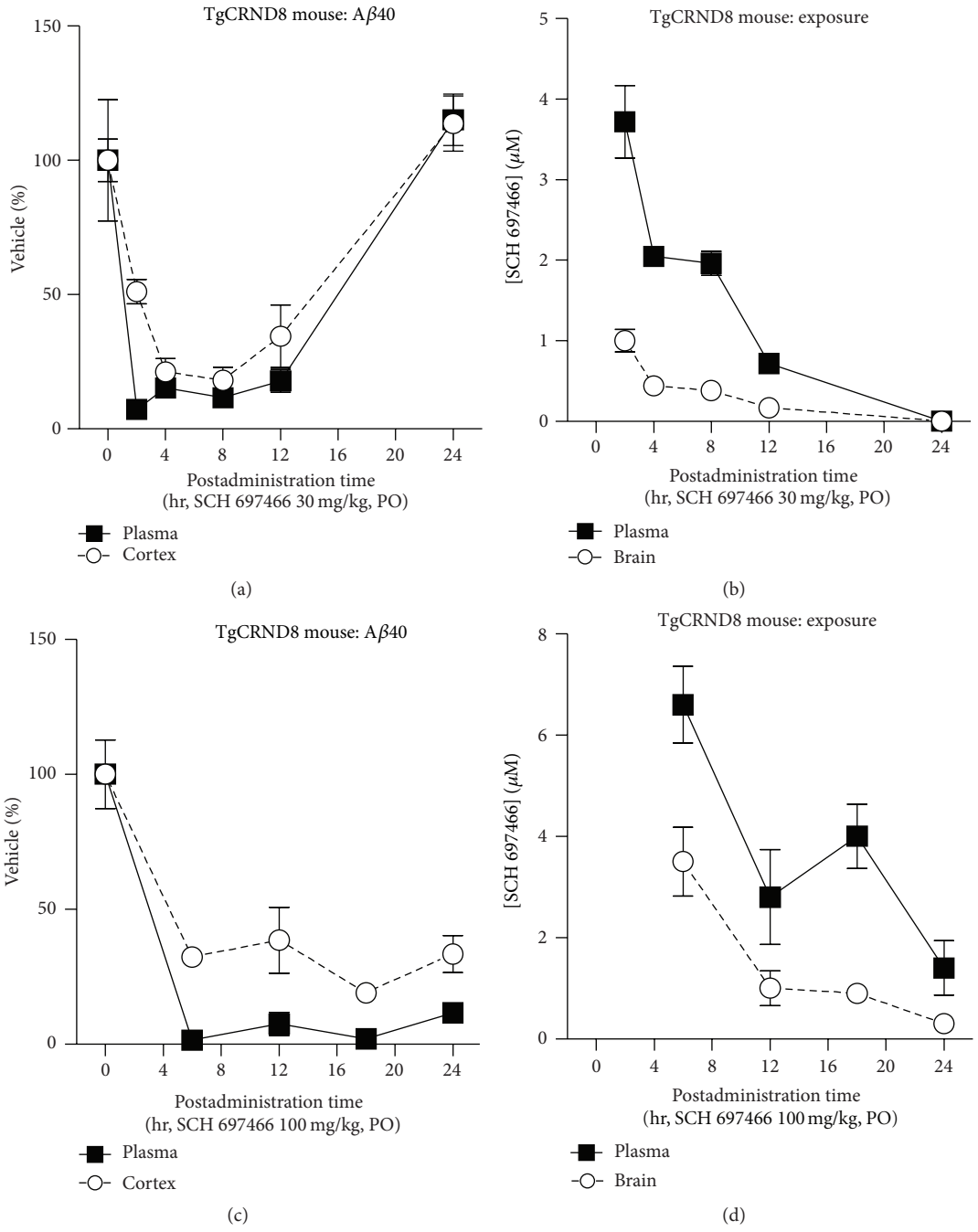

Figure 3: Aβ40 levels over time expressed as a percent of vehicle in plasma and cortex following a single dose of (a) 30 mg/kg or (c) 100 mg/kg of SCH 697466 in TgCRND8 mice. Plasma and brain concentration (μM) of SCH 697466 following a single dose of (b) 30 mg/kg or (d) 100 mg/kg of SCH 697466 in TgCRND8 mice.

Similarly, PAS staining in the ileum was not increased after 11 days of *q.d.* administration of SCH 697466 at 30 and 100 mg/kg, but 100 mg/kg SCH 697466 administered for 6 days *b.i.d.* markedly increased PAS staining in the ileum by about 350% (Figure 5(c); $F(2, 14) = 180.01$, $P < 0.0001$; Figures 5(d)–5(g)). PAS staining in the 100 mg/kg 6 days *b.i.d.* nontransgenic group looked very similar to that observed in TgCRND8 mice following 100 mg/kg 6 days *b.i.d.* SCH 697466 (images not shown). PAS staining was not increased in the 30 mg/kg 6 days *b.i.d.* group.

Contrary to what as observed in the 6 day *b.i.d.* TgCRND8 study, there were no effects of SCH 697466 (up to 100 mg/kg) on body weight or survival in this nontransgenic study (data not shown).

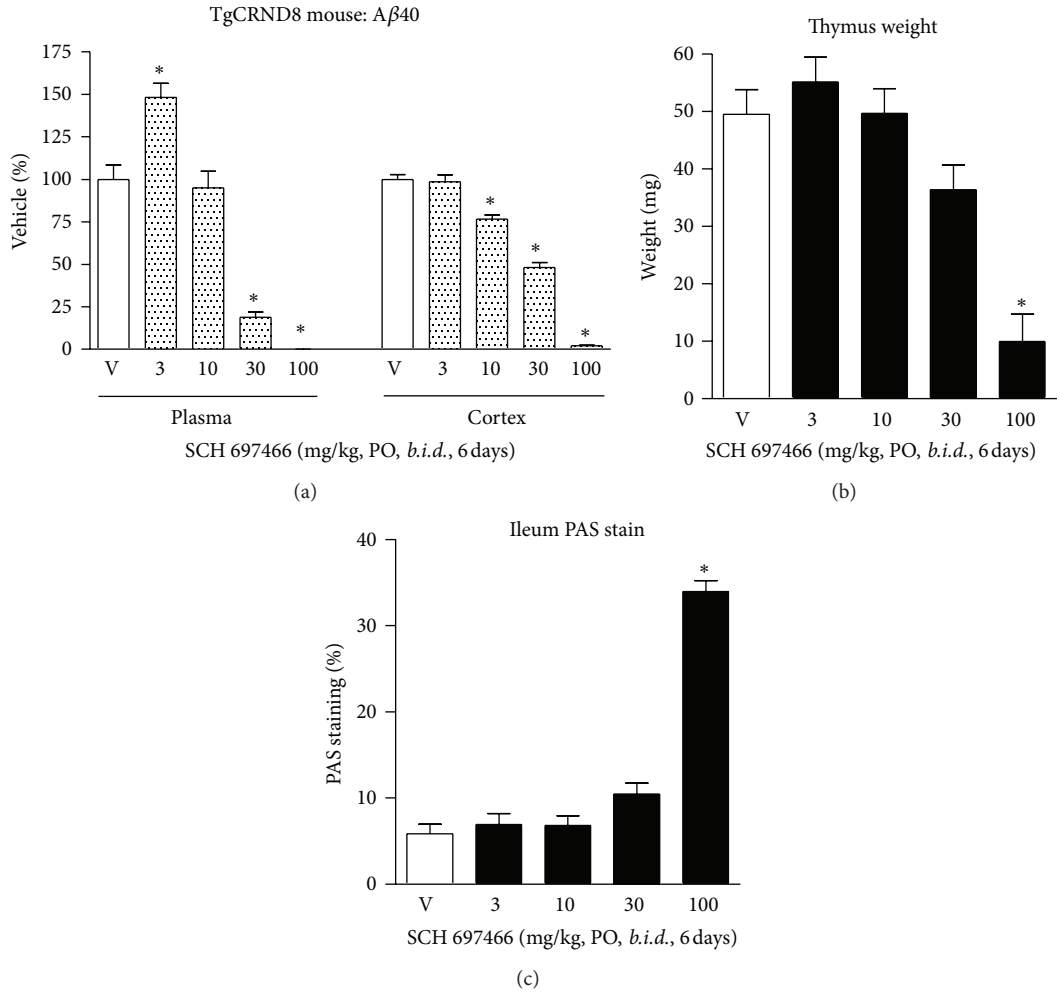

Figure 4: (a) Aβ40 levels expressed as a percent of vehicle in plasma and cortex, (b) thymus weight, and (c) percent area in the ileum covered by PAS stain following 6 days of *b.i.d.* administration of SCH 697466 to TgCRND8 mice. The final dose of SCH 697466 was given on day six 3 hr prior to tissue harvesting. $^{*}P < 0.0006$ versus vehicle, Dunnett post hoc test.

3.5.3. Notch-Related Biomarker Changes. HES-1 gene expression is directly affected by the Notch signaling pathway such that disrupted Notch activity leads to decreased HES-1 expression. Consequently, gene expression of two downstream targets of HES-1, mATH, and KLF4 should be increased following decreased HES-1 expression. As noted in the previous section, only the 100 mg/kg 6 day *b.i.d.* group showed Notch-related pathology.

Both 11 days of *q.d.* administration and 6 days of *b.i.d.* administration of SCH 697466 decreased HES-1 expression in the jejunum (Figure 6(a), main effect of dose: $F(2, 11) = 21.52$ and $F(2, 13) = 14.71$, resp., $P < 0.0005$), with significant decreases observed in both 100 mg/kg groups compared to vehicle-treated mice ($P < 0.02$). mATH1 and KLF4 expression was increased in the jejunum of mice treated for 6 days of *b.i.d.* SCH 697466 (Figures 6(b) and 6(c)); main effect of dose: $F(2, 13) = 7.19$ and 4.51, $P < 0.04$) with increased expression in the 100 mg/kg group for mATH1 and 30 and 100 mg/kg group for KLF4 ($P < 0.04$). mATH1 and KLF expression was unchanged in the 11 day *q.d.* SCH 697466 groups (Figures 6(b) and 6(c)). Adipsin, another downstream target of HES-1, expression in the jejunum was very low in all groups (data not shown).

In the blood, HES-1 expression was affected by treatment with SCH 697466 (Figure 6(d); main effect of dose: $F(2, 11) = 4.48$ and $F(2, 13) = 6.86$, $P < 0.04$) with decreased expression in the 100 mg/kg groups of both dosing paradigms (significant decrease for the 100 mg/kg *b.i.d.* group, $P < 0.04$). Although KLF4 expression was affected by SCH 697466 when administered for 11 days *q.d.* (Figure 6(e); main effect of dose: $F(2, 11) = 5.81$, $P < 0.02$), none of the dosed groups differed from vehicle-treated mice. MATH1 and adipsin expression was not detected in the blood.

3.5.4. Exposure. There was a dose-related increase (although in some cases it was more than dose-proportional) in the concentration of SCH 697466 in plasma and brain (3 hr posttreatment) in each dosing paradigm (Table 3). Overall, drug levels at corresponding doses were similar between the

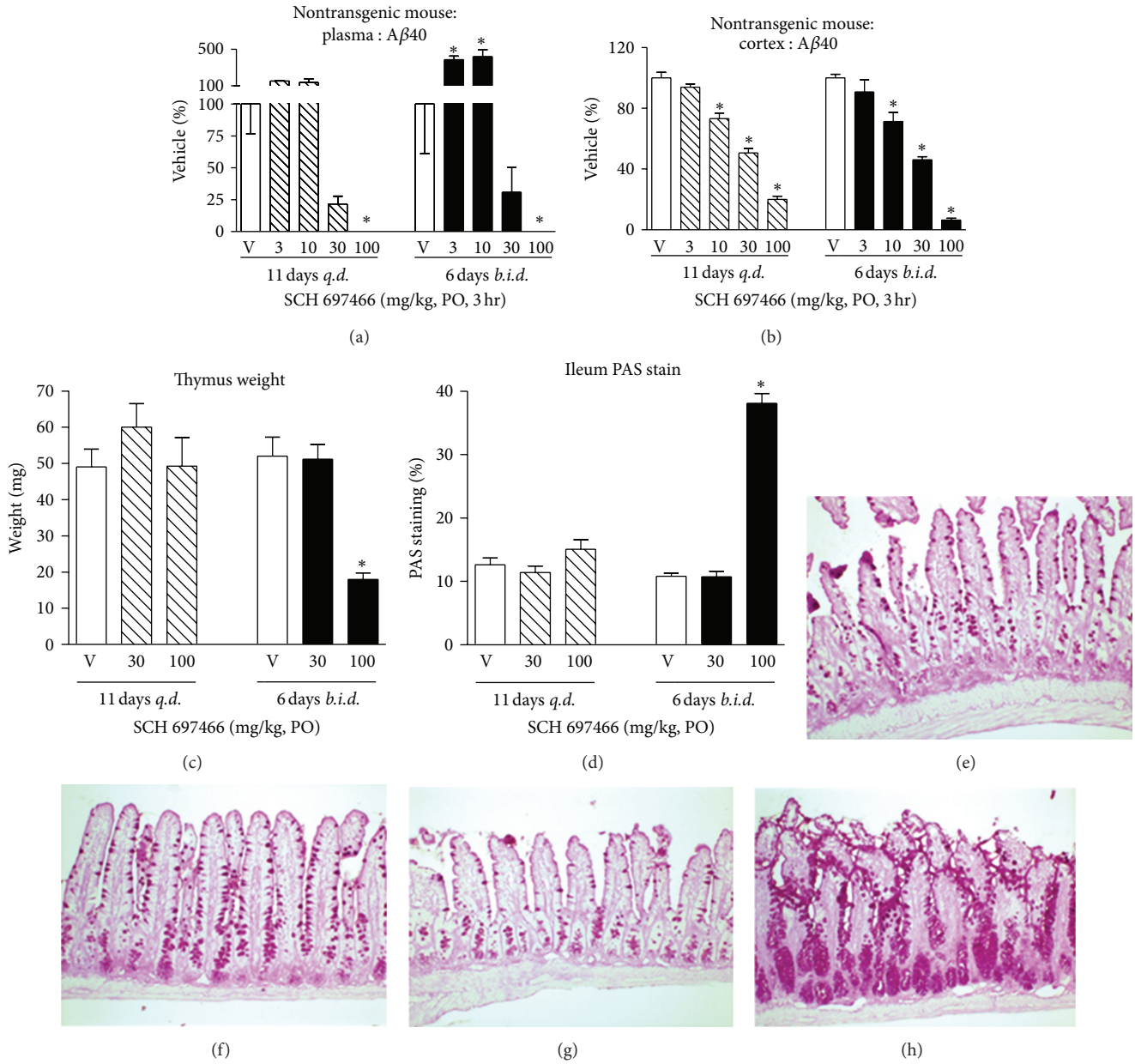

FIGURE 5: Aβ40 levels expressed as a percent of vehicle in (a) plasma and (b) cortex, (c) thymus weight, and (d) percent area in the ileum covered by PAS stain following 11 days of *q.d.* administration (left side of graphs) or 6 days of *b.i.d.* administration (right side of graphs) of SCH 697466 in nontransgenic B6C3F1 mice. The final dose of SCH 697466 was given 3 hr prior to tissue harvesting. Representative examples of the PAS stained ileum from (e) 11 day *q.d.* vehicle-treated mouse; 13% PAS staining, (f) 11 day *q.d.* 100 mg/kg SCH 697466 treated mouse; 16% PAS staining, (g) 6 day *b.i.d.* vehicle-treated mouse; 11% PAS staining, and (h) 6 day *b.i.d.* 100 mg/kg SCH 697466 treated mouse; 39% PAS staining. Increased PAS staining was only observed in the 6 day *b.i.d.* 100 mg/kg treated group. $^{*}P < 0.003$ versus vehicle, Dunnett post hoc test.

dosing paradigm groups and similar to what was observed acutely in rats, TgCRND8 mice, and nontransgenic mice and after 6 days of *b.i.d.* administration in TgCRND8 mice (except here we did not observe the very high brain exposure that was observed in the 100 mg/kg 6 days *b.i.d.* TgCRND8 group). Therefore, the Notch-related side effects and biomarker changes specifically observed in the 100 mg/kg 6 days *b.i.d.* group are not likely to be due to drug accumulation and higher exposure.

4. Discussion

Substantial evidence implicates Aβ peptides in the etiology of Alzheimer's disease. Given that Aβ is produced by cleavage of APP by β- and γ-secretase, γ-secretase inhibition is a promising disease modifying treatment for Alzheimer's disease.

SCH 697466 [34] is a novel, potent, orally available γ-secretase inhibitor that reduced Aβ in plasma and brain of

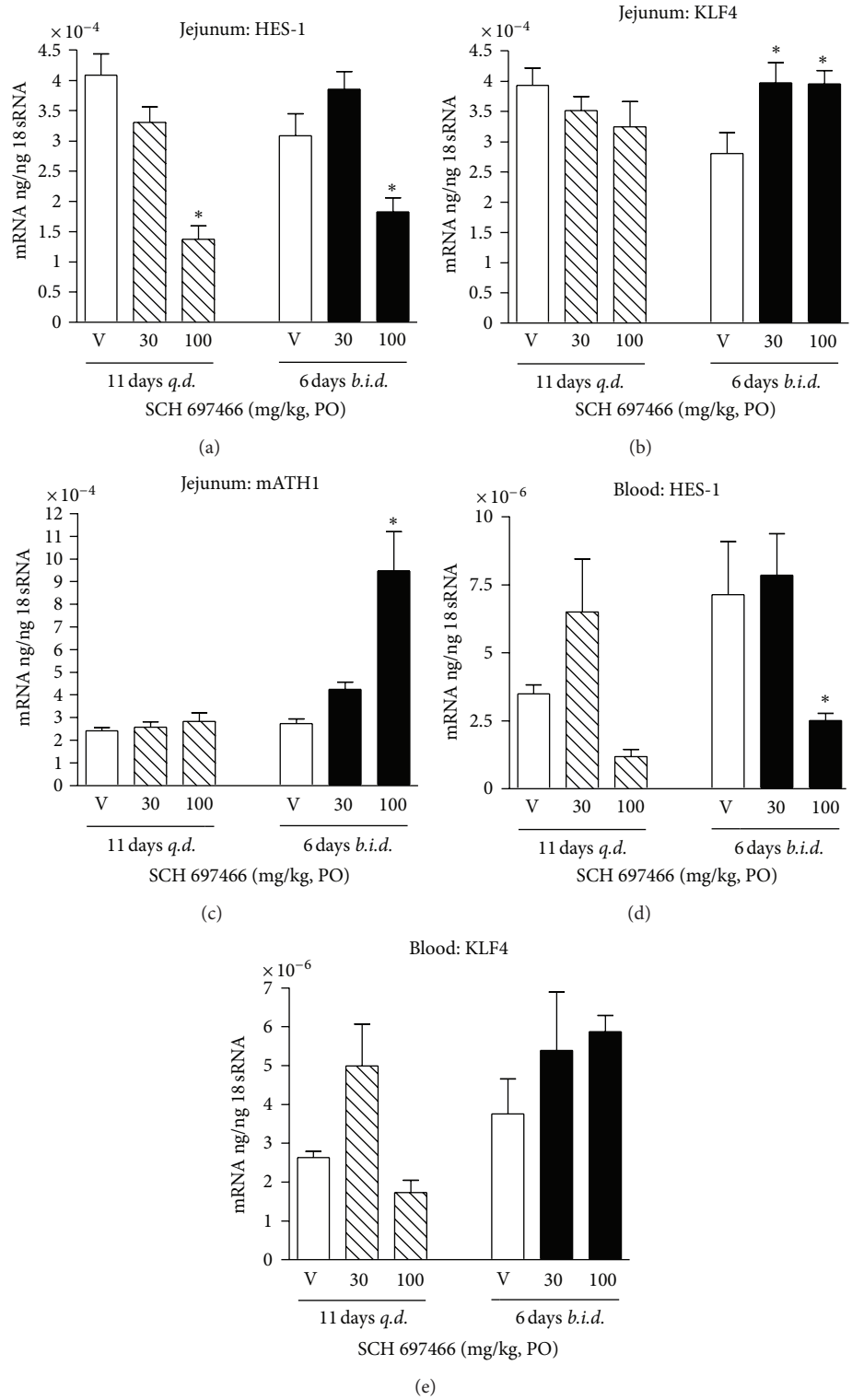

Figure 6: (a) HES-1, (b) KLF4, and (c) mATH gene expression in the jejunum and (d) HES-1 and (e) KLF4 gene expression in white blood cells following 11 days of *q.d.* administration (left side of graphs) or 6 days of *b.i.d.* administration (right side of graphs) of SCH 697466 in nontransgenic B6C3F1 mice. The final dose of SCH 697466 was given 3 hr prior to tissue harvesting. $^{*}P < 0.04$ versus vehicle, Dunnett post hoc test.

rats, preplaque TgCRND8 mice, and nontransgenic mice. The acute effects of SCH 697466 on Aβ levels were relatively similar between the rodent species and genotypes with about 50% lowering of Aβ in plasma, cortex, and CSF occurring between 10 and 30 mg/kg (or between ~0.4 and 3 μM plasma concentration of SCH 697466) and near complete lowering of Aβ occurring at 100 mg/kg (or about 5–8 μM plasma concentration). Therefore, as has been reported for other γ-secretase inhibitors, SCH 697466 was effective at reducing Aβ in vivo.

Although γ-secretase inhibitors reduce Aβ well in peripheral and central compartments, some γ-secretase inhibitors also produce mechanism-based side effects including a reduction in thymus size and an increase in intestinal goblet cell hyperplasia [5, 27–29]. Both of these effects are likely mediated by a disruption of Notch processing [30, 41, 42]. Based on our experience in rodents, these Notch-related side effects seem to be typically observed at doses that give continuous, near complete lowering Aβ in plasma for at least 3 days [5]. Alternatively, we and others have shown that "partial inhibition" doses of these same compounds provide reasonable lowering of Aβ (about >50% reduction) without Notch-related side effects [5, 18]. However, it is not clear how partial inhibition can best be applied in the management of Notch-related side effects, that is, is it preferable to aim for incomplete inhibition for a sustained period of time or complete inhibition for a short period of time? Therefore, we conducted additional subchronic studies with SCH 697466 to address this question as well as to assess the in vivo therapeutic window of this compound.

As was observed acutely in TgCRND8 mice, subchronic *b.i.d.* administration of SCH 697466 dose-dependently lowered Aβ in plasma and cortex with about 50% inhibition occurring between 10 and 30 mg/kg (or between 2–10 μM plasma exposure). SCH 697466 given at 100 mg/kg *b.i.d.* provided sustained and almost complete lowering of plasma Aβ, but also produced Notch-related side effects, including a reduction in thymus size and increased goblet cell hyperplasia. Alternatively, SCH 697466 given at 30 mg/kg *b.i.d.* to TgCRND8 mice provided sustained, although not complete, lowering of Aβ (48% reduction in cortex) without Notch-related side effects. Similar results were previously reported with another γ-secretase inhibitor, LY-411,575 [5]. Thus, although both the 30 and 100 mg/kg doses of SCH 697466 provided sustained lowering of Aβ, only the dose that also provided nearly complete lowering (100 mg/kg) produced Notch-related side effects, while the "partial" inhibition dose (30 mg/kg) did not. In other words, a short duration of action does not seem to be required to mitigate Notch-related side effects, just incomplete inhibition.

Interestingly, although SCH 697466 had a reasonable in vitro separation between IC_{50}s for Aβ lowering and Notch processing (~24-fold), this did not translate in vivo. After subchronic 6 day *b.i.d.* administration of SCH 697466, the ED_{50} for reducing brain Aβ40 was about 30 mg/kg and Notch-related side effects were observed at 100 mg/kg. Therefore, although there was a clear therapeutic window for SCH 697466 in vivo, it was small (~3-fold based on dose and ~5-fold based on plasma concentrations) and significantly less than the therapeutic window predicted by in vitro experiments. It is important to note that SCH 697466 was less potent at lowering the more amyloidogenic Aβ42 species especially in brain suggesting that the in vivo therapeutic index will likely be smaller if Aβ42 data were used instead.

Given that the duration of action of SCH 697466 at 100 mg/kg is relatively long (>24 hr), both *b.i.d.* and *q.d.* administration would provide sustained and near complete lowering of Aβ. It was hypothesized, however, that *q.d.* administration of SCH 697466 might decrease the incidence of Notch-related side effects compared to those observed with *b.i.d.* administration while maintaining excellent lowering of Aβ (>80% reduction). Indeed, in a study with nontransgenic mice, although lowering of plasma and brain Aβ was very similar between the *b.i.d.* and *q.d.* dosing paradigms, the Notch-related side effects were strikingly different such that Notch-related pathology was only observed at 100 mg/kg when administered *b.i.d.* and not *q.d.* This did not seem to be due to large increases in exposure or drug accumulation in the *b.i.d.* group. Of note, although nontransgenic mice tolerated high doses of SCH 697466 better than TgCRND8 mice as measured by body weight loss and survival, both groups of mice showed similar reduction in thymus weight and increase in intestinal goblet cell hyperplasia at 100 mg/kg *b.i.d.* Thus, Notch-related side effects can be managed even with sustained and near complete lowering of Aβ by optimizing the frequency of dosing of γ-secretase inhibitors. However, it cannot be completely excluded that longer term administration of γ-secretase inhibitors even with an optimized frequency of dosing might eventually result in Notch-related side effects; further studies would be required to address this possibility.

Recent data suggest that there may be additional options for mitigating Notch-related side effects with γ-secretase inhibition. A study by Das et al. [43] showed that treating transgenic mice with the γ-secretase inhibitor LY-411,575 for a short period of time during a key, early phase of amyloid accumulation resulted in long-lasting beneficial effects on brain Aβ without the need for continuous drug treatment. These data along with our own suggest that there may be ways to safely and effectively lower brain Aβ with γ-secretase inhibition. Further studies would be required to determine how useful these approaches would be in the clinic.

Based on our findings that Notch-related side effects can be managed with sustained but incomplete lowering of Aβ, or near complete lowering of Aβ but with more intermittent administration, it is possible that some of the "Notch-sparing" and "APP-selective" γ-secretase inhibitors reported in the literature may be managing Notch-related side effects by using these strategies instead of the molecules really being "Notch sparing" in vivo. For example, after 7 days of *b.i.d.* dosing of ELN 475516, an "APP-selective" γ-secretase inhibitor, there was no evidence of Notch-related toxicity as measured by thymus weight and goblet cell hyperplasia in the ileum and the doses and frequency of drug administration utilized provided sustained but incomplete (~74%) lowering of Aβ [10]. Perhaps if this compound was able to obtain near complete lowering of Aβ in a sustained fashion, Notch-related side effects may have indeed been observed.

It is important to note that in these studies, we were using reduction in thymus size and intestinal goblet cell hyperplasia as representative measures of "Notch-related side effects." However, it is possible that there are other toxicities or effects related to γ-secretase inhibition and/or altered Notch signaling that we did not measure and that may not be mitigated or avoided with partial inhibition and/or intermittent dosing paradigms. Further, the translatability of these treatment approaches or mitigation strategies in rodents to humans is not clear.

Although some Notch-related side effects are reversible [5], it would be useful to have a clinically tractable biomarker to monitor potential effects of γ-secretase inhibitors on Notch processing in the clinic. HES-1 gene expression is directly affected by the Notch signaling pathway such that disrupted Notch activity leads to decreased HES-1 expression. Consequently, gene expression of two downstream targets of HES-1, mATH and KLF4, is increased following decreased HES-1 expression [32, 33]. In certain cases, the gene expression profiles of these Notch-related biomarkers paralleled the Notch-related pathology observed. For example, the 100 mg/kg dose of SCH 697466 when given *b.i.d.* induced Notch-related pathology and also decreased HES-1 in the jejunum and in the blood and increased mATH1 and KLF4 expression in the jejunum. The biomarker data did not completely align with the in vivo data though, for example, HES-1 gene expression was decreased in the jejunum of mice treated with 100 mg/kg *q.d.* when no pathology was observed and KLF4 gene expression was increased in mice treated with 30 mg/kg *b.i.d.* when no pathology was observed and when HES-1 expression (upstream of KLF4) was not decreased. It is also possible that the biomarker changes that were observed in the absence of pathology reflect relevant changes in Notch signaling that after a longer period of dosing would indeed result in observations of Notch-related pathology. In general, however, when clear Notch-related pathology was observed, changes in Notch-related biomarkers were simultaneously observed. This is in agreement with other reports using expression of these same genes as potential biomarkers for Notch-related pathology [10].

Interestingly and perhaps paradoxically in several studies an *increase* in plasma Aβ was observed at lower doses of SCH 697466 (e.g., 3 and 10 mg/kg). This increase in plasma Aβ or "Aβ rise" has been frequently observed with other γ-secretase inhibitors in vivo, including in humans, and occurs at low concentrations likely under conditions of partial enzyme occupancy [15, 40, 44, 45]. In addition, the Aβ rise was more prominent in nontransgenic mice than transgenic mice as has been supported elsewhere [40, 44]. Importantly, we never observed an increase in Aβ levels in the cortex with SCH 697466.

To summarize, SCH 697466 is a novel, potent γ-secretase inhibitor that is effective at reducing Aβ in plasma, CSF, and brain in rodents. SCH 697466 has a small, but distinct, in vivo therapeutic index between Aβ lowering and Notch-related side effects in the ileum and thymus in mice. A partial inhibition dose of SCH 697466 provided reasonable reduction of Aβ (~50%) that was sustained over 24 hr when given *b.i.d.* without evidence of Notch-related side effects. Although the reasons are not entirely clear, *q.d.* dosing provided another way to maintain excellent, continuous inhibition of Aβ (>80%) with SCH 697466, but without Notch-related side effects. Therefore, by utilizing partial, but sustained, inhibition doses or optimizing the frequency of administration, it may be possible to obtain robust and sustained lowering of Aβ without Notch-related side effects using γ-secretase inhibitors. Finally, HES-1 expression in blood may be a useful Notch-related biomarker in the clinic.

Acknowledgments

The authors would like to thank Marco Baptista, Carina Bleickardt, Benjamin Eschle, Nicholas Jones, Sherry Lu, and Julie Strain for help with the tissue collections; Howard Jones and Marie Sondey for their help with some of the histology; Ronald Manning for breeding and genotyping the TgCRND8 mice; and Greg Tucker, Lucy Xu, Jing Lan, James Jean, and Lynn Rogers for analyzing the plasma and brain samples.

References

[1] D. J. Selkoe, "The molecular pathology of Alzheimer's disease," *Neuron*, vol. 6, no. 4, pp. 487–498, 1991.

[2] J. A. Hardy and G. A. Higgins, "Alzheimer's disease: the amyloid cascade hypothesis," *Science*, vol. 256, no. 5054, pp. 184–185, 1992.

[3] J. Hardy and D. J. Selkoe, "The amyloid hypothesis of Alzheimer's disease: progress and problems on the road to therapeutics," *Science*, vol. 297, no. 5580, pp. 353–356, 2002.

[4] D. M. Barten, J. E. Meredith Jr., R. Zaczek, J. G. Houston, and C. F. Albright, "γ-secretase inhibitors for Alzheimer's disease: balancing efficacy and toxicity," *Drugs in R and D*, vol. 7, no. 2, pp. 87–97, 2006.

[5] L. A. Hyde, N. A. McHugh, J. Chen et al., "Studies to investigate the in vivo therapeutic window of the γ-secretase inhibitor N2-[(2S)-2-(3,5-difluorophenyl)-2-hydroxyethanoyl]-N1-[(7S)-5-methyl-6-oxo-6,7-dihydro-5H-dibenzo[b,d] azepin-7-yl]-L-alaninamide (LY411,575) in the CRND8 mouse," *Journal of Pharmacology and Experimental Therapeutics*, vol. 319, no. 3, pp. 1133–1143, 2006.

[6] J. D. Best, M. T. Jay, F. Otu et al., "In vivo characterization of Aβ(40) changes in brain and cerebrospinal fluid using the novel γ-secretase inhibitor N-[cis-4-[(4-chlorophenyl)sulfonyl]-4-(2,5-difluorophenyl)cyclohexyl]-1,1,1-trifluoromethan-
esulfonamide (MRK-560) in the rat," *Journal of Pharmacology and Experimental Therapeutics*, vol. 317, no. 2, pp. 786–790, 2006.

[7] C. V. C. Prasad, M. Zheng, S. Vig et al., "Discovery of (S)-2-((S)-2-(3,5-difluorophenyl)-2-hydroxyacetamido)-*N-((S,Z)*-3-methyl-4-oxo-4,5-dihydro-3H-benzo[d][1,2]diazepin-5-yl)propanamide (BMS-433796): a γ-secretase inhibitor with Aβ lowering activity in a transgenic mouse model of Alzheimer's disease," *Bioorganic and Medicinal Chemistry Letters*, vol. 17, no. 14, pp. 4006–4011, 2007.

[8] R. L. Martone, H. Zhou, K. Atchison- et al., "Begacestat (GSI-953): a novel, selective thiophene sulfonamide inhibitor of amyloid precursor protein gamma-secretase for the treatment of Alzheimer's disease," *Journal of Pharmacology and Experimental Therapeutics*, vol. 331, no. 2, pp. 598–608, 2009.

[9] K. W. Gillman, J. E. Starrett, M. F. Parker et al., "Discovery and evaluation of BMS-708163, a potent, selective and orally bioavailable $\hat{1}^3$-Secretase Inhibitor," *ACS Medicinal Chemistry Letters*, vol. 1, no. 3, p. 120, 2010.

[10] G. S. Basi, S. Hemphill, E. F. Brigham et al., "Amyloid precursor protein selective gamma-secretase inhibitors for treatment of Alzheimer's disease," *Alzheimer's Research & Therapy*, vol. 2, no. 6, p. 36, 2010.

[11] T. A. Lanz, K. M. Wood, K. E. G. Richter et al., "Pharmacodynamics and pharmacokinetics of the γ-secretase inhibitor PF-3084014," *Journal of Pharmacology and Experimental Therapeutics*, vol. 334, no. 1, pp. 269–277, 2010.

[12] Y. Mitani, J. Yarimizu, K. Saita et al., "Differential effects between gamma-secretase inhibitors and modulators on cognitive function in amyloid precursor protein-transgenic and nontransgenic mice," *Journal of Neuroscience*, vol. 32, no. 6, pp. 2037–2050, 2012.

[13] D. B. Henley, P. C. May, R. A. Dean, and E. R. Siemers, "Development of semagacestat (LY450139), a functional γ-secretase inhibitor, for the treatment of Alzheimer's disease," *Expert Opinion on Pharmacotherapy*, vol. 10, no. 10, pp. 1657–1664, 2009.

[14] R. J. Bateman, E. R. Siemers, K. G. Mawuenyega et al., "A γ-secretase inhibitor decreases amyloid-β production in the central nervous system," *Annals of Neurology*, vol. 66, no. 1, pp. 48–54, 2009.

[15] G. Tong, J. S. Wang, O. Sverdlov et al., "Multicenter, randomized, double-blind, placebo-controlled, single-ascending dose study of the oral gamma-secretase inhibitor BMS-708163 (Avagacestat): tolerability profile, pharmacokinetic parameters, and pharmacodynamic markers," *Clinical Therapeutics*, vol. 34, no. 3, pp. 654–667, 2012.

[16] A. S. Fleisher, R. Raman, E. R. Siemers et al., "Phase 2 safety trial targeting amyloid beta production with a gamma-secretase inhibitor in Alzheimer disease," *Archives of Neurology*, vol. 65, no. 8, pp. 1031–1038, 2008.

[17] E. R. Siemers, J. F. Quinn, J. Kaye et al., "Effects of a γ-secretase inhibitor in a randomized study of patients with Alzheimer disease," *Neurology*, vol. 66, no. 4, pp. 602–604, 2006.

[18] J. D. Best, D. W. Smith, M. A. Reilly et al., "The novel γ secretase inhibitor N-[cis-4-[(4-chlorophenyl)sulfonyl]-4-(2,5-difluorophenyl)cyclohexyl]-1,1,1-trifluoromethanesulfonamide (MRK-560) reduces amyloid plaque deposition without evidence of notch-related pathology in the Tg2576 mouse," *Journal of Pharmacology and Experimental Therapeutics*, vol. 320, no. 2, pp. 552–558, 2007.

[19] D. Abramowski, K. H. Wiederhold, U. Furrer et al., "Dynamics of Aβ turnover and deposition in different β-amyloid precursor protein transgenic mouse models following γ-secretase inhibition," *Journal of Pharmacology and Experimental Therapeutics*, vol. 327, no. 2, pp. 411–424, 2008.

[20] S. J. Pollack and H. Lewis, "γ-Secretase inhibitors for Alzheimer's disease: challenges of a promiscuous protease," *Current Opinion in Investigational Drugs*, vol. 6, no. 1, pp. 35–47, 2005.

[21] A. Lleo and C. A. Saura, "gamma-secretase substrates and their implications for drug development in Alzheimer's disease," *Current Topics in Medicinal Chemistry*, vol. 11, no. 12, pp. 1513–1527, 2011.

[22] B. De Strooper, W. Annaert, P. Cupers et al., "A presenilin-1-dependent γ-secretase-like protease mediates release of notch intracellular domain," *Nature*, vol. 398, no. 6727, pp. 518–522, 1999.

[23] S. Artavanis-Tsakonas, M. D. Rand, and R. J. Lake, "Notch signaling: cell fate control and signal integration in development," *Science*, vol. 284, no. 5415, pp. 770–776, 1999.

[24] D. C. Cole, J. R. Stock, A. F. Kreft et al., "(S)-N-(5-Chlorothiophene-2-sulfonyl)-β,β-diethylalaninol a Notch-1-sparing γ-secretase inhibitor," *Bioorganic and Medicinal Chemistry Letters*, vol. 19, no. 3, pp. 926–929, 2009.

[25] A. Kreft, B. Harrison, S. Aschmies et al., "Discovery of a novel series of Notch-sparing γ-secretase inhibitors," *Bioorganic and Medicinal Chemistry Letters*, vol. 18, no. 14, pp. 4232–4236, 2008.

[26] S. C. Mayer, A. F. Kreft, B. Harrison et al., "Discovery of begacestat, a Notch-1-sparing γ-secretase inhibitor for the treatment of Alzheimer's disease," *Journal of Medicinal Chemistry*, vol. 51, no. 23, pp. 7348–7351, 2008.

[27] G. H. Searfoss, W. H. Jordan, D. O. Calligaro et al., "Adipsin, a biomarker of gastrointestinal toxicity mediated by a functional gamma-secretase inhibitor," *Journal of Biological Chemistry*, vol. 278, no. 46, pp. 46107–46116, 2003.

[28] G. T. Wong, D. Manfra, F. M. Poulet et al., "Chronic treatment with the gamma-secretase inhibitor LY-411,575 inhibits beta-amyloid peptide production and alters lymphopoiesis and intestinal cell differentiation," *Journal of Biological Chemistry*, vol. 279, no. 13, pp. 12876–12882, 2004.

[29] J. Milano, J. McKay, C. Dagenais et al., "Modulation of Notch processing by γ-secretase inhibitors causes intestinal goblet cell metaplasia and induction of genes known to specify gut secretory lineage differentiation," *Toxicological Sciences*, vol. 82, no. 1, pp. 341–358, 2004.

[30] J. H. Van Es, M. E. Van Gijn, O. Riccio et al., "Notch/γ-secretase inhibition turns proliferative cells in intestinal crypts and adenomas into goblet cells," *Nature*, vol. 435, no. 7044, pp. 959–963, 2005.

[31] M. Katoh and M. Katoh, "Notch signaling in gastrointestinal tract (Review)," *International Journal of Oncology*, vol. 30, no. 1, pp. 247–251, 2007.

[32] H. Zheng, D. M. Pritchard, X. Yang et al., "KLF4 gene expression is inhibited by the notch signaling pathway that controls goblet cell differentiation in mouse gastrointestinal tract," *American Journal of Physiology*, vol. 296, no. 3, pp. G490–G498, 2009.

[33] C. A. Richmond and D. T. Breault, "Regulation of gene expression in the intestinal epithelium," *Progress in Molecular Biology and Translational Science*, vol. 96, pp. 207–229, 2010.

[34] T. Asberom, Z. Zhao, T. A. Bara et al., "Discovery of γ-secretase inhibitors efficacious in a transgenic animal model of Alzheimer's disease," *Bioorganic and Medicinal Chemistry Letters*, vol. 17, no. 2, pp. 511–516, 2007.

[35] M. A. Chishti, D. S. Yang, C. Janus et al., "Early-onset amyloid deposition and cognitive deficits in transgenic mice expressing a double mutant form of amyloid precursor protein 695," *Journal of Biological Chemistry*, vol. 276, no. 24, pp. 21562–21570, 2001.

[36] L. A. Hyde, T. M. Kazdoba, M. Grilli et al., "Age-progressing cognitive impairments and neuropathology in transgenic CRND8 mice," *Behavioural Brain Research*, vol. 160, no. 2, pp. 344–355, 2005.

[37] T. A. Lanz, C. S. Himes, G. Pallante et al., "The γ-secretase inhibitor N-[N-(3,5-difluorophenacetyl)-lalanyl]-S-phenylglycine t-butyl ester reduces Aβ levels in vivo in plasma and cerebrospinal fluid in young (plaque-free) and aged (plaque-bearing) Tg2576 mice," *Journal of Pharmacology and Experimental Therapeutics*, vol. 305, no. 3, pp. 864–871, 2003.

[38] D. M. Barten, V. L. Guss, J. A. Corsa et al., "Dynamics of β-amyloid reductions in brain, cerebrospinal fluid, and plasma of β-amyloid precursor protein transgenic mice treated with a γ-secretase inhibitor," *Journal of Pharmacology and Experimental Therapeutics*, vol. 312, no. 2, pp. 635–643, 2005.

[39] L. Zhang, L. Song, G. Terracina, Y. Liu, B. Pramanik, and E. Parker, "Biochemical characterization of the γ-secretase activity that produces β-amyloid peptides," *Biochemistry*, vol. 40, no. 16, pp. 5049–5055, 2001.

[40] C. R. Burton, J. E. Meredith, D. M. Barten et al., "The amyloid-β rise and γ-secretase inhibitor potency depend on the level of substrate expression," *Journal of Biological Chemistry*, vol. 283, no. 34, pp. 22992–23003, 2008.

[41] J. Jensen, E. E. Pedersen, P. Galante et al., "Control of endodermal endocrine development by Hes-1," *Nature Genetics*, vol. 24, no. 1, pp. 36–44, 2000.

[42] S. Fre, M. Huyghe, P. Mourikis, S. Robine, D. Louvard, and S. Artavanis-Tsakonas, "Notch signals control the fate of immature progenitor cells in the intestine," *Nature*, vol. 435, no. 7044, pp. 964–968, 2005.

[43] P. Das, C. Verbeeck, L. Minter et al., "Transient pharmacologic lowering of Abeta production prior to deposition results in sustained reduction of amyloid plaque pathology," *Molecular Neurodegeneration*, vol. 7, p. 39, 2012.

[44] T. A. Lanz, M. J. Karmilowicz, K. M. Wood et al., "Concentration-dependent modulation of amyloid-β in vivo and in vitro using the γ-secretase inhibitor, LY-450139," *Journal of Pharmacology and Experimental Therapeutics*, vol. 319, no. 2, pp. 924–933, 2006.

[45] E. Siemers, M. Skinner, R. A. Dean et al., "Safety, tolerability, and changes in amyloid β concentrations after administration of a γ-secretase inhibitor in volunteers," *Clinical Neuropharmacology*, vol. 28, no. 3, pp. 126–132, 2005.

Hindawi Publishing Corporation
International Journal of Alzheimer's Disease
Volume 2012, Article ID 591392, 7 pages
doi:10.1155/2012/591392

Review Article

γ-Secretase-Dependent Proteolysis of Transmembrane Domain of Amyloid Precursor Protein: Successive Tri- and Tetrapeptide Release in Amyloid β-Protein Production

Mako Takami[1,2] and Satoru Funamoto[1]

[1] *Department of Neuropathology, Graduate School of Life and Medical Sciences, Doshisha University, Kyotanabe, Kyoto 610-0934, Japan*
[2] *Pharma Eight Co. Ltd., Kyoto, Kyoto 602-0841, Japan*

Correspondence should be addressed to Satoru Funamoto, sfunamot@mail.doshisha.ac.jp

Received 13 September 2012; Revised 27 November 2012; Accepted 12 December 2012

Academic Editor: Jeremy Toyn

γ-Secretase cleaves the carboxyl-terminal fragment (βCTF) of APP not only in the middle of the transmembrane domain (γ-cleavage), but also at sites close to the membrane/cytoplasm boundary (ε-cleavage), to produce the amyloid β protein (Aβ) and the APP intracellular domain (AICD), respectively. The AICD49–99 and AICD50–99 species were identified as counterparts of the long Aβ species Aβ48 and Aβ49, respectively. We found that Aβ40 and AICD50–99 were the predominant species in cells expressing wild-type APP and presenilin, whereas the production of Aβ42 and AICD49–99 was enhanced in cells expressing familial Alzheimer's disease mutants of APP and presenilin. These long Aβ species were identified in cell lysates and mouse brain extracts, which suggests that ε-cleavage is the first cleavage of βCTF to produce Aβ by γ-secretase. Here, we review the progress of research on the mechanism underlying the proteolysis of the APP transmembrane domain based on tri- and tetrapeptide release.

1. Introduction

The amyloid precursor protein (APP) is a type I membrane protein. After ectodomain shedding by β-secretase, the carboxyl-terminal fragment (βCTF) of APP becomes a direct substrate of γ-secretase and is processed into the amyloid β protein (Aβ) and the APP intracellular domain (AICD) [1–5]. γ-secretase is an enigmatic protease composed of presenilin 1/2, nicastrin, Aph-1, and Pen-2 that catalyzes proteolysis in the hydrophobic environment of the lipid bilayer [6–15]. Currently, over 50 molecules are reported as γ-secretase substrates, which reflects the physiological importance of this enzyme [16]. For instance, the Notch receptor on the plasma membrane is cleaved by γ-secretase upon ligand binding and the liberated Notch intracellular domain (NICD) translocates into the nucleus and activates the expression of transcription factors to suppress neuronal differentiation [17, 18]. This indicates that inhibition of γ-secretase for suppression of Aβ production causes harmful side effects. To avoid this risk in anti-Alzheimer's disease (AD) therapeutics, it is very important to elucidate the molecular mechanism underlying γ-secretase-dependent proteolysis. Recently, it was revealed that γ-secretase forms a hydrophilic pore and three water-accessible cavities [19–23]. Here, we review the progress of research on the mechanism underlying the proteolysis of the transmembrane domain of βCTF.

2. Discovery of ε-Cleavage during APP Processing

After the β-secretase-dependent cleavage of APP, the ectodomain of APP is released into the extracellular space and βCTF (as a stub in the lipid bilayer) is the direct substrate of γ-secretase [2, 3, 24]. βCTF is composed of 99 amino acids and is eventually processed into the 38–43-residue-long Aβ, suggesting that the counterparts of those Aβ species should

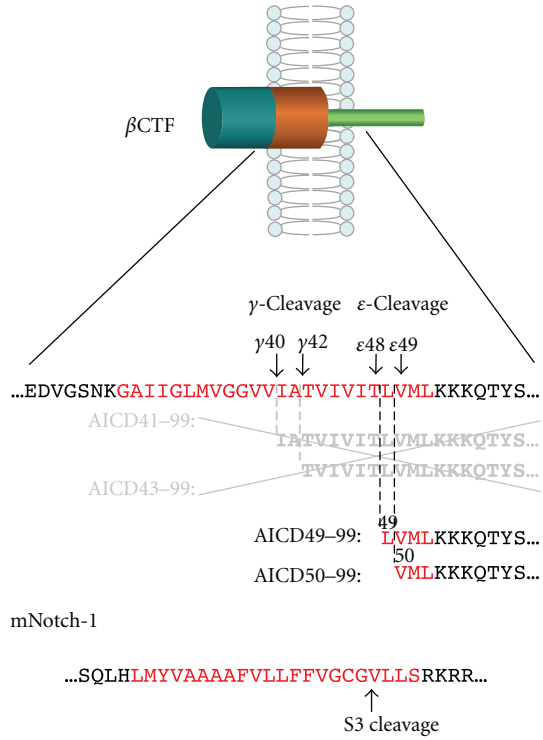

Figure 1: βCTF is cleaved at the membrane-cytoplasm boundary and not in the middle of the transmembrane domain (ε-cleavage), to release the AICD49–99 and AICD50–99 species. The production of AICD species was inhibited in the presence of a γ-secretase inhibitor. ε-Cleavage is analogous to the S3 cleavage of mNotch-1. Red indicates the transmembrane domain.

contain 56–61 residues [4, 25–29]. However, 50-51-residue-long AICDs were identified that correspond to residues 49–99 and 50–99 of βCTF (AICD49–99 and AICD50–99), instead of 56–61-residue-long species (Figure 1) [30–32]. These AICD species were suppressed by L-685,458, a transition state analogue γ-secretase inhibitor, and by expression of a dominant-negative mutant of presenilin (PS), suggesting that γ-secretase cleaves βCTF not only in the middle of the transmembrane domain (γ-cleavage), but also at sites close to the membrane/cytoplasm boundary (ε-cleavage), releasing AICD49–99 and AICD50–99. ε-Cleavage sites are analogues of the Notch S3 cleavage site, which is located at the membrane, near the cytoplasm (Figure 1). Cleavages similar to the APP ε-cleavage were identified in other proteins, such as amyloid precursor-like protein 1 (APLP-1), APLP-2, CD44, Delta 1, E-cadherin, ErbB4, and LRP1 [30, 33–37]. It is reasonable to consider that the water molecules required for proteolysis have access to the catalytic center of γ-secretase from the cytoplasm, rather than from the extracellular space, and that ε-cleavage precedes γ-cleavage during APP processing.

3. Relationship between γ- and ε-Cleavage

CHO cells expressing familial AD (FAD) mutants of PS or APP increase production ratio of Aβ42 (Aβ43) to Aβ40 compared to cells expressing wild-type PS or APP these longer Aβ species are more hydrophobic and more prone to form neurotoxic aggregates. CHO cells expressing wild-type PS preferentially release AICD50–99, whereas those expressing a subset of familial AD (FAD) mutants of PS or APP exhibit an increased proportion of AICD49–99 (Figure 2(a)) [42]. As those FAD mutations cause an increase in the Aβ42/Aβ40 ratio, a potential link between γ- and ε-cleavage was assumed. To test this, we expressed Aβ49 and Aβ48, which are potential counterparts of AICD50–99 and AICD49–99, respectively, in CHO cells. The cells expressing Aβ49 predominantly secreted Aβ40, whereas those expressing Aβ48 exhibited a significantly increased proportion of Aβ42/Aβ40 (Figure 2(b)) [43]. These data indicate that ε-cleavage sites determine the preference for γ- and ε-cleavage sites to produce Aβ40 and Aβ42. Long Aβ species, Aβ49 and Aβ48, have been identified in cell lysates and mouse brain extracts, which suggests that ε-cleavage is the first cleavage of βCTF to produce Aβ by γ-secretase [44]. On the other hand, ε-cleavage can be considered as endopeptidase activity of γ-secretase. FAD mutations did not consistently impair the endopeptidase activity on APP, Notch, ErbB4, and N-Cadherin, but altered γ-cleavage of APP, especially fourth cleavage to produce Aβ40 and Aβ38 from Aβ43 and Aβ42, respectively [45]. Such dissociation between ε-cleavage and γ-cleavage was also proposed by Quintero-Monzon et al. [46].

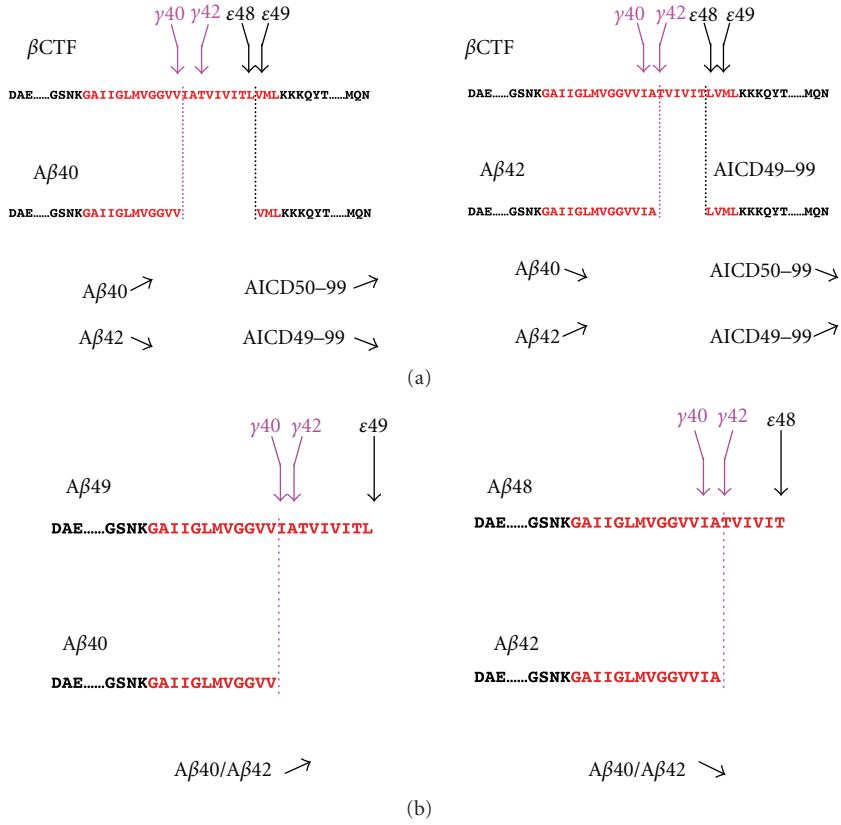

Figure 2: Relationship between γ- and ε-cleavage. (a) Cells expressing wild-type PS or APP predominantly produce Aβ40 and AICD50–99, while cells expressing a FAD mutant of PS or APP exhibited increased proportion of Aβ42 and AICD49–99. (b) Expression of Aβ49 results in an increase in Aβ40/Aβ42 ratio, whereas expression of Aβ48 leads to opposite results. ↗ increase, ↘ decrease.

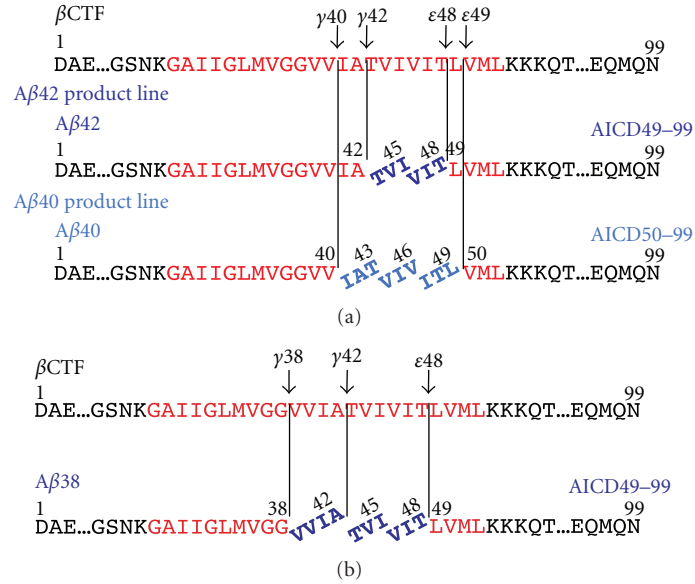

Figure 3: Tri- and tetrapeptide release from βCTF. (a) Upon ε-cleavage at ε48, γ-secretase releases the VIT and TVI tripeptides successively to produce Aβ42. (b) In the Aβ40 product line, after ε-cleavage at ε49, βCTF is converted into Aβ40 by releasing ITL, VIV, and IAT. Aβ42 is a direct substrate during Aβ38 production, which acts by releasing the VVIA tetrapeptide.

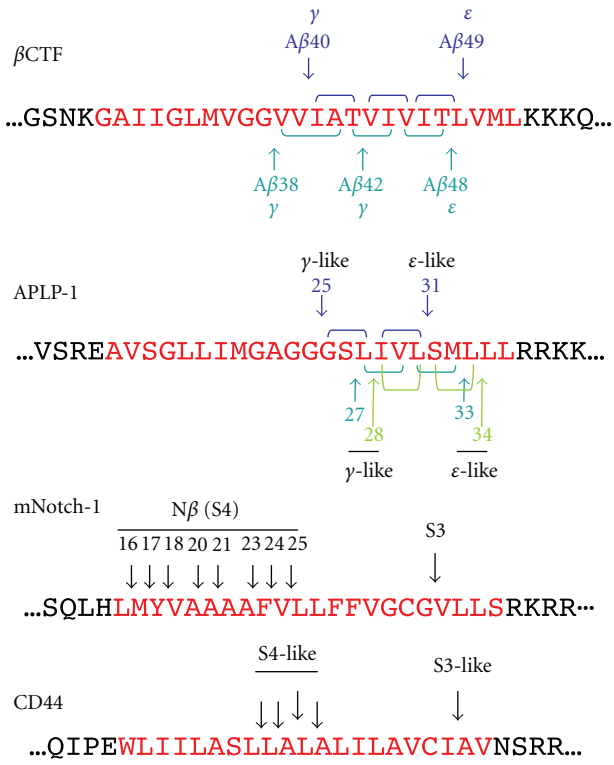

Figure 4: Multiple cleavage sites on the transmembrane domain of γ-secretase substrates. APP [38], APLP-1 [30, 39], mNotch-1 [40], and CD44 [41].

4. Tripeptide Hypothesis

Treatment with N-[N-(3,5-difluorophenacetyl)-L-alanyl]-(S)-phenylglycine t-butyl ester (DAPT), a γ-secretase inhibitor, suppressed extracellular Aβ in cells expressing APP [47]. The levels of the intracellular Aβ40 and Aβ42 species also decreased after DAPT treatment; however, intracellular Aβ43 and Aβ46 increased in a dose-dependent manner [44, 48, 49]. Tryptophan substitutions of γ-cleavage site (41–43) of APP attenuated Aβ secretion, but accumulated Aβ45 species in cell lysate. Tryptophan substitutions of ε-cleavage site (48–52) of APP decreased Aβ production and allowed longer AICD46–99 production. Tryptophan substitutions of ξ-cleavage site (45–47) also suppressed Aβ production. These substitution studies also implied successive cleavage of APP for Aβ production after ε-cleavage [50].

γ-Secretase containing mature nicastrin accumulates in lipid rafts, which indicates that active γ-secretase mainly localizes to the lipid raft of cells [51]. Lipid rafts are an ideal material to investigate Aβ production in the membrane environment. Aβ46 was the dominant species in a lipid raft isolated from DAPT-treated cells. Interestingly, incubating this lipid raft in the absence of DAPT resulted in production of Aβ40 and Aβ43, but not of Aβ42 [52]. These data suggest that Aβ46 is mainly converted into Aβ40 by releasing VIV and IAT tripeptides (successive tripeptide release, tripeptide hypothesis; Aβ40 product line) (Figure 3(a)). On the other hand, CHO cells expressing an FAD mutant of presenilin 2 exhibited a decrease in intracellular Aβ42 and a concomitant increase in intracellular Aβ45 levels in the presence of DAPT, suggesting that Aβ45 is a precursor of Aβ42 by releasing TVI (Aβ42 product line) (Figure 3(a)) [53]. It is reasonable to consider that two major product lines lead to Aβ40 and Aβ42 production (Figure 3(a)).

5. Identification of Tri- and Tetrapeptides Released from βCTF

The most effective approach to confirm tripeptide release from βCTF is the identification of those tripeptides directly in the reaction mixture of Aβ production. CHAPSO soluble γ-secretase was isolated and incubated with the βCTF substrate. LC-MS/MS analysis identified five major tripeptides, and γ-secretase inhibitors abolished the production of these molecules. ITL, VIV, and IAT were predicted tripeptides in the Aβ40 product line (Figure 3(a)). The amounts of Aβ40 and Aβ43 in the reaction mixture, as assessed using Western blotting, corresponded roughly to the predicted Aβ40 and Aβ43 levels, respectively [38]. VIT and TVI were also detected in the Aβ42 product line, as predicted (Figure 3(a)). Interestingly, the VVIA tetrapeptide was detected in the reaction mixture only in the absence of γ-secretase inhibitors (Figure 3(b)). We postulated that VVIA was released from Aβ42 to produce Aβ38. No significant difference was detected between the level of Aβ42 by Western blot quantification and that by LC-MS/MS quantitative estimation. These results indicate that γ-secretase releases

tri- and tetrapeptides successively upon ε-cleavage of βCTF, to produce Aβ species. These tri- and tetrapeptides released from βCTF were detected even in the lipid raft fraction (Takami, unpublished observation).

6. Is Tripeptide Release a General Property of Substrate Cleavage by γ-Secretase?

Successive tripeptide release was observed in βCTF processing by γ-secretase. We also found that γ-secretase released tri- and tetrapeptides successively from αCTF substrate (Takami, unpublished observation). Recently, tripeptide spacing of endoproteolysis on presenilin has been reported [54]. These suggest that successive tri- and tetrapeptide release is a general property of γ-secretase-mediated intramembrane proteolysis.

Yanagida et al. reported that APLP-1 was also cleaved into three Aβ-like peptides [39]. As three ε-like cleavages are known, it is likely that APLP-1 is processed in three product lines by successive tripeptide release [30] (Figure 4). The transmembrane domain of mNotch-1 is cleaved by γ-secretase after ectodomain shedding to liberate NICD (S3 cleavage). NICD containing V1744 was found as the prominent species produced by S3 cleavage [55]. To date, it seems reasonable to suppose that there is a single cleavage site in S3. γ-Secretase also cleaves mNotch-1 at the lumen-membrane boundary (S4 cleavage) to release Notch β peptides (Nβ) (Figure 4) [40, 56, 57]. Fenofibrate treatment increased the proportion of Nβ25, but not that of Nβ21, which implies that Nβ25 and Nβ21 correspond to Aβ42 and Aβ40, respectively [57]. However, it is unlikely that several Nβ product lines exist in Notch processing because of the single S3 site. The production of Nβ species may not fit the tripeptide-processing model (Figure 4). CD44 is cleaved not only at the membrane-cytoplasm boundary, but also at the middle of the transmembrane domain, which results in the release of Aβ-like peptides [33, 41]. Similar to Notch, the processing of the CD44 transmembrane domain may not fit the tripeptide-processing model (Figure 4).

7. Conclusion and Perspectives

The tripeptide hypothesis was confirmed in the processing of the APP transmembrane domain, which accounts for the production of Aβ species. Although the physiological significance of the multiple cleavage of the transmembrane domain is unknown, it is important to illustrate the cleavage mechanisms of other γ-secretase substrates, because the limitation of this stepwise mechanism would help to elucidate the substrate-specific inhibition of Aβ production. As shown in Figure 4, APLP-1 may be cleaved by tripeptide release; however, Notch and CD44 do not fit this processing model [40, 41]. γ-Secretase is widely believed to be a promiscuous protease; however, the cleavage mechanisms of APP and Notch, at least, seem to be different (Figure 4), which indicates that γ-secretase distinguishes substrates during proteolysis. Perhaps absence of helix breaker glycine residues in mid-portion of transmembrane domain allows multiple S4 cleavages even after single S3 cleavage in Notch. From this point of view, uncovering the mechanisms underlying γ-secretase-dependent cleavage offers a basis for new therapeutic approaches that are aimed at substrate-specific Aβ inhibition.

Abbreviations

Aβ:	Amyloid β protein
AICD:	APP intracellular domain
APP:	Amyloid precursor protein
βCTF:	Carboxyl terminal fragment of APP
DAPT:	N-[N-(3,5-difluorophenacetyl)-L-alanyl]-(*S*)-phenylglycine *t*-butylester
FAD:	Familial Alzheimer's disease
LC-MS/MS:	Liquid chromatography-tandem mass spectrometry
Nβ:	Notch β peptide
NICD:	Notch intracellular domain
PS:	Presenilin.

Acknowledgments

The authors thank Nobuto Kakuda for critical comments on this paper. Work in the authors' laboratories is supported in part by the Core Research for Evolutional Science and Technology of JST and by MEXT-Supported Program for the Strategic Research Foundation at Private Universities 2012–2016.

References

[1] C. Haass, E. H. Koo, A. Mellon, A. Y. Hung, and D. J. Selkoe, "Targeting of cell-surface β-amyloid precursor protein to lysosomes: alternative processing into amyloid-bearing fragments," *Nature*, vol. 357, no. 6378, pp. 500–503, 1992.

[2] M. Citron, D. B. Teplow, and D. J. Selkoe, "Generation of amyloid β protein from its precursor is sequence specific," *Neuron*, vol. 14, no. 3, pp. 661–670, 1995.

[3] R. Vassar, B. D. Bennett, S. Babu-Khan et al., "β-Secretase cleavage of Alzheimer's amyloid precursor protein by the transmembrane aspartic protease BACE," *Science*, vol. 286, no. 5440, pp. 735–741, 1999.

[4] I. Pinnix, U. Musunuru, H. Tun et al., "A novel γ-secretase assay based on detection of the putative C-terminal fragment-γ of amyloid β protein precursor," *Journal of Biological Chemistry*, vol. 276, no. 1, pp. 481–487, 2001.

[5] D. J. Selkoe, "Alzheimer's disease: genes, proteins, and therapy," *Physiological Reviews*, vol. 81, no. 2, pp. 741–766, 2001.

[6] B. De Strooper, P. Saftig, K. Craessaerts et al., "Deficiency of presenilin-1 inhibits the normal cleavage of amyloid precursor protein," *Nature*, vol. 391, no. 6665, pp. 387–390, 1998.

[7] B. De Strooper and G. König, "Alzheimer's disease. A firm base for drug development," *Nature*, vol. 402, no. 6761, pp. 471–472, 1999.

[8] M. S. Wolfe, W. Xia, B. L. Ostaszewski, T. S. Diehl, W. T. Kimberly, and D. J. Selkoe, "Two transmembrane aspartates in presenilin-1 required for presenilin endoproteolysis and γ-secretase activity," *Nature*, vol. 398, no. 6727, pp. 513–517, 1999.

[9] G. Struhl and I. Greenwald, "Presenilin is required for activity and nuclear access of notch in drosophila," *Nature*, vol. 398, no. 6727, pp. 522–525, 1999.

[10] G. Yu, M. Nishimura, S. Arawaka et al., "Nicastrin modulates presenilin-mediated notch/glp-1 signal transduction and βAPP processing," *Nature*, vol. 407, no. 6800, pp. 48–54, 2000.

[11] C. Goutte, "Genetics leads the way to the accomplices of presenilins," *Developmental Cell*, vol. 3, no. 1, pp. 6–7, 2002.

[12] R. Francis, G. McGrath, J. Zhang et al., "aph-1 and pen-2 are required for Notch pathway signaling, γ-secretase cleavage of βAPP, and presenilin protein accumulation," *Developmental Cell*, vol. 3, no. 1, pp. 85–97, 2002.

[13] D. Edbauer, E. Winkler, J. T. Regula, B. Pesold, H. Steiner, and C. Haass, "Reconstitution of γ-secretase activity," *Nature Cell Biology*, vol. 5, no. 5, pp. 486–488, 2003.

[14] W. T. Kimberly, M. J. LaVoie, B. L. Ostaszewski, W. Ye, M. S. Wolfe, and D. J. Selkoe, "γ-Secretase is a membrane protein complex comprised of presenilin, nicastrin, aph-1, and pen-2," *Proceedings of the National Academy of Sciences of the United States of America*, vol. 100, no. 11, pp. 6382–6387, 2003.

[15] N. Takasugi, T. Tomita, I. Hayashi et al., "The role of presenilin cofactors in the γ-secratase complex," *Nature*, vol. 422, no. 6930, pp. 438–441, 2003.

[16] A. J. Beel and C. R. Sanders, "Substrate specificity of γ-secretase and other intramembrane proteases," *Cellular and Molecular Life Sciences*, vol. 65, no. 9, pp. 1311–1334, 2008.

[17] M. S. Brown, J. Ye, R. B. Rawson, and J. L. Goldstein, "Regulated intramembrane proteolysis: a control mechanism conserved from bacteria to humans," *Cell*, vol. 100, no. 4, pp. 391–398, 2000.

[18] M. S. Wolfe and R. Kopan, "Intramembrane proteolysis: theme and variations," *Science*, vol. 305, no. 5687, pp. 1119–1123, 2004.

[19] A. Tolia, K. Horré, and B. De Strooper, "Transmembrane domain 9 of presenilin determines the dynamic conformation of the catalytic site of γ-secretase," *Journal of Biological Chemistry*, vol. 283, no. 28, pp. 19793–19803, 2008.

[20] S. Takagi, A. Tominaga, C. Sato, T. Tomita, and T. Iwatsubo, "Participation of transmembrane domain 1 of presenilin 1 in the catalytic pore structure of the γ-secretase," *Journal of Neuroscience*, vol. 30, no. 47, pp. 15943–15950, 2010.

[21] C. Sato, S. Takagi, T. Tomita, and T. Iwatsubo, "The C-terminal PAL motif and transmembrane domain 9 of presenilin 1 are involved in the formation of the catalytic pore of the γ-secretase," *Journal of Neuroscience*, vol. 28, no. 24, pp. 6264–6271, 2008.

[22] K. Takeo, N. Watanabe, T. Tomita, and T. Iwatsubo, "Contribution of the γ-secretase subunits to the formation of catalytic pore of presenilin 1 protein," *Journal of Biological Chemistry*, vol. 287, no. 31, pp. 25834–25843, 2012.

[23] P. Osenkowski, H. Li, W. Ye et al., "Cryoelectron microscopy structure of purified γ-secretase at 12 Å resolution," *Journal of Molecular Biology*, vol. 385, no. 2, pp. 642–652, 2009.

[24] M. Citron, T. Oltersdorf, C. Haass et al., "Mutation of the β-amyloid precursor protein in familial Alzheimer's disease increases β-protein production," *Nature*, vol. 360, no. 6405, pp. 672–674, 1992.

[25] J. T. Jarrett, E. P. Berger, and P. T. Lansbury, "The carboxy terminus of the β amyloid protein is critical for the seeding of amyloid formation: implications for the pathogenesis of Alzheimer's disease," *Biochemistry*, vol. 32, no. 18, pp. 4693–4697, 1993.

[26] R. Wang, D. Sweeney, S. E. Gandy, and S. S. Sisodia, "The profile of soluble amyloid β protein in cultured cell media. Detection and quantification of amyloid β protein and variants by immunoprecipitation-mass spectrometry," *Journal of Biological Chemistry*, vol. 271, no. 50, pp. 31894–31902, 1996.

[27] M. Citron, D. Westaway, W. Xia et al., "Mutant presenilins of Alzheimer's disease increase production of 42-residue amyloid β-protein in both transfected cells and transgenic mice," *Nature Medicine*, vol. 3, no. 1, pp. 67–72, 1997.

[28] N. J. Clarke, A. J. Tomlinson, Y. Ohyagi, S. Younkin, and S. Naylor, "Detection and quantitation of cellularly derived amyloid β peptides by immunoprecipitation-HPLC-MS," *FEBS Letters*, vol. 430, no. 3, pp. 419–423, 1998.

[29] D. Beher, J. D. J. Wrigley, A. P. Owens, and M. S. Shearman, "Generation of C-terminally truncated amyloid-β peptides is dependent on γ-secretase activity," *Journal of Neurochemistry*, vol. 82, no. 3, pp. 563–575, 2002.

[30] Y. Gu, H. Misonou, T. Sato, N. Dohmae, K. Takio, and Y. Ihara, "Distinct intramembrane cleavage of the beta-amyloid precursor protein family resembling gamma-secretase-like cleavage of Notch," *Journal of Biological Chemistry*, vol. 276, no. 38, pp. 35235–35238, 2001.

[31] M. Sastre, H. Steiner, K. Fuchs et al., "Presenilin-dependent γ-secretase processing of β-amyloid precursor protein at a site corresponding to the S3 cleavage of Notch," *EMBO Reports*, vol. 2, no. 9, pp. 835–841, 2001.

[32] A. Weidemann, S. Eggert, F. B. M. Reinhard et al., "A novel ε-cleavage within the transmembrane domain of the Alzheimer amyloid precursor protein demonstrates homology with notch processing," *Biochemistry*, vol. 41, no. 8, pp. 2825–2835, 2002.

[33] I. Okamoto, Y. Kawano, D. Murakami et al., "Proteolytic release of CD44 intracellular domain and its role in the CD44 signaling pathway," *Journal of Cell Biology*, vol. 155, no. 5, pp. 755–762, 2001.

[34] H. J. Lee, K. M. Jung, Y. Z. Huang et al., "Presenilin-dependent γ-secretase-like intramembrane cleavage of ErbB4," *Journal of Biological Chemistry*, vol. 277, no. 8, pp. 6318–6323, 2002.

[35] P. Marambaud, J. Shioi, G. Serban et al., "A presenilin-1/γ-secretase cleavage releases the E-cadherin intracellular domain and regulates disassembly of adherens junctions," *EMBO Journal*, vol. 21, no. 8, pp. 1948–1956, 2002.

[36] P. May, Y. Krishna Reddy, and J. Herz, "Proteolytic processing of low density lipoprotein receptor-related protein mediates regulated release of its intracellular domain," *Journal of Biological Chemistry*, vol. 277, no. 21, pp. 18736–18743, 2002.

[37] T. Ikeuchi and S. S. Sisodia, "The Notch ligands, Delta1 and Jagged2, are substrates for presenilin-dependent "γ-secretase" cleavage," *Journal of Biological Chemistry*, vol. 278, no. 10, pp. 7751–7754, 2003.

[38] M. Takami, Y. Nagashima, Y. Sano et al., "γ-Secretase: successive tripeptide and tetrapeptide release from the transmembrane domain of β-carboxyl terminal fragment," *Journal of Neuroscience*, vol. 29, no. 41, pp. 13042–13052, 2009.

[39] K. Yanagida, M. Okochi, S. Tagami et al., "The 28-amino acid form of an APLPl-derived Aβ-like peptide is a surrogate marker for Aβ42 production in the central nervous system," *EMBO Molecular Medicine*, vol. 1, no. 4, pp. 223–235, 2009.

[40] J. Wanngren, J. Ottervald, S. Parpal et al., "Second generation γ-secretase modulators exhibit different modulation of notch β and Aβ production," *Journal of Biological Chemistry*, vol. 287, no. 39, pp. 32640–32650, 2012.

[41] S. Lammich, M. Okochi, M. Takeda et al., "Presenilin-dependent intramembrane proteolysis of CD44 leads to the liberation of its intracellular domain and the secretion of an

Aβ-like peptide," *Journal of Biological Chemistry*, vol. 277, no. 47, pp. 44754–44759, 2002.

[42] T. Sato, N. Dohmae, Y. Qi et al., "Potential link between amyloid beta-protein 42 and C-terminal fragment gamma 49-99 of beta-amyloid precursor protein," *Journal of Biological Chemistry*, vol. 278, no. 27, pp. 24294–20301, 2003.

[43] S. Funamoto, M. Morishima-Kawashima, Y. Tanimura, N. Hirotani, T. C. Saido, and Y. Ihara, "Truncated carboxyl-terminal fragments of β-amyloid precursor protein are processed to amyloid β-proteins 40 and 42," *Biochemistry*, vol. 43, no. 42, pp. 13532–13540, 2004.

[44] Y. Qi-Takahara, M. Morishima-Kawashima, Y. Tanimura et al., "Longer forms of amyloid β protein: implications for the mechanism of intramembrane cleavage by γ-secretase," *Journal of Neuroscience*, vol. 25, no. 2, pp. 436–445, 2005.

[45] L. Chévez-Gutiérrez, L. Bammens, I. Benilova et al., "The mechanism of γ-Secretase dysfunction in familial Alzheimer disease," *EMBO Journal*, vol. 31, no. 10, pp. 2261–2274, 2012.

[46] O. Quintero-Monzon, M. M. Martin, M. A. Fernandez, C. A. Cappello, P. Osenkowski, and M. S. Wolfe, "Dissociation between the processivity and total activity of γ-secretase: implications for the mechanism of Alzheimer's disease-causing presenilin mutations," *Biochemistry*, vol. 50, no. 42, pp. 9023–9035, 2011.

[47] H. F. Dovey, V. John, J. P. Anderson et al., "Functional gamma-secretase inhibitors reduce beta-amyloid peptide levels in brain," *Journal of Neurochemistry*, vol. 76, no. 1, pp. 173–181, 2001.

[48] G. Zhao, G. Mao, J. Tan et al., "Identification of a new presenilin-dependent ζ-cleavage site within the transmembrane domain of amyloid precursor protein," *Journal of Biological Chemistry*, vol. 279, no. 49, pp. 50647–50650, 2004.

[49] G. Zhao, M. Z. Cui, G. Mao et al., "γ-cleavage is dependent on ζ-cleavage during the proteolytic processing of amyloid precursor protein within its transmembrane domain," *Journal of Biological Chemistry*, vol. 280, no. 45, pp. 37689–37697, 2005.

[50] T. Sato, Y. Tanimura, N. Hirotani, T. C. Saido, M. Morishima-Kawashima, and Y. Ihara, "Blocking the cleavage at mid-portion between γ- and ε-sites remarkably suppresses the generation of amyloid β-protein," *FEBS Letters*, vol. 579, no. 13, pp. 2907–2912, 2005.

[51] K. S. Vetrivel, H. Cheng, W. Lin et al., "Association of γ-secretase with lipid rafts in post-golgi and endosome membranes," *Journal of Biological Chemistry*, vol. 279, no. 43, pp. 44945–44954, 2004.

[52] S. Yagishita, M. Morishima-Kawashima, S. Ishiura, and Y. Ihara, "Aβ46 is processed to Aβ40 and Aβ43, but not to Aβ42, in the low density membrane domains," *Journal of Biological Chemistry*, vol. 283, no. 2, pp. 733–738, 2008.

[53] S. Yagishita, M. Morishima-Kawashima, Y. Tanimura, S. Ishiura, and Y. Ihara, "DAPT-induced intracellular accumulations of longer amyloid β-proteins: further implications for the mechanism of intramembrane cleavage by γ-secretase," *Biochemistry*, vol. 45, no. 12, pp. 3952–3960, 2006.

[54] A. Fukumori, R. Fluhrer, H. Steiner, and C. Haass, "Three-amino acid spacing of presenilin endoproteolysis suggests a general stepwise cleavage of γ-secretase-mediated intramembrane proteolysis," *Journal of Neuroscience*, vol. 30, no. 23, pp. 7853–7862, 2010.

[55] S. Osawa, S. Funamoto, M. Nobuhara et al., "Phosphoinositides suppress γ-secretase in both the detergent-soluble and -insoluble states," *Journal of Biological Chemistry*, vol. 283, no. 28, pp. 19283–19292, 2008.

[56] M. Okochi, H. Steiner, A. Fukumori et al., "Presenilins mediate a dual intramembranous γ-secretase cleavage of Notch-1," *EMBO Journal*, vol. 21, no. 20, pp. 5408–5416, 2002.

[57] M. Okochi, A. Fukumori, J. Jiang et al., "Secretion of the Notch-1 Aβ-like peptide during Notch signaling," *Journal of Biological Chemistry*, vol. 281, no. 12, pp. 7890–7898, 2006.

Hindawi Publishing Corporation
International Journal of Alzheimer's Disease
Volume 2012, Article ID 210756, 10 pages
doi:10.1155/2012/210756

Research Article

Modulation of Gamma-Secretase for the Treatment of Alzheimer's Disease

Barbara Tate, Timothy D. McKee, Robyn M. B. Loureiro, Jo Ann Dumin, Weiming Xia, Kevin Pojasek, Wesley F. Austin, Nathan O. Fuller, Jed L. Hubbs, Ruichao Shen, Jeff Jonker, Jeff Ives, and Brian S. Bronk

Satori Pharmaceuticals, Inc., 281 Albany Street, Cambridge, MA 02139, USA

Correspondence should be addressed to Barbara Tate, barbara.tate@satoripharma.com

Received 13 August 2012; Accepted 8 November 2012

Academic Editor: Jeremy Toyn

The Amyloid Hypothesis states that the cascade of events associated with Alzheimer's disease (AD)—formation of amyloid plaques, neurofibrillary tangles, synaptic loss, neurodegeneration, and cognitive decline—are triggered by Aβ peptide dysregulation (Kakuda et al., 2006, Sato et al., 2003, Qi-Takahara et al., 2005). Since γ-secretase is critical for Aβ production, many in the biopharmaceutical community focused on γ-secretase as a target for therapeutic approaches for Alzheimer's disease. However, pharmacological approaches to control γ-secretase activity are challenging because the enzyme has multiple, physiologically critical protein substrates. To lower amyloidogenic Aβ peptides without affecting other γ-secretase substrates, the epsilon (ε) cleavage that is essential for the activity of many substrates must be preserved. Small molecule modulators of γ-secretase activity have been discovered that spare the ε cleavage of APP and other substrates while decreasing the production of Aβ_{42}. Multiple chemical classes of γ-secretase modulators have been identified which differ in the pattern of Aβ peptides produced. Ideally, modulators will allow the ε cleavage of all substrates while shifting APP cleavage from Aβ_{42} and other highly amyloidogenic Aβ peptides to shorter and less neurotoxic forms of the peptides without altering the total Aβ pool. Here, we compare chemically distinct modulators for effects on APP processing and *in vivo* activity.

1. Introduction

Gamma-secretase (γ-secretase) is required for the production of amyloid beta peptides (Aβ) and decreasing Aβ production as a disease modifying approach for the treatment of Alzheimer's disease (AD) has received intense interest. The initial focus was on the discovery of compounds that would decrease γ-secretase activity. γ-Secretase cleaves the membrane bound C-terminal domain (C99) of APP at the ε site to produce the intracellular domain, AICD. The enzyme then makes sequential cuts of the remaining intramembrane APP fragment at each turn of the alpha helix (every 3-4 amino acids) until Aβ peptides are formed and released into the extracellular space [1–3]. This protein processivity produces Aβ peptides that vary in size, from 43–34 amino acids in length [4, 5]. In Alzheimer's disease, a greater number of the longer forms of Aβ, including Aβ_{42} and Aβ_{43}, or a high ratio of the long peptides to the shorter forms, appear to occur [6]. These longer Aβ peptides readily oligomerize, forming toxic species, as well as becoming the seeds for amyloid plaques [7, 8].

The full inhibition of γ-secretase appeared to be a sound approach. However, it was found that γ-secretase plays a broader biological role and cleaves multiple proteins to yield physiologically essential products. Thus, total inhibition results in severe adverse effects *in vivo* [9–11]. This played out in the clinic in the trial of the γ-secretase inhibitor, semagacestat from Eli Lilly [12–14]. Patients treated with this drug developed skin and gastrointestinal side effects that are characteristic of the inhibition of γ-secretase processing of Notch, leading to the discontinuation of the clinical trial in 2010 [13, 14].

The discovery of compounds that could decrease the production of the more amyloidogenic Aβ_{42} peptide while preserving total Aβ levels and γ-secretase cleavage of other substrates led to a clinical trial of one of these newly

identified, first generation gamma-secretase modulators (GSMs) [15]. The NSAID-derived, Flurizan from Myriad Genetics was tested in a Phase 3 trial in mild to moderate AD patients. However, Flurizan is a very weak modulator of γ-secretase, with an IC_{50} of ~250 μM [16]. In addition, this compound has very poor distribution into the central nervous system [16, 17]. Not surprisingly, the combination of these less than desirable properties resulted in no exposure in the brain, and a failed Phase III trial in June 2008 [18].

Second and now third generation GSMs have been discovered and are proceeding toward clinical trials in AD. These GSMs are significantly more potent than Flurizan and appear to have better drug-like properties. However, the majority of these compounds fall into one of two chemical classes, with little structural diversity within each of these classes and the development of some has been discontinued because of toxicities and biopharmaceutical limitations that other class members may also share [19]. A structurally unique GSM derived from a core molecule isolated from a natural product is also moving through preclinical testing [20]. While all three chemical series of GSMs share some common pharmacological properties, they differ in other fundamental ways. Here we present data contrasting the pharmacology of members of several structural series of GSMs and how modulation may avoid the pitfalls associated with γ-secretase inhibitors (GSIs).

2. Materials and Methods

2.1. Test Compounds. LY411575, GSI-953, BMS-708163, MK-GSM1, JNJ-40418677, and E-2012 were prepared according to published methods. SPI-1802 and SPI-1810 were prepared at Satori Pharmaceuticals.

2.2. Cell Culture and Compound Treatment. SUP-T1 cells (ATCC) were cultured in T75 flasks in RPMI media (Mediatech 10-041-CV) supplemented with 10% FBS and penicillin/streptomycin at 37°C in a 5% CO_2 atmosphere. One hour prior to drug treatment, six well plates were seeded with 1.5 mL of media containing 2% FBS and cells at a density of 1.5×10^6 cells/mL. Test compounds in DMSO were diluted 100-fold directly into the media with the cells and incubated for 18 hours at 37°C. After treatment 100 μL aliquots of treated cells were assayed for viability with the Promega Cell Titer Glo assay system. The conditioned media and cells were further processed to measure Aβ levels and NICD levels, respectively.

CHO-2B7 cells (Mayo Clinic) are Chinese hamster ovary cells stably transfected with human βAPP 695 wt [38, 39]. The cells were cultured in Ham's F12 media (Thermo Fisher SH30026.01) supplemented with 10% FBS, 0.25 mg/mL Zeocin and penicillin/streptomycin at 37°C in a 5% CO_2 atmosphere. For compound treatment, cells were plated in 96-well plates at a density of 1.0×10^5 cells/mL and allowed to grow to 100% confluence over two days. Test compounds in DMSO were diluted 100-fold directly into the media before adding to the cells. Immediately prior to adding compound-containing media to the cells, they were washed once with 1XPBS. Conditioned media from CHO-2B7 cells were collected after 5 hours of treatment and the levels of Aβ peptides were assessed as described below.

H4 human neuroglioma cells (ATCC) were cultured in 10% FBS/DMEM (Media Tech) with Pen/Strep (50 units/50 μg/mL; Invitrogen). Human WT APP stably transfected CHO cells were cultured in 10% FBS/HAM'S F-12 growth media (Media Tech) supplemented with Pen/Strep and G418 (500 μg/mL; Promega). Cells were plated and grown to confluency in 96-well plates prior to dosing. Cells were washed with PBS and 100 μL of media containing DMSO alone (vehicle) or test compounds in DMSO at a final DMSO concentration of 1% (v/v). Conditioned media was collected after 18 hours of treatment and diluted 1 : 1 with MSD blocking buffer (1% BSA in MSD wash buffer).

2.3. Solid Phase Extraction. Wells of 30 mg Oasis HLB 96-well extraction plates (Waters Corporation) were activated by addition of 1 mL of methanol followed by rinsing with 1 mL of water utilizing a vacuum plate manifold. 1 mL of SUP-T1 conditioned media was added and wells were then washed sequentially with 2 mL of 10% methanol and then with 2 mL of 30% methanol. Samples were eluted into sample collection tubes by adding 250 μL of 90% methanol with 2% ammonium hydroxide to each well. Eluted samples were concentrated to dryness under vacuum without heating.

2.4. Aβ In Vitro Assay Measurement. Conditioned media was collected after 5–18 hours of treatment and diluted with 1 volume of MSD blocking buffer (1% BSA in MSD wash buffer). Alternatively, dried films of SUP-T1 conditioned media after solid phase extraction were resuspended with 1 volume of MSD blocking buffer (1% BSA in MSD wash buffer). Samples were transferred to blocked MSD Human (6E10) Aβ 3-Plex plates and incubated for 2 hours at room temperature with orbital shaking followed by washing and reading according to the manufacturer's instructions (SECTOR Imager 2400 Meso Scale Discovery, Gaithersburg MD).

2.5. NICD Assay. The remaining cells were washed twice in PBS and then lysed with Promega reporter lysis buffer containing a complete protease inhibitor cocktail (Roche) for 1 hour at 4°C. Lysates were spun at 5,000 RPM for 5 minutes and supernatants were collected. Total protein levels were measured and adjusted to 1-2 mg/mL total protein using the BCA total protein assay (Thermo Scientific). NICD levels were then measured with a cleavage specific Notch1 sandwich ELISA (Cell Signaling Technologies) according to the manufacturer's instructions.

2.6. Immunoprecipitation and Matrix-Assisted Laser Desorption/Ionization Time-of-Flight (MALDI-TOF) Mass Spectrometry. Chinese Hamster Ovary cells stably transfected with wild-type human APP were treated for 6 hrs with γ-secretase modulators at an approximate concentration of 10-fold the IC_{50} (Merck GSM1 at 1 μM, JNJ-40418677 at 2 μM, SPI-1802 at 3 μM, and SPI-1810 at 2 μM.) Monoclonal Aβ antibodies 6E10 (specific for amino acids 1–16 of Aβ) and 4G8 (specific for amino acids 17–24 of Aβ; Covance, Dedham, MA) were immobilized with agarose resin using the

AminoLink Plus reagents (Thermo Scientific, Rockport, IL). Conditioned media from treated cells was precleared with agarose resin overnight, and the supernatant was incubated with agarose-conjugated 6E10/4G8 for 6 hrs. Immunoprecipitates were washed extensively prior to analysis.

Analyses were performed on a Shimadzu Biotech Axima TOF2 (Shimadzu Instruments) matrix-assisted-laser desorption/ionization time-of-flight (MALDI-TOF) mass spectrometer. Peptides were analyzed in positive ion linear mode. For intact peptide mass measurement the instrument was set with a mass range extending up to 6000 m/z using a pulsed extraction setting of 3500. An average mass external standard was used which consisted of angiotensin II (1047.2), P14R (1534.86) and ACTH clip 18–39 (2465.20), insulin B (3496.67), and insulin (5734.51). For sample preparation, 5 μL aliquots of Aβ containing immunoprecipitates were diluted with 10 μL of 0.1% TFA and then desalted using a C18 Zip Tip (Millipore, Corp.). Samples were directly deposited from the Zip Tip onto the MALDI sample target and then mixed with 0.5 μL of matrix solution which consisted of 5 mg/mL of alpha cyano-4-hydroxy cinnamic acid in acetonitrile: 0.1% TFA (50 : 50). Data was acquired manually using a set laser power and averaging 1500–2000 laser shots.

2.7. In Vivo Study Methods. All animal handling and procedures were conducted in full compliance to AAALAC International and NIH regulations and guidelines regarding animal care and welfare.

Either transgenic mice (Tg2576, 3 mos; $N = 21$) or wild-type Sprague Dawley rats (200–225 g; $N = 8$) were utilized to assess *in vivo* efficacy. All animals were acclimated to the test facility for a minimum of two days prior to initiation of the study. Compounds were dosed orally in 10 : 20 : 70 Ethanol/Solutol/Water via oral gavage. Samples were harvested at 6 hrs after dose for Aβ and compound exposure levels. Blood samples were collected into K2EDTA and stored on wet ice until processed to plasma by centrifugation (3500 rpm at 5°C) within 30 minutes of collection. Each brain was dissected into three parts: left and right hemispheres and cerebellum. Brain tissues were rinsed with ice cold phosphate buffered saline (without Mg^{2+} or Ca^{2+}), blotted dry and weighed. Plasma and cerebella were analyzed for parent drug via LC/MS/MS. Parent drug levels were compared to a standard curve to establish the unknown levels.

2.8. Rodent Aβ Determination. This protocol is a modification of protocols described by Lanz et al. [40] and Rogers et al. [41]. Frozen hemispheres were weighed into tared homogenization tubes (MP Biomedicals#6933050 for rat; MP Biomedicals, Solon, OH) and (Simport#T501-4AT; Simport, Beloeil, Qc, Canada) containing one 5 mm stainless steel bead (Qiagen#69989) for mouse). For every gram of brain, 10 mLs of 6 M guanidine hydrochloride (wild-type rat) or 0.2% diethyl amine in 50 mM NaCl (transgenic mouse) was added to the brain-containing tubes on wet ice. Rat hemispheres were homogenized for one minute and mouse hemispheres were homogenized for 30 seconds at the 6.5 setting using the FastPrep-24 Tissue and Cell homogenizer (MP Biomedicals#116004500). Homogenates were rocked for two hours at 4°C, then precleared by ultracentrifugation at 100,000 ×g for one hour at 4°C. Precleared wild-type rat homogenates were concentrated over solid phase extraction (SPE) columns (Oasis HLB 96-well SPE plate 30 um, Waters#WAT058951; Waters Corp., Milford, MA). Briefly, SPE columns were prepared by wetting with 1 mL of 100% methanol followed by dH_2O using vacuum to pull liquids through. Brain homogenates were then added to the prepared columns (1.0 mL from rat). Columns were washed twice with 10% methanol followed by two washes with 30% methanol. Labeled eluent collection tubes (Costar cluster tubes #4413; Corning Inc., Corning, NY) were placed under SPE columns and samples were eluted under very mild vacuum with 300 μL of 2% NH_4OH/90% methanol. Eluents were dried to films under vacuum with no heat in a speed vacuum microcentrifuge. Films were resuspended in 150 μL of Meso Scale Discovery (MSD, Gaithersburg MD) blocking buffer (1% BSA in MSD wash buffer) for one hour at room temperature with occasional vortexing. A volume of 45 μL of precleared transgenic mouse brain homogenates were diluted into 450 μL of blocking buffer and were neutralized with 5 μL of 0.5 M Tris pH 6.8. For Aβ38, 40, and 42 measurements, MSD 96 well multispot Human/Rodent (4G8) Aβ triplex ultrasensitive ELISA plates were blocked with MSD blocking buffer for 1 hour at room temperature with orbital shaking. A volume of 25 μL of neat resuspended wild-type rat brain homogenate films or diluted transgenic mouse brain homogenates were added in duplicates to the blocked 3-plex Aβ MSD plates with SULFO-TAG 4G8 antibody (MSD). The Aβ 3-Plex plates were incubated for 2 hours at room temperature with orbital shaking followed by washing and reading according to the manufacturer's instructions (SECTOR Imager 2400, MSD). The average Aβ concentrations from duplicate measurements of each animal were converted to percent vehicle values and the treatment group averages were statistically compared by ANOVA analysis.

3. Results and Discussion

γ-Secretase is a complex enzyme with multiple substrates and multiple cleavage sites on at least some of these substrates, including APP. Complete inhibition of γ-secretase activity by targeting the ε cleavage site prevents the processing of multiple physiologically relevant proteins, leading to the severe side effects reported in AD patients [12, 13]. On the other hand, chemically modulating the enzyme with a GSM is a more precise mechanism to enhance certain cleavage events while preventing the cut that yields the amyloidogenic peptide, Aβ_{42} which is linked to the pathophysiological initiation of AD (Figure 6). In preclinical toxicological testing, GSMs appear to be free of the mechanism-based toxicities attributed to the inhibition of Notch processing that have plagued the enzyme inhibitors. *In vitro* data demonstrate that Notch cleavage to NICD is not inhibited by any of several represented GSMs at concentrations that do not disrupt cell viability (Figure 1). Treatment with GSMs in rodents have not shown the classical Notch-related toxicities that are associated with GSIs, suggesting that the complete processing of Notch to NICD can occur in the presence of GSMs.

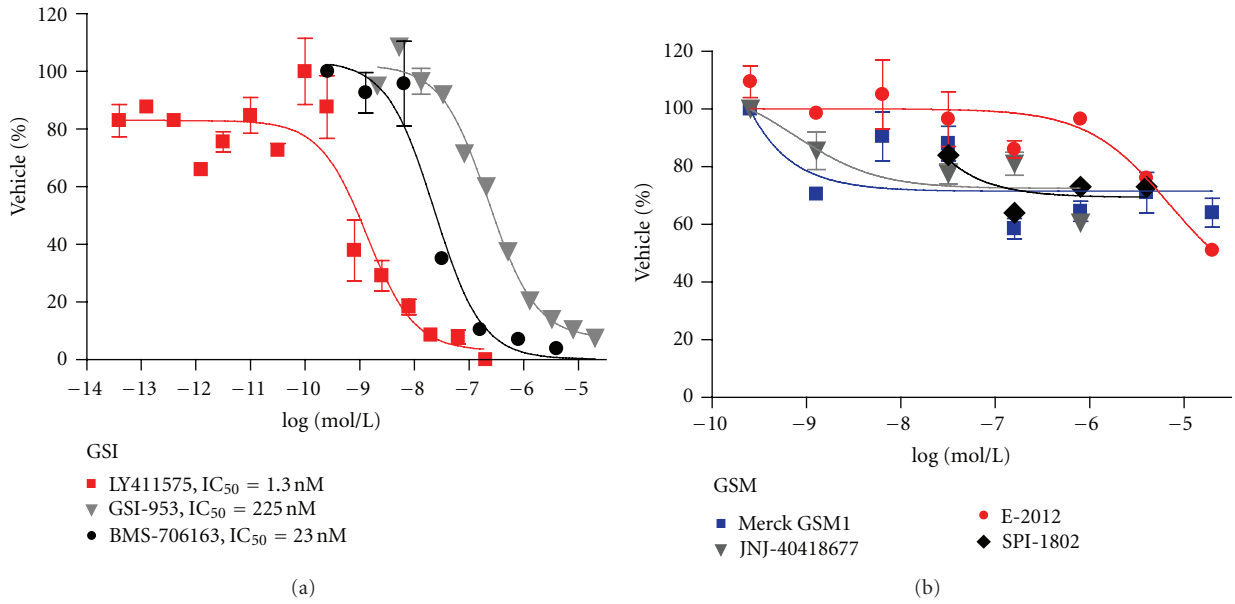

Figure 1: Multiple GSI and GSMs were examined in for their ability to inhibit NOTCH cleavage using the SUP-T1 cellular assay.

3.1. GSMs Do Not Show a Potency Shift with Changes in Substrate Concentration. γ-Secretase inhibitors can show a significant shift in potency in APP transfected cell-based assays depending on the level of expression of APP. Table 1 compares the IC_{50} for $A\beta_{42}$ lowering of different GSIs in multiple cell lines with varying levels of APP expression. In the highest expressing cell lines, the GSIs assayed here appear more potent (lower IC_{50}s in the high expressing, transfected CHO-2B7 cell line) than when the same compounds are tested in assays using lower expressing cell lines (native H4 cell line). This potency shift seen with GSIs has been attributed to a shift in the enzyme/substrate ratio [42], where there is a higher ratio in wild-type cells versus those that overexpress APP. This higher ratio in turn requires more compounds to inhibit the enzymatic reaction. Interestingly, the potency shift due to substrate concentration that occurs with GSIs does not occur with GSMs. As seen in Table 1, the IC_{50} for all the GSMs shown are consistent across cell lines, regardless of the APP expression levels. While this potency shift is not well understood, these data do suggest that GSIs and GSMs affect the enzyme in fundamentally different ways.

3.2. Structural Diversity of GSMs. Many of the second generation GSMs were inspired by the NSAIDs (Figure 2). For instance, all compounds shown in the figure were initially derived from the aryl acetic acid motif found in **1** and similar NSAIDs [21]. The similarity between these compounds makes for a crowded patent landscape, with some compounds potentially covered in multiple patent applications from different sponsors. In addition, for this structural series, the physicochemical properties indicate that all of these compounds carry an increased safety risk due to the high logP, low PSA [43–45], and high degree of aromaticity [46, 47]. Compounds **7–9** are designed to improve upon these properties, but are still considered high risk due to these same physicochemical based *in silico* models [27–29]. *In vivo* preclinical toxicity testing will ultimately be needed to assess the safety profile of these similar structures. However, the lack of progression of compounds from this class into and through clinical development suggests that this scaffold may have challenges that will continue to slow or prevent successful conduct of the studies required for registration.

A second class of GSMs that has received significant attention is summarized in Figure 3. Following initial disclosure of **10** and **11**, a number of pharmaceutical companies pursued structurally related chemical series [30, 48]. Although this class offers clear distinction from the NSAID-inspired compounds above, their physicochemical properties also reside outside of the molecular space most frequently affiliated with marketed agents for oral therapy. For example, the number of aromatic rings and clogP of the representatives shown are higher than the average for oral compounds on the market [46, 47], leading to a higher probability of safety and biopharmaceutical challenges with this class. Although some groups have been successful in developing promising structural alternatives, as exemplified by **16–18**, little has been reported on the development of any representatives from this general scaffold [34–36].

A novel and structurally distinct chemical architecture of a third class of GSMs has been reported by Satori Pharmaceuticals. This scaffold was first isolated from black cohosh, leading to the characterization of initial hit **19** (Figure 4) [20]. A combination of synthetic and medicinal chemistry optimization led to **20**, which is reported to have better drug properties than **19** [20]. To date, the compounds reported by Satori also fall outside of the guidelines most typically associated with good *in vivo* disposition. The group notes, however, that the majority of marketed agents derived from natural products also violate these same guidelines, a trend that has led some to conclude that molecules derived via

Table 1: GSMs do not show a potency shift with APP overexpression.

Cell line	H4	H4-APP	CHO-SW	CHO-7W	CHO-2B7
Aβ_{42} Levels (pg/mL)	20	110	131	834	200
Inhibitors			Aβ_{42} IC_{50} (nM) per cell line		
LY411575	1.40	1.20	0.20	ND	0.05
GSI-953	706	52	5.20	8.70	2.50
BMS-708163	40	8	0.98	1.10	0.20
Modulators			Aβ_{42} IC_{50} (nM) per cell line		
GSM1	54	64	154	73	62
JNJ-40418677	115	133	190	122	172
E-2012	42	84	54	36	33

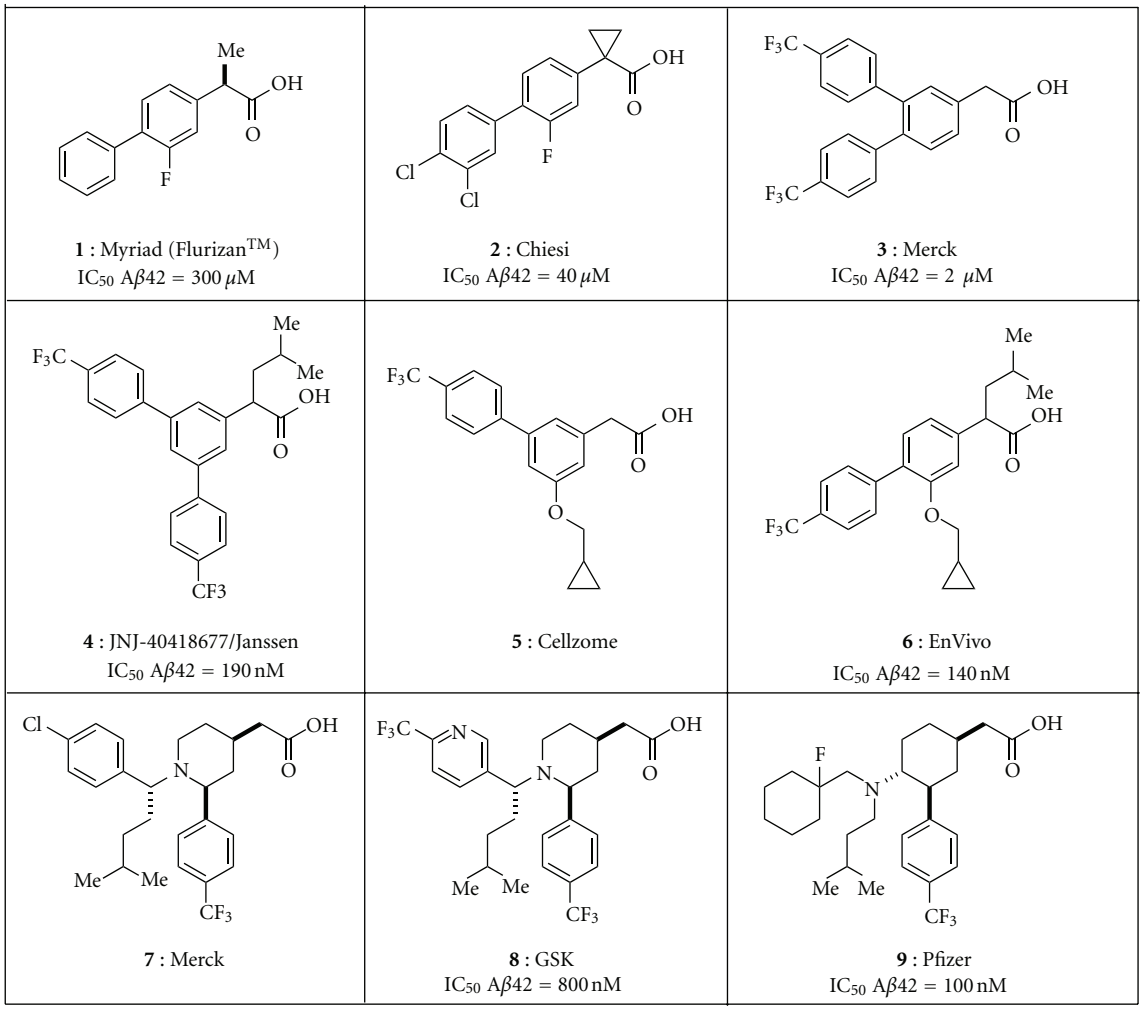

Figure 2: Representative NSAID-inspired GSMs. Compounds **1–6** are aryl acetic acids [21–26], compounds **7** and **8** are piperidine acetic acids [27, 28] and compound **9** is a cyclohexane acetic acid [29].

semisynthesis on natural product scaffolds define a different set of guidelines. Compounds from this class are now proceeding through preclinical development.

3.3. Aβ Peptide Profiling of Structurally Diverse GSMs. When the NSAID-type of GSMs was first described (Figure 2), the changes in Aβ peptides that were seen, a decrease in Aβ_{42}, an increase in Aβ_{38} and little or no change on Aβ_{40} or total Aβ were labeled the "modulator profile," nomenclature that was reinforced by the pharmacology reported for the GSMs represented by the structures in Figure 3. However, since that time, additional Aβ peptide profiles have been reported for the chemically distinct scaffold disclosed by Satori Pharmaceuticals, as well as molecules more closely

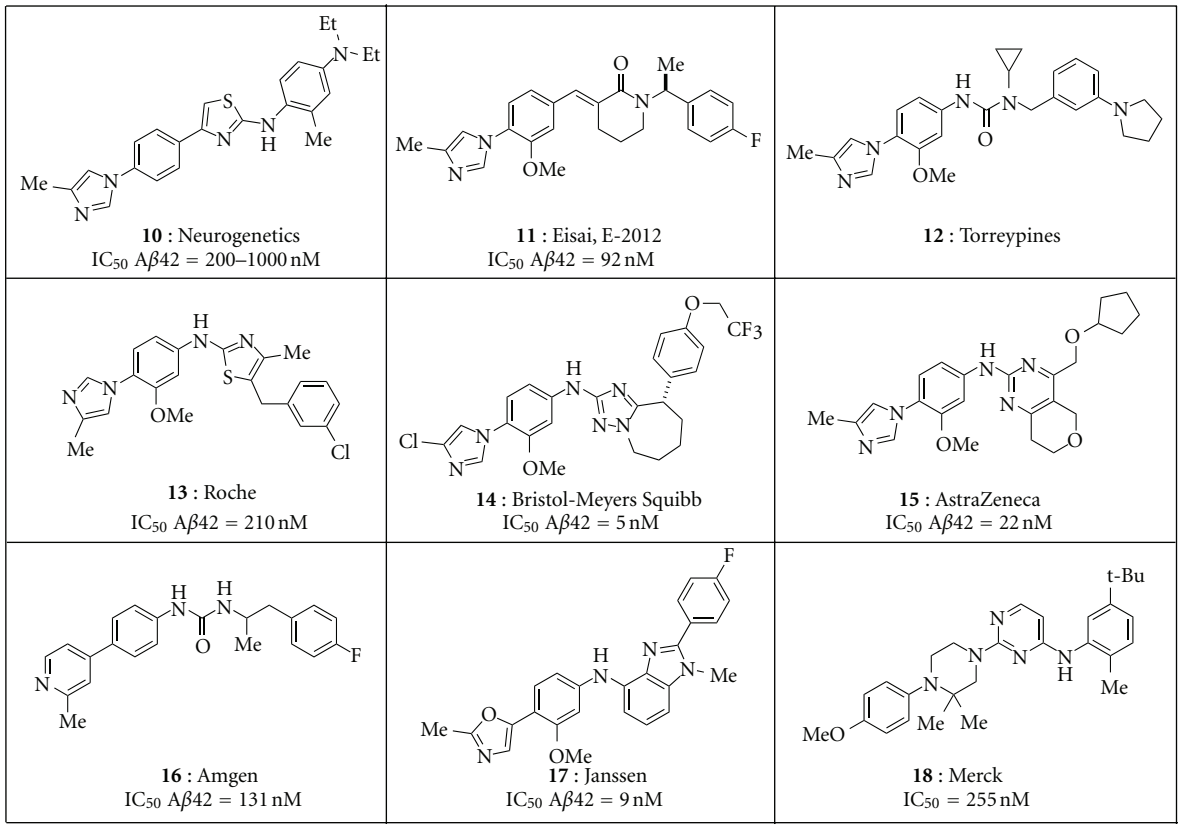

Figure 3: Representative aryl imidazole inspired GSMs [30–33]. Compounds **16–18** are the most unique because the aryl imidazole has been replaced by a bioisostere [34–36].

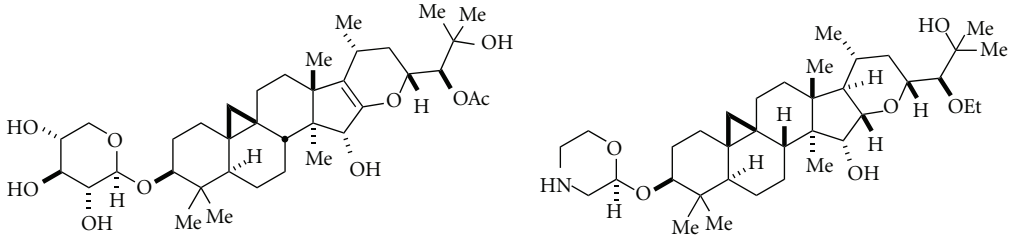

Figure 4: Two examples of Satori GSMs.

related to those in Figure 3. Examples of the variety of Aβ peptide profiles produced by GSMs are shown in Figure 6. Merck GSM1 and JNJ-40418677 lower Aβ_{42} while increasing Aβ_{38}, with little or no effect on Aβ_{40}. Alternatively, the Satori Pharmaceutical compounds, SPI-1802 and SPI-1810 (structures shown in Figure 5) decrease both Aβ_{42} and Aβ_{38}, but maintain total Aβ levels by increasing Aβ_{37} and Aβ_{39}. Yet, all of these compounds can be classified as "gamma secretase modulators" based on the commonality of sparing the ε cleavage of C99 and other substrates (e.g., Notch), decreasing Aβ_{42}, and not affecting total Aβ levels.

Based on these data, modulation of γ-secretase is more accurately defined as a shift of the Aβ pool to shorter, but variable length, Aβ peptides. A physiological role for Aβ peptides has not been discovered, but *in vitro* studies have demonstrated that shorter peptides are incapable of aggregation and oligomerization [19] and may even prevent the oligomerization of Aβ_{42} by binding to it, suggesting that preserving the total pool of Aβ may be beneficial.

The molecular mechanism by which GSMs modulate γ-secretase activity is not completely understood. The variety of Aβ peptide profiles that result from treatment of cells

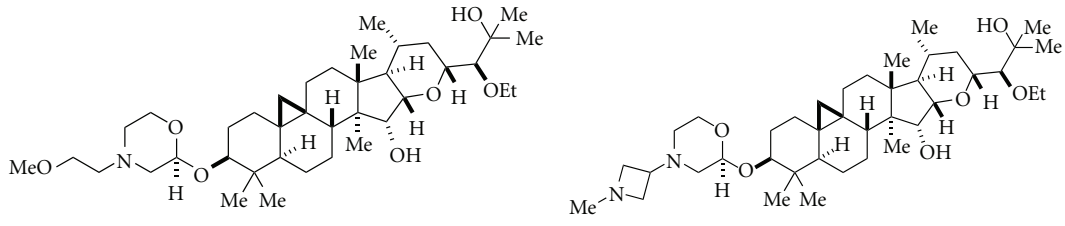

(a) (b)

Figure 5: Structures of SPI-1802 and SPI-1810 [20, 37].

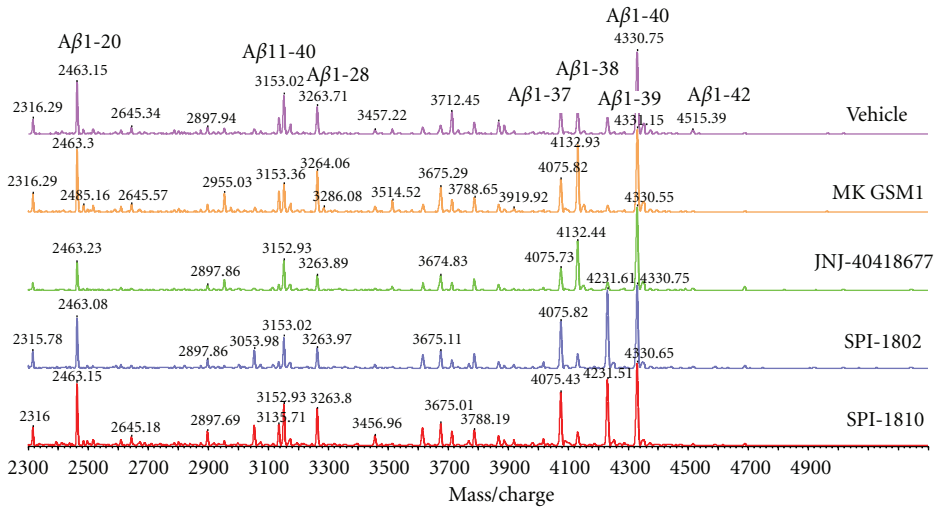

Figure 6: MALDI-TOF analysis of Aβ peptides from conditioned media of APP-overexpressing CHO cells treated with GSMs. The immunoprecipitated Aβ peptides were subjected to MALDI-TOF analysis to visualize individual Aβ fragments. Using a combination of two Aβ antibodies, 6E10, and 4G8 allows precipitation of full length and N- and C-terminal truncated Aβ peptides.

with different γ-secretase modulators suggests that the enzyme has numerous allosteric modulatory sites. These are not necessarily completely unique sites and published data suggests the sites may be overlapping [49]. The modulator binding sites thus far identified all seem to reside on the presenilin component of γ-secretase [50].

3.4. In Vivo Activity of GSMs. *In vivo*, GSMs exhibit the same Aβ profile as observed *in vitro* with reductions in $A\beta_{42}$ and increases or decreases of other Aβ peptides and no effect on total Aβ levels. However, the amount of compound required to generate these effects has been surprisingly high when compared to the *in vitro* potency of the molecules. For example, the Eisai GSM E-2012 has an *in vitro* IC_{50} of 33 nM in a cell-based assay. *In vivo*, 4.9 μM plasma concentrations of the compound were required to reduce brain Aβ by 25%. Similarly, Merck GSM1, JNJ-40418677, and SPI-1810 also require high plasma levels in order to achieve 25% lowering (Table 2), a factor that does not appear to be readily attributable to plasma protein binding. These high compound levels are not required for *in vivo* efficacy with GSIs which further suggests that the interaction with γ-secretase by a GSM is different from that of a GSI. Why high concentrations of some GSMs are required to modulate γ-secretase activity *in vivo* is not completely understood. Less than ideal pharmacokinetic properties, such as low free fraction or poor blood brain barrier permeability may contribute to the need for high plasma concentrations of GSMs to see efficacy in the brain *in vivo*. In addition, there are data indicating that GSMs can bind to both active and inactive forms of presenilin since the binding site of the modulators is available even prior to endoproteolysis that creates the active form of γ-secretase [51, 52]. Conversely, data indicate that GSIs require complex formation prior to binding [53], which may mean more binding sites are available for GSMs than for GSIs.

4. Conclusions

Small molecule modulators of γ-secretase are now in the early stages of clinical testing. In preclinical toxicology studies, these modulators are free of the mechanism-based toxicities that have been seen with GSIs, most of which appear to be due to inhibition of Notch processing by directly targeting the ε cleavage site. Both *in vitro* and *in vivo* data support the conclusion that GSMs do not interfere with Notch

Table 2: GSM potency versus plasma exposure in mice.

	E-2012	JNJ-40418677	GSM1	SPI-1810
In vitro $A\beta_{42}$ IC_{50} (nM) CHO-2B7 cells	33	172	62	114
Plasma exposure (μM)	4923	7764	2744	14638
Plasma fold over $A\beta_{42}$ IC_{50} for 25% reduction	149	45	44	128
Brain exposure (μM)	2749	7497	8681	20368
Brain fold over $A\beta_{42}$ IC_{50} for 25% reduction	83	44	140	179

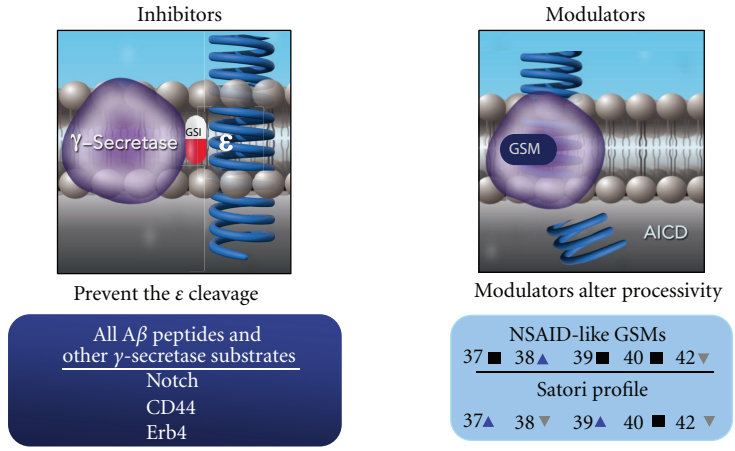

Figure 7: Diagram highlighting the differences between inhibitors and modulators.

processing, but instead, via slight shifts in the cleavage site on APP, lower $A\beta_{42}$ production to produce the other normal $A\beta$ peptide products (Figures 6 and 7). Thus, modulation of γ-secretase may represent the most selective approach to treating Alzheimer's disease via a decrease in production of $A\beta_{42}$, more selective that an inhibitor of either beta or γ-secretase . Modulators do differ both in chemical structure and in their effects on APP processing, producing the desired decrease in $A\beta_{42}$ and a variety of changes in other $A\beta$ peptides. Understanding the molecular basis of these varying profiles may shed further light on the biology of γ-secretase.

Disclosures

All authors are or were employees of Satori Pharmaceuticals, Inc.

Acknowledgments

A portion of this work was presented at the AAIC Annual meetings in 2011 and 2012. The authors would like to thank Dr. John Leszyk from the University of Massachusetts for MALDI-TOF $A\beta$ profile analysis and Kelly Ames, Business Manager at Satori Pharmaceuticals, Inc.

References

[1] N. Kakuda, S. Funamoto, S. Yagishita et al., "Equimolar production of amyloid β-protein and amyloid precursor protein intracellular domain from β-carboxyl-terminal fragment by γ-secretase," *Journal of Biological Chemistry*, vol. 281, no. 21, pp. 14776–14786, 2006.

[2] T. Sato, N. Dohmae, Y. Qi et al., "Potential link between amyloid β-protein 42 and C-terminal fragment γ 49-99 of β-amyloid precursor protein," *Journal of Biological Chemistry*, vol. 278, no. 27, pp. 24294–20301, 2003.

[3] Y. Qi-Takahara, M. Morishima-Kawashima, Y. Tanimura et al., "Longer forms of amyloid β protein: implications for the mechanism of intramembrane cleavage by γ-secretase," *Journal of Neuroscience*, vol. 25, no. 2, pp. 436–445, 2005.

[4] M. Takami, Y. Nagashima, Y. Sano et al., "γ-Secretase: successive tripeptide and tetrapeptide release from the transmembrane domain of β-carboxyl terminal fragment," *Journal of Neuroscience*, vol. 29, no. 41, pp. 13042–13052, 2009.

[5] T. E. Golde, Y. Ran, and K. M. Felsenstein, "Shifting a complex debate on γ-secretase cleavage and Alzheimer's disease," *The EMBO Journal*, vol. 31, no. 10, pp. 2237–2239, 2012.

[6] N. Suzuki, T. T. Cheung, X. D. Cai et al., "An increased percentage of long amyloid β protein secreted by familial amyloid β protein precursor (βAPP717) mutants," *Science*, vol. 264, no. 5163, pp. 1336–1340, 1994.

[7] T. Saito, T. Suemoto, N. Brouwers et al., "Potent amyloidogenicity and pathogenicity of $A\beta$ 243," *Nature Neuroscience*, vol. 14, no. 8, pp. 1023–1032, 2011.

[8] J. T. Jarrett, E. P. Berger, and P. T. Lansbury Jr., "The carboxy terminus of the β amyloid protein is critical for the seeding of amyloid formation: Implications for the pathogenesis of Alzheimer's disease," *Biochemistry*, vol. 32, no. 18, pp. 4693–4697, 1993.

[9] J. Milano, J. McKay, C. Dagenais et al., "Modulation of Notch processing by γ-secretase inhibitors causes intestinal goblet cell metaplasia and induction of genes known to specify gut secretory lineage differentiation," *Toxicological Sciences*, vol. 82, no. 1, pp. 341–358, 2004.

[10] G. H. Searfoss, W. H. Jordan, D. O. Calligaro et al., "Adipsin, a biomarker of gastrointestinal toxicity mediated by a functional

γ-secretase inhibitor," *Journal of Biological Chemistry*, vol. 278, no. 46, pp. 46107–46116, 2003.

[11] G. T. Wong, D. Manfra, F. M. Poulet et al., "Chronic treatment with the γ-secretase inhibitor LY-411,575 inhibits γ-amyloid peptide production and alters lymphopoiesis and intestinal cell differentiation," *Journal of Biological Chemistry*, vol. 279, no. 13, pp. 12876–12882, 2004.

[12] E. Lilly, "Lilly Halts Development of Semagacestat for Alzheimer's Disease Based on Preliminary Results of Phase III Clinical Trials," 2010, http://newsroom.lilly.com/releasedetail.cfm?releaseid=499794.

[13] D. J. Selkoe, "Resolving controversies on the path to Alzheimer's therapeutics," *Nature Medicine*, vol. 17, no. 9, pp. 1060–1065, 2011.

[14] B. P. Imbimbo, F. Panza, V. Frisardi et al., "Therapeutic intervention for Alzheimer's disease with γ-secretase inhibitors: still a viable option?" *Expert Opinion on Investigational Drugs*, vol. 20, no. 3, pp. 325–341, 2011.

[15] S. Weggen, J. L. Eriksen, P. Das et al., "A subset of NSAIDs lower amyloidogenic Aβ42 independently of cyclooxygenase activity," *Nature*, vol. 414, no. 6860, pp. 212–216, 2001.

[16] T. E. Golde, L. S. Schneider, and E. H. Koo, "Anti-Aβ therapeutics in alzheimer's disease: the need for a paradigm shift," *Neuron*, vol. 69, no. 2, pp. 203–213, 2011.

[17] B. P. Imbimbo, "Why did tarenflurbil fail in alzheimer's disease?" *Journal of Alzheimer's Disease*, vol. 17, no. 4, pp. 757–760, 2009.

[18] R. C. Green, L. S. Schneider, D. A. Amato et al., "Effect of tarenflurbil on cognitive decline and activities of daily living in patients with mild Alzheimer disease: a randomized controlled trial," *Journal of the American Medical Association*, vol. 302, no. 23, pp. 2557–2564, 2009.

[19] B. Bulic, J. Ness, S. Hahn, A. Rennhack, T. Jumpertz, and S. Weggen, "Chemical biology, molecular mechanism and clinical perspective of γ-secretase modulators in Alzheimer's disease," *Current Neuropharmacology*, vol. 9, no. 4, pp. 598–622, 2011.

[20] J. L. Hubbs, N. O. Fuller, W. F. Austin et al., "Optimization of a natural product-based class of gamma-secretase modulators," *Journal of Medicinal Chemistry*, vol. 55, no. 21, pp. 9270–9282, 2012.

[21] E. H. M. Koo, T. E. Golde, and D. R. Galasko, "Nonsteroidal antiinflammatory drug (NSAID) and NSAID derivative amyloid Aβ42 polypeptide-lowering agents for the treatment of Alzheimer's disease, and screening methods," pp. 73, Mayo Foundation for Medical Education and Research, USA, 2001.

[22] L. Raveglia, I. Peretto, S. Radaelli, B. P. Imbimbo, A. Rizzi, and G. Villetti, "Preparation of 1-phenylalkanecarboxylic acid derivatives for the treatment of neurodegenerative diseases," pp. 91, Chiesi Farmaceutici S.p.A., Italy, 2004.

[23] P. Blurton et al., "Arylacetic acids and related compounds and their preparation, pharmaceutical compositions and their use for treatment of diseases associated with the deposition of β-amyloid peptides in the brain such as Alzheimer's disease," pp. 58, Merck Sharp & Dohme Limited, UK, 2006.

[24] C. Y. Ho, *Preparation of Biphenyl Derivatives as γ-secretAse Modulators*, Janssen Pharmaceutica, Belg, Germany, 2009.

[25] F. Wilson, A. Reid, V. Reader et al., "Preparation of biphenylacetic acids as γ-secretase modulators for the treatment of Alzheimer's disease," pp. 57, Cellzome, Germany, 2006.

[26] G. Shapiro and R. Chesworth, "1,3,4-Trisubstituted benzenes as γ-secretase inhibitors and their preparation and use in the treatment of neurodegenerative diseases," pp. 165, Envivo Pharmaceuticals, USA, 2009.

[27] J. J. Kulagowski, A. Madin, P. M. Ridgill, and M. E. Seward, "Preparation of piperidines and related compounds for treatment of Alzheimer's disease," pp. 178, Merck Sharp & Dohme Limited, UK, 2006.

[28] A. Hall, R. L. Elliott, G. M. P. Giblin et al., "Piperidine-derived γ-secretase modulators," *Bioorganic and Medicinal Chemistry Letters*, vol. 20, no. 3, pp. 1306–1311, 2010.

[29] E. C. W. Am et al., "Aminocyclohexanes and aminotetrahydropyrans as γ-secretase modulators and their preparation and use for thetreatment of neurological and psychiatric diseases," pp. 91, Pfizer, USA, 2011.

[30] S. Cheng, D. D. Comer, L. Mao, G. P. Balow, and D. Pleynet, "Aryl compounds and uses in modulating amyloid β," pp. 178, Neurogenetics, USA 2004.

[31] K. Baumann et al., "Preparation of thiazolyl-substituted imidazolylphenylamine derivatives and related compounds as modulators of amyloid beta," pp. 32, Hoffmann-La Roche, USA, 2008.

[32] L. R. Marcin et al., "Preparation of bicyclic compounds, especially bicyclic triazoles, for the reduction of beta-amyloid protein production," pp. 242, Bristol-Myers Squibb Company, USA, 2010.

[33] R. Forsblom, K. Paulsen, M. Waldman, D. Rotticci, and E. Santangelo, "Preparation of 2-aminopyrimidines as amyloid beta modulators," pp. 227, AstraZeneca AB, Sweden, 2010.

[34] K. Biswas, J. J. Chen, J. R. Falsey et al., "Preparation of urea compounds as gamma secretase modulators," pp. 116, Amgen, USA, 2009.

[35] H. J. M. Gijsen, A. I. Velter, G. J. MacDonald et al., "Novel substituted bicyclic heterocyclic compounds as gamma secretase modulators and their preparation and use in the treatment of diseases," pp. 164, Ortho-Mcneil-Janssen Pharmaceuticals, USA, 2010.

[36] P. Blurton et al., "Preparation of heteroarylpiperazine derivatives for use in treatment of Alzheimer's disease," pp.68, Merck & Co., Merck Sharp & Dohme Limited, USA, 2008.

[37] M. A. Findeis, F. Schroeder, T. D. McKee et al., "Discovery of a novel pharmacological and structural class of gamma secretase modulators derived from the extract of actaea racemosa," *ACS Chemical Neuroscience*, vol. 3, no. 11, pp. 941–951, 2012.

[38] S. J. Haugabook, D. M. Yager, E. A. Eckman, T. E. Golde, S. G. Younkin, and C. B. Eckman, "High throughput screens for the identification of compounds that alter the accumulation of the Alzheimer's amyloid β peptide (Aβ)," *Journal of Neuroscience Methods*, vol. 108, no. 2, pp. 171–179, 2001.

[39] M. P. Murphy, S. N. Uljon, P. E. Fraser et al., "Presenilin 1 regulates pharmacologically distinct γ-secretase activities: implications for the role of presenilin in γ-secretase cleavage," *Journal of Biological Chemistry*, vol. 275, no. 34, pp. 26277–26284, 2000.

[40] T. A. Lanz, M. J. Karmilowicz, K. M. Wood et al., "Concentration-dependent modulation of amyloid-β in vivo and in vitro using the γ-secretase inhibitor, LY-450139," *Journal of Pharmacology and Experimental Therapeutics*, vol. 319, no. 2, pp. 924–933, 2006.

[41] K. Rogers et al., "Optimization of a natural product-based class of gamma secretase modulators," in *International Conference on Alzheimer's Disease*, Vienna, Austria, 2009.

[42] C. R. Burton, J. E. Meredith, D. M. Barten et al., "The amyloid-β rise and γ-secretase inhibitor potency depend on the level of substrate expression," *Journal of Biological Chemistry*, vol. 283, no. 34, pp. 22992–23003, 2008.

[43] J. D. Hughes, J. Blagg, D. A. Price et al., "Physiochemical drug properties associated with in vivo toxicological outcomes,"

Bioorganic and Medicinal Chemistry Letters, vol. 18, no. 17, pp. 4872–4875, 2008.

[44] T. T. Wager, X. Hou, P. R. Verhoest, and A. Villalobos, "Moving beyond rules: the development of a central nervous system multiparameter optimization (CNS MPO) approach to enable alignment of druglike properties," *ACS Chemical Neuroscience*, vol. 1, no. 6, pp. 435–449, 2010.

[45] T. T. Wager, R. Y. Chandrasekaran, X. Hou et al., "Defining desirable central nervous system drug space through the alignment of molecular properties, in vitro ADME, and safety attributes," *ACS Chemical Neuroscience*, vol. 1, no. 6, pp. 420–434, 2010.

[46] F. Lovering, J. Bikker, and C. Humblet, "Escape from flatland: increasing saturation as an approach to improving clinical success," *Journal of Medicinal Chemistry*, vol. 52, no. 21, pp. 6752–6756, 2009.

[47] T. J. Ritchie and S. J. F. Macdonald, "The impact of aromatic ring count on compound developability—are too many aromatic rings a liability in drug design?" *Drug Discovery Today*, vol. 14, no. 21-22, pp. 1011–1020, 2009.

[48] T. Kimura, K. Kawano, E. Doi et al., "Preparation of cinnamide, 3-benzylidenepiperidin-2-one, phenylpropynamide compounds as amyloid β production inhibitors," pp. 679, Eisai, Japan, 2005.

[49] A. Ebke, T. Luebbers, A. Fukumori et al., "Novel γ-secretase enzyme modulators directly target presenilin protein," *Journal of Biological Chemistry*, vol. 286, pp. 37181–37186, 2011.

[50] M. S. Wolfe, "gamma-Secretase inhibitors and modulators for Alzheimer's disease," *Journal of Neurochemistry*, vol. 120, supplement 1, pp. 89–98, 2012.

[51] Y. Ohki, T. Higo, K. Uemura et al., "Phenylpiperidine-type γ-secretase modulators target the transmembrane domain 1 of presenilin 1," *The EMBO Journal*, vol. 30, no. 23, pp. 4815–4824, 2011.

[52] S. Weggen and D. Beher, "Molecular consequences of amyloid precursor protein and presenilin mutations causing autosomal-dominant Alzheimer's disease," *Alzheimer's Research and Therapy*, vol. 4, no. 2, Article ID 9, 2012.

[53] K. Takeo, N. Watanabe, T. Tomita, and T. Iwatsubo, "Contribution of the γ-secretase subunits to the formation of catalytic pore of presenilin 1 protein," *Journal of Biological Chemistry*, vol. 287, no. 31, pp. 25834–25843, 2012.

Hindawi Publishing Corporation
International Journal of Alzheimer's Disease
Volume 2012, Article ID 289412, 7 pages
doi:10.1155/2012/289412

Research Article

Morphologic and Functional Effects of Gamma Secretase Inhibition on Splenic Marginal Zone B Cells

Maria Cristina de Vera Mudry,[1] Franziska Regenass-Lechner,[1] Laurence Ozmen,[2] Bernd Altmann,[1] Matthias Festag,[1] Thomas Singer,[1] Lutz Müller,[1] Helmut Jacobsen,[2] and Alexander Flohr[3]

[1] *Non-Clinical Safety, Pharma Research and Early Development, F. Hoffmann-La Roche Ltd., Grenzacherstrasse 124, 4070 Basel, Switzerland*
[2] *Molecular Neuroscience, Pharma Research and Early Development, F. Hoffmann-La Roche Ltd., Grenzacherstrasse 124, 4070 Basel, Switzerland*
[3] *Medicinal Chemistry, Pharma Research and Early Development, F. Hoffmann-La Roche Ltd., Grenzacherstrasse 124, 4070 Basel, Switzerland*

Correspondence should be addressed to Maria Cristina de Vera Mudry, maria_cristina.de_vera_mudry@roche.com

Received 4 August 2012; Accepted 17 November 2012

Academic Editor: Yasuji Matsuoka

The γ-secretase complex is a promising target in Alzheimer's disease because of its role in the amyloidogenic processing of β-amyloid precursor protein. This enzyme also catalyzes the cleavage of Notch receptor, resulting in the nuclear translocation of intracellular Notch where it modulates gene transcription. Notch signaling is essential in cell fate decisions during embryogenesis, neuronal differentiation, hematopoiesis, and development of T and B cells, including splenic marginal zone (MZ) B cells. This B cell compartment participates in the early phases of the immune response to blood-borne bacteria and viruses. Chronic treatment with the oral γ-secretase inhibitor RO4929097 resulted in dose-dependent decreased cellularity (atrophy) of the MZ of rats and mice. Significant decreases in relative MZ B-cell numbers of RO4929097-treated animals were confirmed by flow cytometry. Numbers of MZ B cells reverted to normal after a sufficient RO4929097-free recovery period. Functional characterization of the immune response in relation to RO4929097-related MZ B cell decrease was assessed in mice vaccinated with inactivated vesicular stomatitis virus (VSV). Compared with the immunosuppressant cyclosporin A, RO4929097 caused only mild and reversible delayed early neutralizing IgM and IgG responses to VSV. Thus, the functional consequence of MZ B cell decrease on host defense is comparatively mild.

1. Introduction

The γ-secretase complex is a key enzyme in the amyloidogenic processing of β-amyloid precursor protein (APP) and is a promising drug target for treatment or prevention of Alzheimer's disease [1]. In the first step, the extracellular domain of APP is cleaved off by the "sheddase" activity of either an ADAM protease or β-secretase. The remaining membrane-bound C-terminal fragment is then cleaved by γ-secretase within its transmembrane domain. The cleavage releases a cytoplasmic domain into the cell interior, but produces also the β-amyloid peptides which are released into the extracellular space where they can form toxic aggregates and amyloid plaques. The latter presumably initiate a pathogenic cascade which finally leads to the clinical symptoms of Alzheimer's disease, that is, severe dementia.

A number of additional γ-secretase substrates have been identified and among these are the Notch receptors, CD44 and HER4 [2, 3]. These are all type-1 membrane proteins and their processing follows the same pattern as described for APP. In the case of Notch, the shedding of the extracellular domain is initiated by binding of specific ligands like Delta-like and Jagged. Once released by γ-secretase from its membrane attachment, the cytoplasmic domain of Notch

(ICN, intracellular cellular Notch) translocates to the nucleus where it serves as a transcriptional regulator. Notch signaling is important for cell fate decisions and homeostasis of pluripotent stem cells in the embryo and adult organism [4] and is upregulated in neoplastic cells [5]. Targeted inactivation of the Notch pathway can affect processes such as the renewal of epidermis and gut epithelia and specific populations of lymphocytes, as well as tumors. For this reason, pharmacological inhibition of γ-secretase, for example, as a potential treatment in Alzheimer's disease or neoplasia, can have adverse effects on important physiological processes because of its effects on Notch signaling [6–9].

One group of B lymphocytes that depends on active Notch signaling is the marginal zone B cell [10]. In the current report, we investigated the effects of a selective and potent γ-secretase inhibitor (GSI), RO4929097 [11], on the formation and function of MZ B cells in the rat and mouse *in vivo*. Specifically, the effect of RO4929097 on (1) the number of MZ B cells in the spleen in rats after 13 weeks of oral administration followed by a treatment-free recovery period of 6 weeks, and on (2) the neutralizing antibody formation after challenge with inactivated vesicular stomatitis virus (VSV) in mice after 4 weeks of oral administration was assessed.

2. Materials and Methods

2.1. Compound. The test compound RO4929097 [2,2-dimethyl-N-((S)-6-oxo-6,7-dihydro-5H-dibenzo[b,d]azepin-7-yl)-N-(2,2,3,3,3-pentafluoro-propyl)-malonamide] was synthesized according to the procedure described in patent application (WO2005/023772).

2.2. Animals. Male and female Wistar (HanRCCWIST) SPF rats, 12 weeks of age, and female C57Bl/6JIbm SPF mice, 8–10 weeks of age, (RCC, Füllinsdorf, Switzerland), were used. Animals were provided with pelleted maintenance rodent diet Provimi Kliba 3433 and tap water *ad libitum*. Rats were kept 2 per cage, in Makrolon type III cages, while mice were kept individually in Makrolon type II cages, with autoclaved sawdust bedding. Air-conditioned animal rooms were maintained at 22°C ± 2°C and 40%–80% relative humidity, under periodic bacteriological control. A 12-h light/dark cycle was used and background music was coordinated with light hours. Animals were handled with humane care according to the guidelines of the Institutional Animal Care and Use Committee. The F. Hoffmann-La Roche Pharma Research Basel test facility is certified by the Swiss GLP monitoring authorities to be in compliance with the Swiss Ordinance relating to Good Laboratory Practice (GLP) and is fully accredited by the Association for Assessment and Accreditation of Laboratory Animal Care International.

2.3. Treatments. Rats were administered RO4929097, a potent and selective γ-secretase inhibitor, in the vehicle (Capmul/MCT/Tween 80 solution) at doses of 0, 0.5, 1.5, and 3 mg/kg/day, orally (gavage), once daily for 13 weeks, at a dose volume of 1 mL/kg body weight. Rats were kept for an additional 6 weeks of treatment-free recovery period.

For the VSV vaccination study, female C57Bl/6JIbm mice were administered RO4929097 in 3% Avicel and 0.2% Tween 80 at doses of 0, 3, 10, and 30 mg/kg/day orally (gavage), once daily for 4 weeks. Half of the mice received in addition 60 mg/kg/day cyclosporin A (Sandimmun Neoral, Novartis Pharma) orally from day 5. Ultraviolet (UV) light-inactivated VSV Indiana was kindly provided by Dr. D. Pinschewer (Institute of Experimental Immunology, University Hospital Zürich, Switzerland). All mice were immunized with 4×10^6 PFU equivalents UV-inactivated VSV intravenously on day 9. Serum samples were obtained at different time points to monitor VSV-specific antibody production. Due to technical difficulties during the dosing procedure, some animals did not survive the duration of the study. This resulted in the analysis of 5 mice in the vehicle control group, and 8 mice each in the treated groups.

2.4. Terminal Procedures. Animals were sacrificed with CO_2 and exsanguinated. One-third of the spleen of all animals was taken and placed in 5 mL cold sterile PBS, stored on ice until processing for marginal zone B-cell enumeration. The remainder of the spleen was fixed for at most 24 h in 10% buffered formalin, embedded in Paraplast, sectioned at a nominal thickness of approximately 2–4 μm, and stained for H.E. for routine microscopic examination.

2.5. Flow Cytometric Analysis of Marginal Zone B Cells. Spleen cell suspensions were prepared by passing through a 70 μm cell strainer in cold DMEM (Dulbecco's Minimal Essential Medium). Red blood cells were lysed and washed cells were incubated with a mixture of the following antibodies and acquired in a FACSCanto or FACSCalibur instrument (Becton Dickinson). Analysis was performed using CellQuest software (Becton Dickinson) and results were expressed as percentages of MZ B cells within the leukocyte gate.

Mouse. FITC-conjugated anti-mouse CD21/CD35 (BD Pharmingen), PE-conjugated anti-mouse CD23 (BD Pharmingen), Cy5.5-conjugated anti-mouse B220 (eBioscience), APC-conjugated anti-mouse IgM (BD Pharmingen) were used. MZ B cells were characterized as being IgM^+/$B220^+$/$CD21^{high}$/$CD23^{low}$.

Rat. FITC-conjugated anti-rat HIS57 (BD Pharmingen), PE-conjugated anti-rat IgM (BD Pharmingen), PerCP-conjugated anti-rat Thy1.1 (CD90) (BD Pharmingen) were used. MZ B cells were characterized as IgM^{high}/$CD90^{low/negative}$/$HIS57^+$.

2.6. VSV Neutralization Assay. After intravenous immunization with 2×10^6 PFU (plaque-forming units) VSV-IND, serum was collected from mice at specified times (days 2, 4, 7, 14, and 20 after immunization). In the morning before dosing with RO4929097, approximately 200 μL blood was drawn retroorbitally from mice under light isoflurane anesthesia, centrifuged for 1 h, and the serum frozen at

−20°C. Thawed serum was prediluted 40-fold in DMEM containing 5% FCS and heat-inactivated for 30 min at 56 °C. Serial twofold dilutions were mixed with equal volumes of VSV (500 PFU mL^{-1}) and incubated for 90 min at 37 °C in an atmosphere with 5% CO_2. The serum-virus mixture was transferred onto Vero cell monolayers in 96-well plates and incubated for 1 h at 37 °C. The monolayers were then overlaid with DMEM containing 1% methylcellulose and incubated for 24 h at 37 °C after which the monolayers were fixed and stained with 0.5% crystal violet. The highest dilution of serum that reduced the number of plaques by 50% was taken as the titer. To determine IgG titers, undiluted serum was pretreated with an equal volume of 0.1 mM β-2-mercaptoethanol in saline before heat inactivation and plating onto Vero cells. This treatment has been shown to eliminate only IgM but not IgG from serum [12]. Unreduced samples were taken as IgM titers only, if the corresponding reduced samples had at least a fourfold lower titer, that is, when the IgG present in the unreduced sample could be neglected.

2.7. Statistics. For significance testing of dose-related effects on cellularity of MZ B cells in spleen and VSV neutralizing antibody titers in serum, Student's *t*-test was used. Individual time points (study days) were analyzed separately.

For significance testing of dose-related effects on white blood cell, neutrophil, and lymphocyte numbers in peripheral blood, Jonckheere and the Mann-Whitney *U* tests were used.

3. Results

3.1. 13-Week RO4929097 Treatment in Rats Followed by a 6-Week Treatment-Free Recovery Period. Oral administration of RO4929097 for 13 weeks was generally well tolerated and there were no treatment-related deaths during the course of the study. In the peripheral blood, moderate reductions in lymphocytes and increases in neutrophils from ≥1.5 mg/kg/day in both male and female rats persisted until the end of the 6-week treatment-free recovery period (Tables 1(a) and 1(b)).

Flow cytometry analysis revealed a dose-dependent reduction in the percentage of MZ B cells in the spleen of both male and female rats following oral RO4929097 administration for 13 weeks. Compared with the control, this reduction was statistically significant and greater than 60% reduction at ≥1.5 mg/kg/day (Figure 1(a)). After the recovery period, the percentages of marginal zone B cells of RO4929097-treated rats had normalized and were comparable with those of control animals (Figure 1(b)).

Histopathologic changes were recorded in the spleen of nearly all male and female rats that received ≥1.5 mg/kg/day RO4929097 (Figure 2). These included minimal-to-marked decreased cellularity and infiltration of neutrophils of the marginal zone and periarteriolar lymphoid sheath areas. Individual animals showed minimally increased apoptosis in the marginal zone. In addition, slight-to-moderate stromal change, characterized by a focal, somewhat circumscribed area of occasional pale staining lymphocytes, dendritic cells, eosinophilic hyaline-like deposits, early fibroplasia, necrotic cell debris, and polymorphonuclear leukocyte infiltration, was noted in occasional animals. There were no RO4929097-related findings in the spleen after the 6-week treatment-free recovery period.

3.2. VSV Vaccination Study in Mice. Mice were treated daily with RO4929097 and vaccinated with inactivated VSV in order to characterize the immune response to VSV in relation to a dose-dependent decrease in MZ B cellularity. The immunosuppressant cyclosporin A was used as a positive control. Cyclosporin A is known to suppress the switch from a T-independent IgM to a T-dependent IgG response to VSV in this model [13].

Flow cytometry analysis of spleen cells at the end of the 4-week treatment period showed a dose-dependent reduction of relative MZ B cell counts (Figure 3). There was no significant reduction at 3 mg/kg/day, a 51% reduction at 10 mg/kg/day, and a 95% reduction at 30 mg/kg/day RO4929097. Vehicle or cyclosporin A treatment had no effect on MZ B cellularity.

Dosing with ≥10 mg/kg/day RO4929097 resulted in a delayed appearance of early neutralizing antibodies (presumably of IgM class) in response to VSV, that is, titers were below detection limit at 2 days after vaccination (Figure 4). Notably at 10 mg/kg with an average 51% depletion of MZ B cells, the antibody response to VSV was only affected at the earliest time point on day 2, after which no difference to untreated animals in the immune response was noted. At 4 days after vaccination, antibody titers were detectable in all groups, but these were still reduced in animals dosed with 30 mg/kg/day in comparison to all other groups. In addition, treatment with 30 mg/kg/day RO4929097 resulted in a reduction of neutralizing immunoglobulin titers of the IgG class at 7 days after vaccination (average 7.8-fold reduction), but titers recovered at later time points.

4. Discussion and Conclusion

Previous preclinical toxicity studies with RO4929097 in rats, mice, and dogs have shown that significant effects were attributable to Notch impairment [11]. Similar findings were observed following oral administration of RO4929097 to male and female Wistar rats for 13 weeks. Flow cytometry analysis showed a dose-dependent reduction in relative numbers of splenic MZ B cells that correlated with histopathologic atrophy of the MZ. Marginal zone B cell depletion was completely reversible after a 6-week recovery period. Similarly, a dose-dependent reduction in relative numbers of splenic MZ B cells was seen in female C57Bl/6JIbm mice administered RO4929097 for 4 weeks. Total early neutralizing antibodies (presumably IgM) to inactivated VSV were also reduced, and this was considered to reflect the pharmacological effect of γ-secretase inhibitor RO4929097 on MZ B cells. At the high dose of 30 mg/kg/day RO4929097, neutralizing IgG titers were also reduced at 7 days after vaccination, but recovered at later time points.

Table 1: Effects of RO4929097 on absolute numbers of white blood cells, neutrophils, and lymphocytes in male and female rats.

(a) After 13 weeks of treatment

Dose (mg/kg/day)	Males			Females		
	WBC (10^9/L)	Neutrophils (10^9/L)	Lymphocytes (G/L)	WBC (10^9/L)	Neutrophils (10^9/L)	Lymphocytes (10^9/L)
0						
N	10	10	10	10	10	10
Mean	5.95	1.23	4.26	3.77	0.55	2.94
SD	1.23	0.42	0.92	0.60	0.20	0.47
0.5						
N	10	10	10	10	10	10
Mean	5.65	1.20	4.05	3.68	0.67$^{\#}$	2.76
SD	1.08	0.39	0.75	0.92	0.12	0.86
1.5						
N	10	10	10	9	9	9
Mean	6.31	1.78*	4.01	3.10	1.11**	1.70**
SD	1.39	0.54	1.28	0.85	0.54	0.78
3						
N	10	10	10	10	10	10
Mean	6.37	2.95**	2.70**	2.87	1.10	1.51
SD	1.58	1.29	1.17	0.47	0.24	0.47

Jonckheere test: $^{**}P \leq 1\%$; $^{*}1\% < P \leq 5\%$.
U test: $P \leq 1\%$; $^{\#}1\% < P \leq 5\%$.
N: number of animals.
SD: standard deviation.

(b) After 6 weeks of recovery

Dose (mg/kg/day)	Males			Females		
	WBC (10^9/L)	Neutrophils (10^9/L)	Lymphocytes (10^9/L)	WBC (10^9/L)	Neutrophils (10^9/L)	Lymphocytes (10^9/L)
0						
N	10	10	10	10	10	10
Mean	7.56	1.02	6.19	5.28	0.68	4.36
SD	1.17	0.27	1.18	0.84	0.18	0.76
0.5						
N	10	10	10	10	10	10
Mean	7.28	1.07	5.85	5.06	0.68	4.14
SD	1.37	0.25	1.16	1.00	0.17	0.90
1.5						
N	10	10	10	10	10	10
Mean	8.40	1.70**	6.25	4.01**	1.28**	2.45**
SD	1.34	0.50	1.25	1.03	0.72	0.81
3						
N	10	10	10	10	10	10
Mean	9.13*	3.45**	4.99	3.85**	1.48**	2.08**
SD	2.32	2.10	1.73	0.78	0.54	0.59

Jonckheere test: $^{**}P \leq 1\%$; $^{*}1\% < P \leq 5\%$.
N: number of animals.
SD: standard deviation.

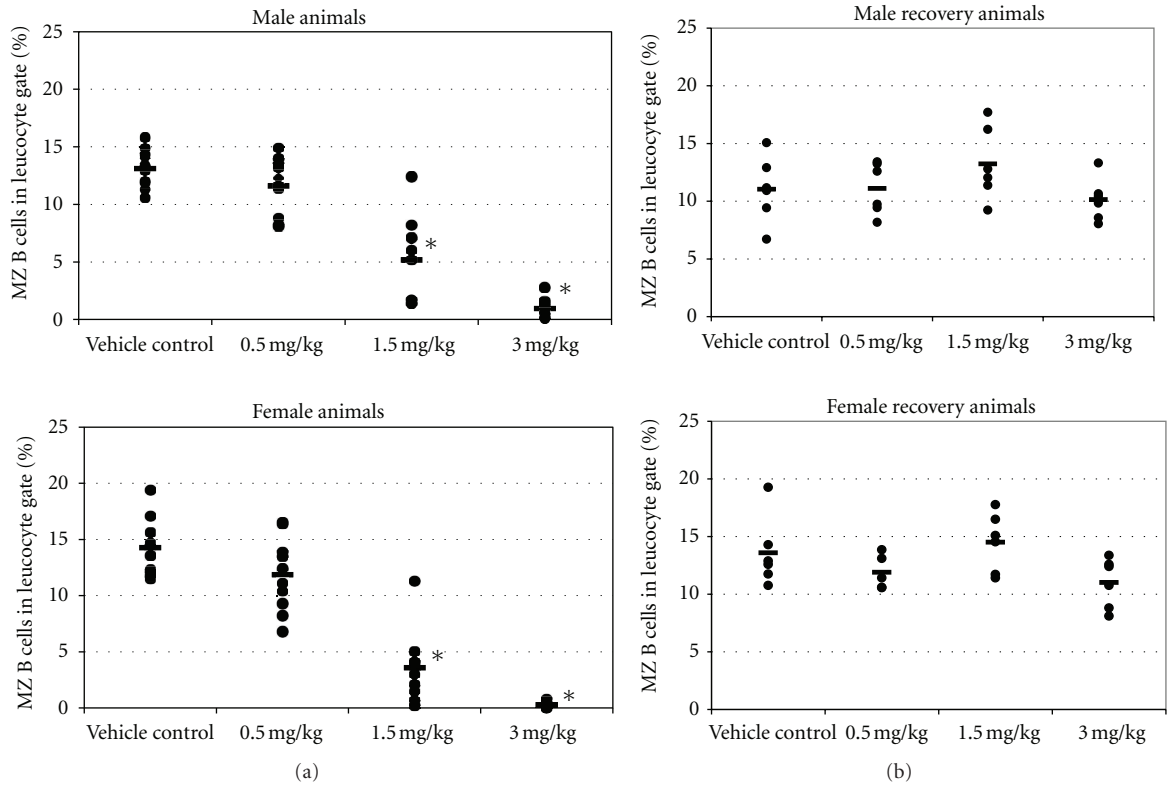

Figure 1: (a) Marginal zone B cells in male and female rats dosed for 13 weeks with RO4929097. Spleen cell suspensions were analyzed by flow cytometry (FACS) using fluorescently labeled antibodies. For each rat the percentage of MZ B cells (= $IgM^{high}/CD90^{low/neg}/HIS57^{+}$) in the leukocyte gate is shown. Dots represent individual rats. - = average per group. $*$ = statistically significant difference to vehicle control ($P < 0.05$). $n = 10$ rats/sex/group. (b) Splenic MZ B cells in male and female rats dosed for 13 weeks with RO4929097 followed by a recovery phase of 6 weeks. Dots represent individual rats. - = average per group. $n = 6$ rats/sex/group.

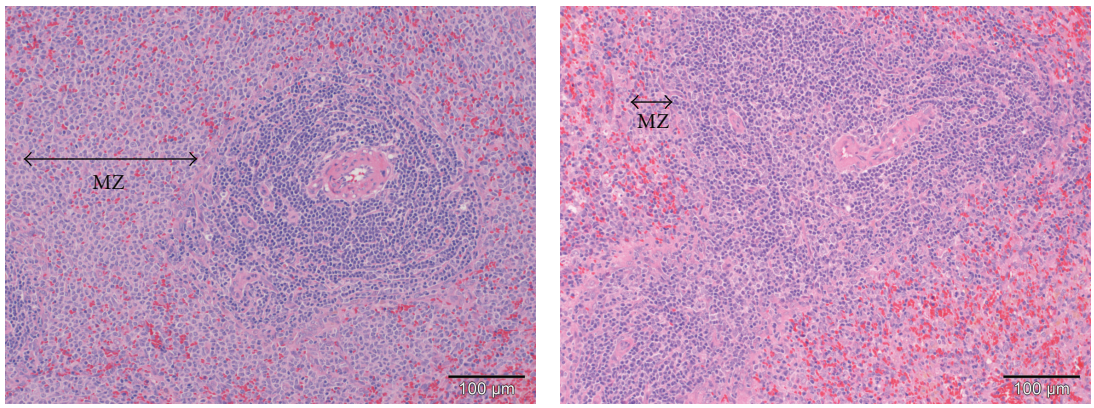

(a) Control (b) RO4929097

Figure 2: Atrophy of the marginal zone (MZ) of the spleen of rats administered 3.0 mg/kg/day RO4929097 for 13 weeks. (hematoxylin-eosin stain).

Class switching from IgM to IgG requires T-cell help, and it is conceivable that high dose RO4929097 not only affected MZ B-cell cellularity but also T-cell function since Notch is also expressed in T cells. Alternatively, a severely reduced MZ B-cell compartment resulted in fewer B cells switching from IgM to IgG. The effect of RO4929097 on IgG antibody formation in these mice was considered relatively mild and a threshold (i.e., 3 mg/kg/day) could be defined where no effects on MZ B-cell counts and neutralizing antibody responses were seen. Originally designed for the treatment of Alzheimer's disease, the efficacious dose of RO4929097 on Aβ reduction was found to be 3 mg/kg in the brain of Aβ transgenic mice, and 10 mg/kg in cerebrospinal fluid of naïve rats. The ED_{50} for mouse MZ B-cell depletion was 10 mg/kg, while for the rat it was lower at 1 mg/kg, but differences in treatment duration should be taken into account. As

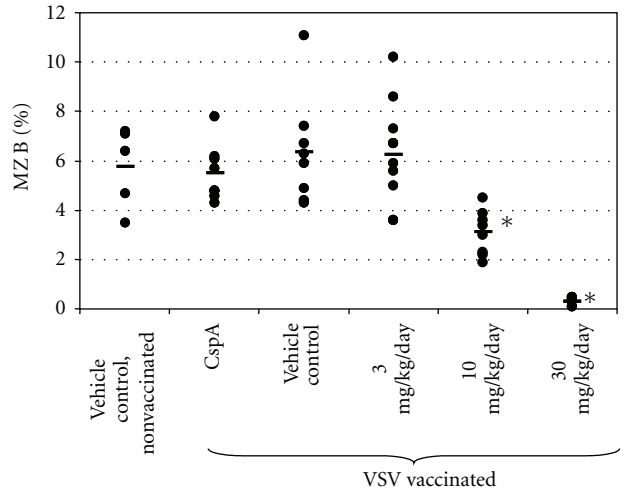

Figure 3: Marginal zone B cells in mice dosed with RO4929097 for 27 days. For each mouse the percentage of MZ B cells (= $IgM^+/B220^+/CD21^{high}/CD23^{low}$) in the leukocyte gate is shown. Dots represent individual mice. - = average per group. ∗ = statistically significant difference to vehicle control ($P < 0.01$). CspA = cyclosporin A. n = 5–8 mice/sex/group.

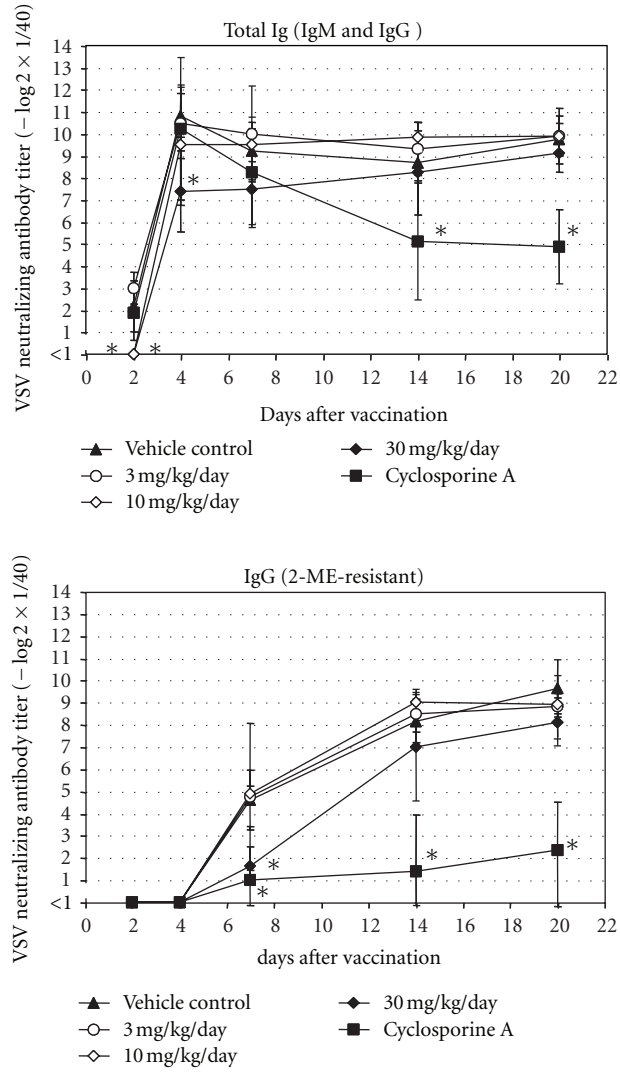

Figure 4: Neutralizing VSV antibodies in mice treated with RO4929097 for 27 days. Neutralizing total Ig (= IgM + IgG) and IgG antibody titers in serum are shown. For each group, average and standard deviation at different time points are shown. ∗ = statistically significant difference to vehicle control ($P < 0.01$) at given time-point. Detection limit of assay was 1 (= 1/40 dilution of serum). Non-vaccinated mice had no detectable VSV neutralizing antibodies in their serum (<1) (not shown). n = 4–8 mice/sex/group.

expected, cyclosporin A showed a much more pronounced effect on neutralizing IgG titers in mice than RO4929097, which was likely due to the known immunosuppressive effect of cyclosporin A on T helper cells, but not on MZ B cells [13].

Much remains unclear regarding development of marginal zone B cells [14]. The immunological consequences of Notch inhibition *in vivo* are not well characterized, and especially little is known about the host response to pathogens under Notch blockade secondary to GSIs. Increased susceptibility to blood-borne bacterial infection has been demonstrated in RBP-J deficient mice [15]. MZ B cells participate in the early phases of the immune response to blood-borne bacteria and viruses. The immune defense of mice to VSV is strongly dependent on the early formation of neutralizing antibodies which in part originate from MZ B cells [15–17]. Therefore the VSV infection or vaccination model can be used to assess the functionality of MZ B cells (and the total B-cell compartment) *in vivo*.

Although RO4929097 was originally designed for the treatment of Alzheimer's disease, the compound is currently under evaluation in clinical studies for oncology. Phase I and other ongoing studies of RO4929097 show that it is generally well tolerated [18–20]. Dose-limiting toxicities arising from administration of γ-secretase inhibitors have been reported as mainly due to effects of Notch inhibition on gut epithelium, rather than on marginal zone B cells, correlating well with preclinical safety studies [6–9]. However, Phase III trials with the γ-secretase inhibitor semagacestat were halted partly because of increased risk of skin cancer that might be attributable to inhibition of Notch1 [21].

Pharmacodynamic biomarkers of Notch inhibition utilizing microarray gene expression of plucked hair follicles have been described in rats [11] and humans [22]. While the hair follicle is a more readily accessible tissue for a biomarker assay, it cannot be used to assess the functional reserve of the marginal zone. It will be interesting to explore further the transcriptional effects of GSIs on marginal zone B cells in the rodent spleen, and their counterpart in humans in the peripheral blood.

Abbreviations

APP: β-amyloid precursor protein
MZ: Marginal zone
VSV: Vesicular stomatitis virus
GSI: γ-secretase inhibitor
FACS: Fluorescence activated cell sorting.

Acknowledgment

The authors would like to thank Dr. D. Pinschewer (Institute of Experimental Immunology, University Hospital Zürich, Switzerland) for kindly providing UV-inactivated VSV Indiana and conducting the VSV neutralization test.

References

[1] S. J. Pollack and H. Lewis, "γ-Secretase inhibitors for Alzheimer's disease: challenges of a promiscuous protease," *Current Opinion in Investigational Drugs*, vol. 6, no. 1, pp. 35–47, 2005.

[2] W. T. Kimberly and M. S. Wolfe, "Identity and function of γ-secretase," *Journal of Neuroscience Research*, vol. 74, no. 3, pp. 353–360, 2003.

[3] D. R. Gibb, M. El Shikh, D. J. Kang et al., "ADAM10 is essential for Notch2-dependent marginal zone B cell development and CD23 cleavage in vivo," *Journal of Experimental Medicine*, vol. 207, no. 3, pp. 623–635, 2010.

[4] M. Baron, "An overview of the Notch signalling pathway," *Seminars in Cell and Developmental Biology*, vol. 14, no. 2, pp. 113–119, 2003.

[5] P. Rizzo, C. Osipo, K. Foreman, T. Golde, B. Osborne, and L. Miele, "Rational targeting of Notch signaling in cancer," *Oncogene*, vol. 27, no. 38, pp. 5124–5131, 2008.

[6] G. H. Searfoss, W. H. Jordan, D. O. Calligaro et al., "Adipsin, a biomarker of gastrointestinal toxicity mediated by a functional γ-secretase inhibitor," *Journal of Biological Chemistry*, vol. 278, no. 46, pp. 46107–46116, 2003.

[7] J. Milano, J. McKay, C. Dagenais et al., "Modulation of Notch processing by γ-secretase inhibitors causes intestinal goblet cell metaplasia and induction of genes known to specify gut secretory lineage differentiation," *Toxicological Sciences*, vol. 82, no. 1, pp. 341–358, 2004.

[8] G. T. Wong, D. Manfra, F. M. Poulet et al., "Chronic treatment with the γ-secretase inhibitor LY-411,575 inhibits γ-amyloid peptide production and alters lymphopoiesis and intestinal cell differentiation," *Journal of Biological Chemistry*, vol. 279, no. 13, pp. 12876–12882, 2004.

[9] J. H. van Es, M. E. van Gijn, O. Riccio et al., "Notch/γ-secretase inhibition turns proliferative cells in intestinal crypts and adenomas into goblet cells," *Nature*, vol. 435, no. 7044, pp. 959–963, 2005.

[10] T. Lopes-Carvalho and J. F. Kearney, "Development and selection of marginal zone B cells," *Immunological Reviews*, vol. 197, pp. 192–205, 2004.

[11] L. Luistro, W. He, M. Smith et al., "Preclinical profile of a potent γ-secretase inhibitor targeting notch signaling with in vivo efficacy and pharmacodynamic properties," *Cancer Research*, vol. 69, no. 19, pp. 7672–7680, 2009.

[12] D. W. Scott and R. K. Gershon, "Determination of total and mercaptoethanol-resistant antibody in the serum sample," *Clinical & Experimental Immunology*, vol. 6, pp. 13–18, 1970.

[13] S. Charan, A. W. Huegin, A. Cerny, H. Hengartner, and R. M. Zinkernagel, "Effects of cyclosporin A on humoral immune response and resistance against vesicular stomatitis virus in mice," *Journal of Virology*, vol. 57, no. 3, pp. 1139–1144, 1986.

[14] I. Maillard, S. H. Adler, and W. S. Pear, "Notch and the Immune System," *Immunity*, vol. 19, no. 6, pp. 781–791, 2003.

[15] K. Tanigaki, H. Han, N. Yamamoto et al., "Notch-RBP-J signaling is involved in cell fate determination of marginal zone B cells," *Nature Immunology*, vol. 3, no. 5, pp. 443–450, 2002.

[16] C. Lutz, B. Ledermann, M. H. Kosco-Vilbois et al., "IgD can largely substitute for loss of IgM function in B cells," *Nature*, vol. 393, no. 6687, pp. 797–801, 1998.

[17] D. Gatto, C. Ruedl, B. Odermatt, and M. F. Bachmann, "Rapid response of marginal zone B cells to viral particles," *Journal of Immunology*, vol. 173, no. 7, pp. 4308–4316, 2004.

[18] http://www.clinicaltrials.gov/ct2/results?term=RO4929097.

[19] A. W. Tolcher, W. A. Messersmith, S. M. Mikulski et al., "Phase I study of RO4929097, a gamma secretase inhibitor of notch signaling, in patients with refractory metastatic or locally advanced solid tumors," *Journal of Clinical Oncology*, vol. 30, no. 19, pp. 2348–2353, 2012.

[20] D. Schepmann and B. Wünsch, "Frontiers in medicinal chemistry 2010: the highlights," *ChemMedChem*, vol. 5, no. 6, pp. 949–954, 2010.

[21] http://newsroom.lilly.com/releasedetail.cfm?releaseid=499794.

[22] S. C. Blackman, J. A. Klappenbach, R. A. Railkar et al., "Identification of a time and dose-responsive transcriptional signature of Notch pathway inhibition in plucked human hair follicles following exposure to the gamma-secretase inhibitor MK-0752," *Molecular Cancer Therapeutics*, vol. 8, supplement 12, 2009, abstract B41.

Hindawi Publishing Corporation
International Journal of Alzheimer's Disease
Volume 2012, Article ID 295207, 10 pages
doi:10.1155/2012/295207

Research Article

γ-Secretase Modulators: Can We Combine Potency with Safety?

Harrie J. M. Gijsen and Marc Mercken

Department of Neuroscience, Janssen Research & Development, Pharmaceutical Companies of Johnson & Johnson, Turnhoutseweg 30, B-2340 Beerse, Belgium

Correspondence should be addressed to Harrie J. M. Gijsen, hgijsen@its.jnj.com

Received 2 August 2012; Accepted 8 November 2012

Academic Editor: Jeremy Toyn

γ-Secretase modulation has been proposed as a potential disease modifying anti-Alzheimer's approach. γ-Secretase modulators (GSMs) cause a product shift from the longer amyloid-beta (Aβ) peptide isoforms to shorter, more soluble, and less amyloidogenic isoforms, without inhibiting APP or Notch proteolytic processing. As such, modulating γ-secretase may avoid some of the adverse effects observed with γ-secretase inhibitors. Since the termination of the GSM tarenfurbil in 2008 due to negative phase III trial results, a considerable progress has been made towards more potent and better brain penetrable compounds. However, an analysis of their lipophilic efficiency indices indicates that their increased potency can be largely attributed to their increased lipophilicity. The need for early and chronic dosing with GSMs will require high-safety margins. This will be a challenge to achieve with the current, highly lipophilic GSMs. We will demonstrate that by focusing on the drug-like properties of GSMs, a combination of high *in vitro* potency and reduced lipophilicity can be achieved and does result in better tolerated compounds. The next hurdle will be to translate this knowledge into GSMs which are highly efficacious and safe *in vivo*.

1. Introduction

With an ageing population, the prevalence of Alzheimer's disease (AD) and the consequent burden to society are rapidly rising [1]. The currently approved medication for AD only offers symptomatic treatment of limited duration without affecting the progression of the disease. Therefore, disease modifying approaches are urgently needed. A hallmark pathology of AD is the presence of amyloid plaques in the brain, which are mainly aggregates of amyloid-beta (Aβ) peptides of varying length, among which Aβ42 is the most amyloidogenic and neurotoxic. These peptides are formed via sequential, proteolytic processing of the amyloid precursor protein (APP) by two aspartyl proteases: β-secretase (BACE) and γ-secretase (GS). Consequently, pharmacological intervention in the activity of these secretases has been heavily investigated for over a decade to prevent both the buildup of the amyloid plaques, as well as the formation of toxic amyloid dimers and oligomers [2, 3]. Small molecules inhibiting either BACE or GS offer a direct way to reduce the production of all amyloid peptides. Where the development of β-secretase inhibitors has been seriously slowed down/hampered due to the difficulty in achieving adequate brain penetration and concomitant *in vivo* efficacy [4], potent, centrally active γ-secretase inhibitors (GSIs) have been discovered and investigated in the clinic and their progress has been reviewed [5, 6]. Phase III clinical trials with the most advanced compound, semagacestat (**1**) (LY450, 139, Figure 1), were prematurely halted in 2010 [6]. Instead of slowing disease progression, **1** was associated with a statistically significant decline in cognition. In addition, an increased risk of skin cancer was reported, most likely related to Notch inhibition.

In comparison with GSIs, γ-secretase modulators (GSMs) cause a product shift from the longer amyloid-beta (Aβ) peptide isoforms to shorter, more soluble, and less amyloidogenic isoforms, without inhibiting APP or Notch proteolytic processing. As such, modulating γ-secretase may avoid the target-related adverse effects observed upon inhibition of GS.

The identification of a subset of NSAIDs as GSMs in 2001 has led to tarenflurbil **2** (Flurizan) as the first NSAID-derived GSM to be tested in the clinic [7, 8]. After negative results in

phase III clinical trials, development was stopped in 2008. This late stage clinical failure can potentially be attributed to the very low brain penetration and weak potency of tarenflurbil [9].

Non-NSAID-derived compounds which do not contain a carboxylic acid group, but are characterized by an imidazole group, were described in a patent application by Neurogenetics in 2004 [10]. Subsequent work by Eisai led to the first compound from this series reaching the clinic, E-2012 (**3**). Although the phase I clinical trial with E-2012 was suspended after lenticular opacity was observed in a high-dose group of a preclinical safety study in rats, in human the compound was reported to reduce plasma Aβ42 levels dose-dependently, with a maximum reduction of ~50% after a 400 mg dose [11].

Since then, many companies have elaborated on these two series, and a considerable progress has been made towards more potent and better brain penetrable compounds in both NSAID- and imidazole-derived chemical series [12, 13]. Despite the efforts spent in this field, very few compounds have made it to the clinic since the termination of tarenflurbil and E-2012. Currently, only two compounds are reported to be in early clinical development: E-2212 and EVP-0962, both with undisclosed structures. In this report, we will provide an overview of our own work and put this into context of the poor drug-like properties of most of the described GSMs to date, especially their high lipophilicity. The need to improve on this in order to obtain safe and efficacious GSMs, suitable for chronic treatment, will also be discussed.

2. Methods

2.1. Calculation of Efficiency Parameters. Mathematically, ligand efficiency (LE) is calculated according to (1), where ΔG represents the binding free energy of a ligand and n is the number of heavy (nonhydrogen) atoms. ΔG can be calculated using (2), where the dissociation constant K_d can be replaced by IC_{50} [14]. Calculation of LE in this paper was done using a temperature (T) of 310 K and using the measured or reported cellular IC_{50} values for the inhibition of Aβ42. As a result, LE is given in kcal/heavy atom according to (3),

$$\mathrm{LE} = \frac{\Delta G}{n}, \tag{1}$$

$$\Delta G = -RT \ln K_d \approx -RT \ln(\mathrm{IC}_{50}), \tag{2}$$

$$\mathrm{LE} = \frac{1.4\mathrm{pIC}_{50}}{n}. \tag{3}$$

Ligand lipophilicity efficiency (LLE) and ligand efficiency-dependent lipophilicity (LELP) were calculated according to (4) and (5), respectively. The octanol-water partition coefficient (clog$P$) is used to describe the lipophilicity of a compound. Log$P$ was calculated (clog$P$) using biobyte software.

$$\mathrm{LLE} = \mathrm{pIC}_{50} - \mathrm{clog}P, \tag{4}$$

$$\mathrm{LELP} = \frac{\mathrm{clog}P}{\mathrm{LE}}. \tag{5}$$

2.2. Biology. For the cellular *in vitro* activity of our own compounds, screening was carried out using SKNBE2 human neuroblastoma cells carrying the hAPP 695 wild-type as described in [15]. For a description of the mouse *in vivo* experiments, see references [15, 16]; for details on the dog *in vivo* experiments, see [17].

3. Discussion

For both the NSAID-derived carboxylic acid GSMs and the imidazole-derived GSMs, we have reported recently on the activity of optimized, potent submicromolar compounds with good *in vivo* activity in lowering Aβ42 levels in mouse brain and/or dog CSF. The structures of the most profiled compounds are shown in Figure 2. Carboxylic acid JNJ-40418677 (**4**) has lowered Aβ42 in cells with an IC_{50} of 200 nM and had a brain/plasma ratio of 0.5–1.0 in mice, depending on the dose [16]. Imidazole JNJ-42601572 (**5**) lowered Aβ42 in cells with an IC_{50} of 16 nM and had a brain/plasma ratio of 0.7–1.1 in mice [15, 17]. A time profile of JNJ-42601572 in mouse is shown in Figure 3. A similar time profile for JNJ-40418677 has been published [16].

Both compounds have been tested in advanced animal models, including repeated dosing in rat and dog. In these studies, early signs of liver toxicity were noted for both compounds, such as bilirubin and ALT/AST increases [17]. Based on these findings, further development was halted. Since then, the dog model combining PK/PD data with early observations of liver toxicity is routinely used in our discovery program to triage compounds [17]. Both JNJ-40418677 and JNJ-42601572 contain a considerable number of conjugated aromatic rings and are characterized by high lipophilicity and molecular weight. In recent years a number of publications have appeared relating such properties with a low probability of success in clinical development [29, 30]. Catchy phrases like "molecular obesity" and "escape from flatland" have been used to describe the issues associated with high molecular weight and number of (hetero) aromatic rings in molecules [31, 32]. Based on analysis of compound properties and their attrition or success in (pre)clinical development, guidelines have been formulated and proposed which can be applied during optimization efforts in medicinal chemistry programs to strive towards more drug-like compounds. The concept of ligand efficiency (LE) is now routinely applied in the drug discovery process [14]. It is defined as the binding energy towards a biological target per (heavy = nonhydrogen) atom in a compound. Since most assays are not directly measuring binding energy, IC_{50} values are often used to make a relative comparison of the LE of compounds. By working towards a high LE,

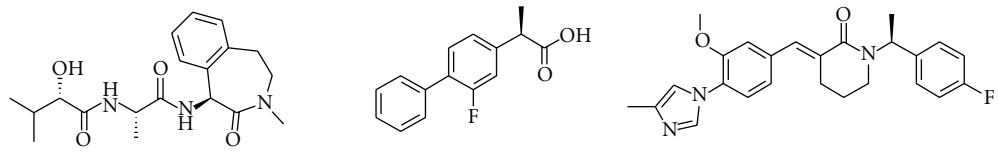

1, semagacestat **2**, tarenflurbil **3**, E-2012

Figure 1

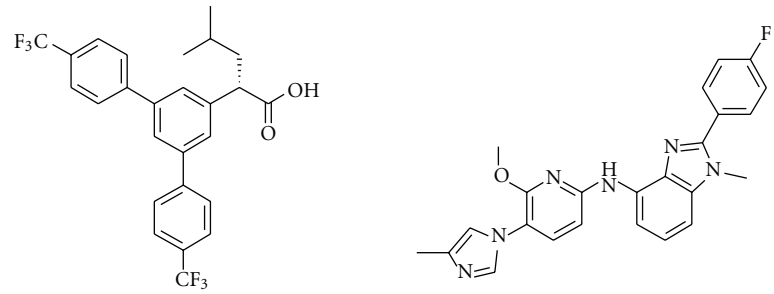

4 Ab42 IC_{50} = 200 nM **5** Ab42 IC_{50} = 16 nM

Figure 2

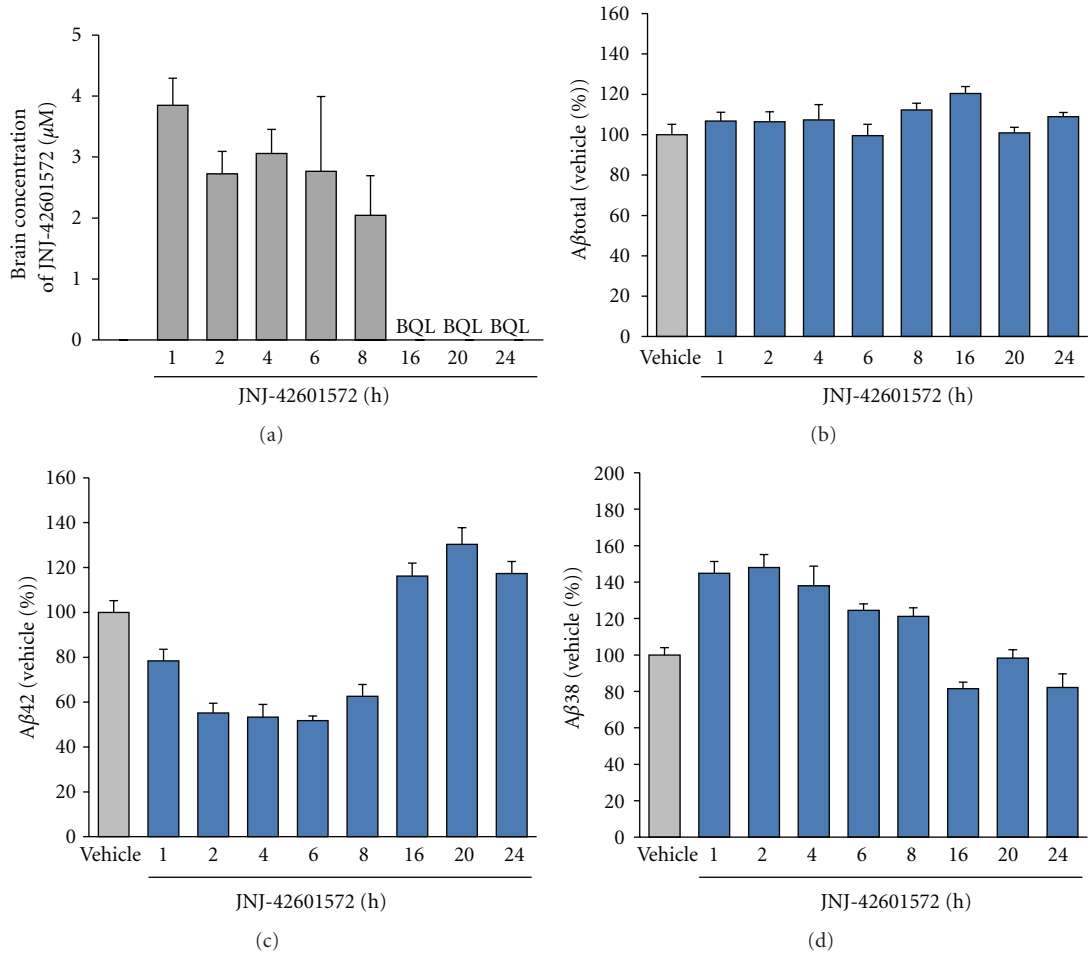

Figure 3: Effects of a single oral dose of 10 mg/kg JNJ-42601572 on Aβ levels in nontransgenic mouse brain as measured with differential ELISAs [16]. Mean (+SEM) brain Aβ levels after drug treatment are expressed as percentage of Aβ levels in brain of vehicle-treated mice. (n = 6 mice per data point). BQL: below quantifiable limits (in brain 0.07–0.12 μM).

molecular weight can be kept in control while optimizing pharmacological activity. Additional parameters have been derived, taking the lipophilicity into account: ligand lipophilicity efficiency (LLE) [33] and ligand efficiency-dependent lipophilicity (LELP) [34] are indices which have been proposed to drive the medicinal chemistry towards an acceptable balance between potency and lipophilicity. Striving for optimal values for these parameters in lead optimization should lead to an increase in potency without increasing lipophilicity. For LLE, a value above 5 is desirable, and for LELP, a value below 10 [35]. In this report we will analyze how the GSM field has evolved in regard to lipophilic efficiency and the implications for their developability.

We have calculated the efficiency indices for a number of representative optimized compounds taken from the literature, including our own compounds. A set of acid-derived GSMs are shown in Table 1, and imidazole-containing GSMs are shown in Table 2. Due to the lack of a direct binding assay to GS, we have calculated the ligand efficiency using the pIC_{50} values for reducing Aβ42 in the cellular assay. Cellular activity can be influenced by additional factors, such as permeability, and can therefore differ substantially from the actual binding of the compounds to the GS complex. Nevertheless, by comparing the various efficiency indices within the two respective chemical classes, we feel the calculated values can still be used to rank order compounds.

In Table 1, the acid-derived GSMs are shown in more or less chronological order. Starting with tarenflurbil, the slightly more potent and brain penetrant CHF5074 is followed by more recently published and considerably more potent analogues JNJ-40418677, BIIB042, and compounds **8** and **9** from GSK and Merck, respectively. The optimization efforts around tarenflurbil have led to an increase in potency and brain penetration, but the ligand and lipophilic efficiency indices for these compounds have hardly been improved. LLE has remained very low for **5**, **6**, and **8**, and although an improvement is seen for **7** and **9**, the values are still below the desirable level (>5). For LELP, all compounds have values well above the desirable upper limit of 10, and no compounds show improvement over tarenflurbil. The increase in potency of GSMs **5**, **7**, and **8** can mainly be attributed to an increase in lipophilicity. For **9**, the lipophilicity has not increased compared to tarenflurbil, and **9** also has a reduced aromatic ring count, compared to the other analogs. However, potency and brain penetration for this compound remain suboptimal. Regarding these metrics, tarenflurbil is still the most drug-like molecule, and indeed the compound was well tolerated during clinical trials despite high dosage [36]. In addition to tarenflurbil, of this set of compounds only the closest analogue, CHF5074 (**6**), has progressed into clinical trials. For all other compounds in Table 1 no further development has been reported.

A similar picture emerges for the nonacidic GSMs, mostly containing an imidazole moiety (Table 2). The early neurogenetic compound **10** has a relatively high ligand efficiency of 0.37 but is characterized by very high lipophilicity, resulting in a low LLE and high LELP value. Going from **10** to E-2012 (**3**), both LLE and LELP have improved. Subsequent work around this series by various companies, as exemplified in Table 2 by **11**–**15** and **5**, has not resulted into a significant further improvement of values relevant for drug-likeness, and in most cases a deterioration of them. The medicinal chemistry program towards **15** was aimed at optimizing lipophilic efficiency [28], which has resulted in the best values for clog*P*, LLE, and LELP within the set of compounds shown in Table 2. However, potency of this compound is still moderate, resulting in a 36% lowering of Aβ42 levels in Guinea pig brain after a 100 mg/kg oral dose [28]. From the compounds in Table 2, only compound **3** (E-2012) has progressed into the clinic. After a single dose of 80 mg/kg of **3** in dog, we have observed liver parameter changes as well as large changes in gene-expression profile in liver tissue obtained in this study [17]. The still suboptimal values for lipophilic efficiency of **3** may have contributed to this, as well as to the termination of **3** in phase 1 clinical trials.

From the *in vivo* data obtained with JNJ-40418677 [16], as well as for JNJ-42601572 shown in Figure 3, two relevant observations can be made, which are also apparent from all other GSMs we have tested *in vivo* up to now. The first observation is that reduction of brain Aβ42 nicely correlates with the compound levels in brain. After the disappearance of the compound from the brain, the Aβ levels quickly return to baseline. This implies that compound levels need to be sustained to maintain a desired change in Aβ levels. The second observation is the large difference between the *in vitro* potency and the compound concentrations required to reduce Aβ42 levels *in vivo*. A considerably higher total compound concentration is required than the *in vitro* IC_{50} to achieve a significant reduction of Aβ42 levels *in vivo*. A common practice is to correct the plasma and brain concentration for the fraction bound to plasma proteins or brain tissue and to use the free compound concentrations. Both JNJ-40418677 and JNJ-42601572 are highly protein/brain tissue bound, with free fractions in plasma and brain of less than 0.1%, resulting in free compound concentrations below the *in vitro* (cellular) IC_{50} values. However, it should be noted that free fractions below 1% are often difficult to be determined accurately, with minor changes in absolute values leading to major differences in calculated free concentrations. After dosing of JNJ-42601572 in dog, the compound concentration in CSF has also been measured, which can be considered as a surrogate for free brain concentrations. After an oral dose of 20 mg/kg, compound levels were only measurable at the plasma Cmax of 4 h, with a CSF/plasma ratio of 0.003. This corresponds to a CSF compound concentration of 11 ± 5 nM, in the same range as the *in vitro* cellular potency (IC_{50}, 16 nM). An increase in free brain concentration as measured by the fraction unbound in brain (F_{ub}) could potentially lead to an improved *in vivo* reduction in Aβ42. A good correlation exists between F_{ub} and the lipophilicity of a compound (Log*P*) [37], giving another reason to aim for a reduced lipophilicity of the compounds. The high lipophilicity required to achieve potency, as evident from all the published GSMs and data shown in Tables 1 and 2, is likely related to the membrane embedded character of the GS proteins and the site where these modulators interact with these proteins. This poses the question if the nature of the target allows for potent compounds with a low lipophilicity.

Table 1: Key parameters and efficiency indices of a set of representative acid GSMs.[a]

Compound	Aβ42 IC_{50} (μM)	Brain/plasma ratio	clog*P*	LE	LLE	LELP	References
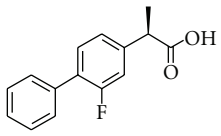 **2**, tarenflurbil	268	~0.01	3.8	0.28	−0.3	14	[8, 18]
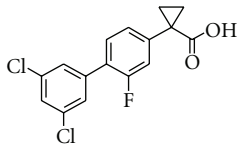 **6**, CHF5074	40	0.03–0.05	5.2	0.29	−0.8	18	[18]
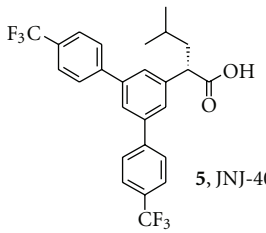 **5**, JNJ-40418677	0.2	0.5–1	8.7	0.28	−2.0	31	[16]
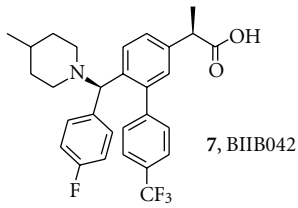 **7**, BIIB042	0.15	~1	5.0	0.27	1.9	18	[19]
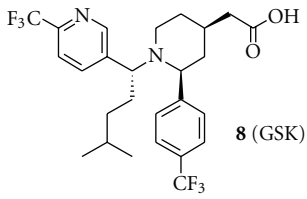 **8** (GSK)	0.32		6.7	0.25	−0.3	26	[20]
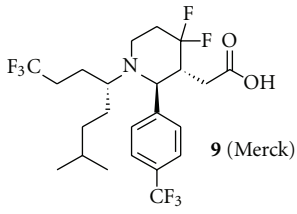 **9** (Merck)	0.6	0.27	3.8	0.25	2.4	15	[21]

[a]LE, LLE, and LELP were calculated using the formulas given in the Methods section. *In vitro* potency values were taken from the indicated references.

Since JNJ-42601572, our GSM program has focused more strongly on improving the drug-like properties, while maintaining good *in vivo* activity. In the design of the next generation of GSMs, we targeted the following profile of the compounds:

(i) lower lipophilicity,

(ii) lower molecular weight,

(iii) reduced aromaticity,

(iv) higher solubility,

(v) higher free fraction.

A representative structure arising from these efforts is shown in Figure 4, including key *in vitro* data and relevant calculated parameters. (The detailed lead optimization

Table 2: Key parameters and efficiency indices of a set of representative nonacid GSMs.[a]

Compound	Aβ42 IC_{50} (nM)	Brain/plasma ratio	clog*P*	LE	LLE	LELP	References
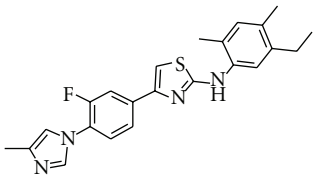 **10** (Neurogenetics)	29		7.5	0.37	0.04	21	[22]
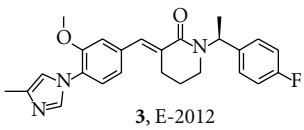 **3**, E-2012	83	~1	4.8	0.32	2.3	15	[23]
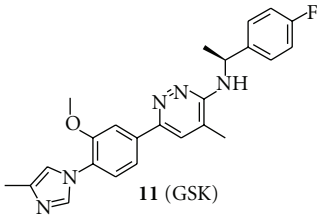 **11** (GSK)	63		5.2	0.33	2.1	16	[24]
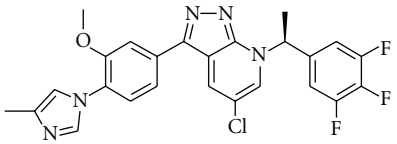 **12** (Schering/Merck)	107		5.4	0.28	1.6	19	[25]
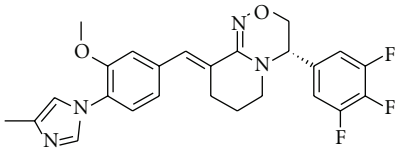 **13** (Schering/Merck)	33		6.6	0.31	0.9	21	[26]
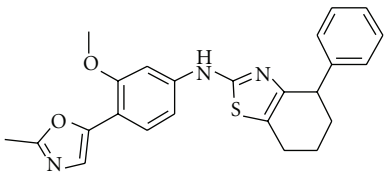 **14** (Roche)	44		6.4	0.35	0.9	19	[27]
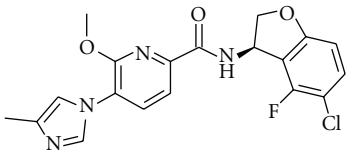 **15** (Pfizer)	188	2.9	4.0	0.34	2.7	12	[28]

Table 2: Continued.

Compound	Aβ42 IC_{50} (nM)	Brain/plasma ratio	clog*P*	LE	LLE	LELP	References
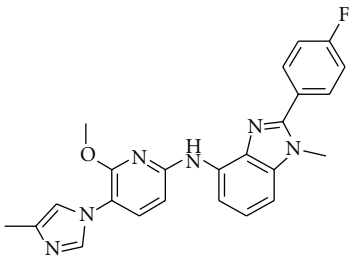 **5**, JNJ-42601572	16	0.7–1.1	5.2	0.34	2.6	15	[15]

[a]LE, LLE, and LELP were calculated using the formulas given in the Methods section. *In vitro* potency values were taken from the indicated references, except for **3**, for which Aβ42 IC_{50} was determined internally.

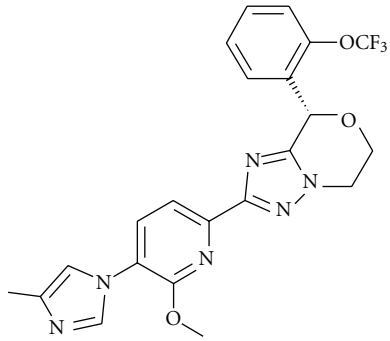

16

Aβ42 IC_{50} = 56 nM
LE 0.32 cLogP 3.1
LLE 4.2
LELP 10
Brain free fraction: F_{ub} 3.9%

Figure 4: "Next generation" GSM.

toward compound **16** will be published elsewhere in due course.)

Although the ligand efficiency of this compound has not improved compared to the previously described structures, the reduced lipophilicity results in a pronounced improvement of LLE and LELP. Also the brain free fraction has increased considerably compared to previous lead JNJ-42601572. When dosed in our dog model at 20 mg/kg p.o., this compound displayed a clear reduction in CSF Aβ42 of 30%–40% at 4 and 8 h after dosing. Despite the high exposure levels in plasma (Cmax at 4 h of 24 ± 3 μM), no increases in bilirubin or ALT levels were observed. In a subsequent limited tolerance study, a two-week daily dose of 200 mg/kg in rats did not lead to overt signs of liver toxicity. These results strengthened our belief that liver toxicity findings with previous GSMs were not target related and that it should be feasible to develop GSMs without liver toxicity.

For **16**, despite the improved free fraction in brain, still high concentrations were required to achieve a significant lowering of Aβ42. CSF compound levels at 4 h were 524 ± 62 nM, considerably above the cellular IC_{50} of 56 nM. This discrepancy is still not fully understood but has also been observed with other analogues with reduced lipophilicity and increased F_{ub}.

Although a lowering of lipophilicity may therefore not necessarily lead to an increased *in vivo* activity at lower total compound concentrations, the improved profile on liver toxicity parameters of the less lipophilic GSMs has warranted further optimization in this direction.

In Figure 5 the evolution in our nonacidic GSM program is plotted in regard to the lipophilic efficiency parameters LLE and LELP. The square in the right bottom corner indicates the desired area with optimal LLE and LELP for successful development related to compound safety and quality, in analogy with the analysis of Tarcsay et al. [35]. The individual squares represent the non-acid GSM compounds prepared and tested in our program with a cellular Aβ42 IC_{50} below 5 μM. The colour is representative for when they were synthesized during the project. Chronologically, going from blue-white-pink to red, the red compounds have been prepared most recently. The yellow dot indicates JNJ-42601572 (**5**), while the green dot indicates **16**. Considering the increased presence of recently prepared (red) compounds closer to the optimal region of the plot, clearly progress has been made towards higher-quality compounds. Within the depicted compounds, only three compounds lie within the desired area. These have been added as reference and are actually three of the GSIs which have been or are still in clinical development: semagacestat, begacestat, and avagacestat. Indeed, the toxic side effects observed with these compounds in the clinic are not related to compound quality but more to target-related (mechanism-based) side effects.

The progress in lipophilic efficiency demonstrates that it is possible to make GSMs with reduced lipophilicity while retaining a good cellular potency. The requirement of high compound exposure to achieve *in vivo* efficacy to change Aβ levels in brain and CSF remains a challenge. CNS targeting compounds, and certainly the more lipophilic ones, tend to have high tissue distribution towards other fatty tissue such as liver, increasing the chance for liver damage further. For example, in a tissue distribution study of JNJ-42601572 in

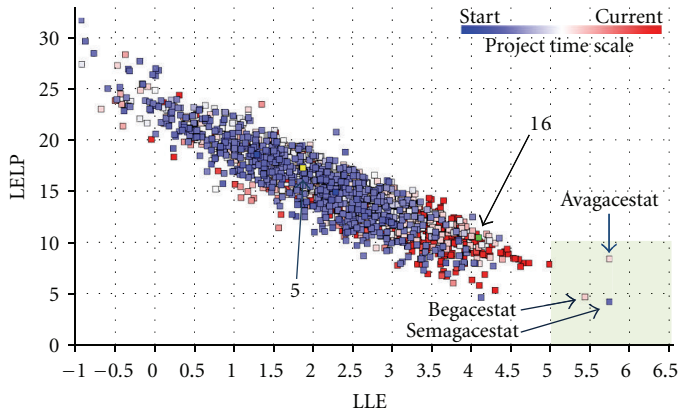

Figure 5: Evolution of our non-acid GSM series in relation to lipophilic efficiency parameters LELP and LLE. (a) LELP and LLE were calculated as described in Section 2. The highlighted section (LELP < 10, LLE > 5) indicates the desired area for drug-like compounds [35]. Each square indicates a compound, with the colour being indicative for when the compound has been synthesized during the project.

rats, a liver/plasma ratio of 8.5 was observed. According to the prevalent theory, an early and likely chronic intervention will be required in order to be effective against AD, certainly for an amyloid cascade targeting a compound like GSM [38]. The safety demands for such a drug will be considerable. A chronic treatment at high, micromolar compound levels, as currently required for significant changes in Aβ levels, is likely to result in adverse effects in at least part of the patient population. How much change in Aβ levels is required to be therapeutically beneficial is still an open question and will certainly influence safety margins for any GSM compound. Chronic treatment of transgenic mice with JNJ-40418677 had a preventive effect on plaque load at compound exposure levels below concentrations required for a reduction in Aβ42 after a single dose [16]. A lower dose than required for acute reduction of Aβ42 levels will translate into increased safety margins. On the other hand, a preventive approach for AD using a GSM potentially requiring lifelong, chronic treatment will certainly increase the safety demand further.

Clearly, a next generation of GSMs beyond the structures discussed in this paper will be needed. Ideally, they should be efficacious *in vivo* at strongly reduced compound concentrations or at least demonstrate significant safety margins. Our efforts in this field have shown progress in optimizing the drug-like properties of GSMs, especially in reducing lipophilicity. Nevertheless, it is clear that we are working at the boundaries of druggable space, with the physicochemical properties required for a highly efficacious GSM conflicting with those required for drug-likeness. A next breakthrough finding may be required to deliver the quality compounds required to test the GSM approach in humans and, if successful, to make it to the market. This will require perseverance in the study of GS and its modulation. Perhaps the evolution of the BACE inhibitor field can serve as an example here: while potent and selective BACE inhibitors were prepared just a few years after the discovery of the BACE enzyme, a decade-long struggle followed to identify brain penetrant, *in vivo* efficacious compounds. But this has ultimately been paid off, and key structural requirements have been identified to achieve good brain penetration [39]. Now, an increasing number of BACE inhibitors are moving forward in(to) the clinic. Unfortunately, in contrast to BACE, no X-ray structures are available of the membrane embedded γ-secretase protein complex to allow for structure-based design. More insight into the precise molecular mechanism of GSMs could be of great help in further optimization. Several photoaffinity labelling studies with carboxylic acid [40, 41] and imidazole [42] derived GSMs have now been reported, suggesting that compounds of both classes bind to the N-terminal fragment of presenilin. This does not preclude additional interactions with membrane lipids or the membrane embedded amino acid residues of APP, and hopefully future research will pinpoint the site of action more precisely.

Novel chemical series of GSMs have started to appear, such as natural product-derived triterpene derivatives [43, 44]. Although these are again highly lipophilic and high molecular weight compounds, aromaticity is strongly reduced. Their different profile in Aβ-level modulation may be the result of an alternative interaction or a binding site within GS and illustrate that there may be a potential for additional chemical space to modulate the activity of GS.

4. Concluding Remarks

In regard to the intervention in amyloid peptide production, γ-secretase modulation can be clearly distinguished from the straightforward inhibition by either GS or BACE. GSMs have actually been proposed as GS activators by enhancing the cleavage of the longer, more amyloidogenic peptides towards shorter amyloid peptides Aβ39-Aβ37 [45]. As such, GSMs may counter the loss of GS function linked to many familial AD causing mutations [46]. Another clear differentiation of GSMs compared to BACE and GS inhibitors lies in the multiple proteins processed by BACE and GS, and the potential adverse effects when inhibiting the processing of these proteins. Where inhibition of BACE has so far not been related to overt toxicities, inhibition of GS has led

to especially Notch-related toxicity. Based on these distinctions, GS modulation deserves an optimal effort to obtain drugable, high quality GSMs. Where the principle of modulation makes on-target side effects less likely, the potential for off-target-related side effects is considerable with the currently required high, micromolar concentrations of relatively lipophilic compounds. With the compounds from the chemical series described in this paper, the question in the title "can we combine potency with safety?" cannot be answered positively yet. Nevertheless, progress towards less lipophilic, more drug-like GSMs has been made. A next generation of increased drug-likeness, potency, and/or *in vivo* efficacy, will be required. Further insight into the structure of the GS complex and the interaction with GSMs may provide the required insight on how to get to novel chemical space. In addition, the use of ligand efficiency parameters as discussed in this paper and other drug-likeness guidelines during the optimization process will be crucial to ultimately deliver a high quality-GSM.

Acknowledgments

The authors sincerely thank the many coworkers in the neuroscience and supporting departments who have contributed to the GSM project, including the collaborators at Cellzome and VIB, especially Professor Bart De Strooper.

References

[1] Alzheimer's Association, "2012 Alzheimer's disease facts and figures," *Alzheimer's and Dementia*, vol. 8, pp. 131–168, 2012.

[2] J. Hardy and D. J. Selkoe, "The amyloid hypothesis of Alzheimer's disease: progress and problems on the road to therapeutics," *Science*, vol. 297, no. 5580, pp. 353–356, 2002.

[3] B. De Strooper, R. Vassar, and T. Golde, "The secretases: enzymes with therapeutic potential in Alzheimer disease," *Nature Reviews Neurology*, vol. 6, no. 2, pp. 99–107, 2010.

[4] J. Varghese, *BACE: Lead Target for Orchestrated Therapy of Alzheimer's Disease*, John Wiley & Sons, Hoboken, NJ, USA, 2010.

[5] A. F. Kreft, R. Martone, and A. Porte, "Recent advances in the identification of γ-secretase inhibitors to clinically test the Aβ oligomer hypothesis of Alzheimer's disease," *Journal of Medicinal Chemistry*, vol. 52, no. 20, pp. 6169–6188, 2009.

[6] G. D'Onofrio, F. Panza, V. Frisardi et al., "Advances in the identification of γ-secretase inhibitors for the treatment of Alzheimer's disease," *Expert Opinion on Drug Discovery*, vol. 7, no. 1, pp. 19–37, 2012.

[7] S. Weggen, J. L. Eriksen, P. Das et al., "A subset of NSAIDs lower amyloidogenic Aβ42 independently of cyclooxygenase activity," *Nature*, vol. 414, no. 6860, pp. 212–216, 2001.

[8] J. L. Eriksen, S. A. Sagi, T. E. Smith et al., "NSAIDs and enantiomers of flurbiprofen target γ-secretase and lower Aβ42 in vivo," *Journal of Clinical Investigation*, vol. 112, no. 3, pp. 440–449, 2003.

[9] B. P. Imbimbo, "Why did tarenflurbil fail in alzheimer's disease?" *Journal of Alzheimer's Disease*, vol. 17, no. 4, pp. 757–760, 2009.

[10] S. Cheng, D. D. Comer, L. Mao, G. P. Balow, and D. Pleynet, "Aryl compounds and uses in modulating amyloid β," WO 2004110350, 2004.

[11] C. Nagy, E. Schuck, A. Ishibashi, Y. Nakatani, B. Rege, and V. Logovinsky, "E2012, a novel gamma-secretase modulator, decreases plasma amyloid-beta (Aβ) levels in humans," *Journal of Alzheimer's Disease*, vol. 6, no. 4, p. S574, 2010.

[12] H. Zettl, S. Weggen, P. Schneider, and G. Schneider, "Exploring the chemical space of γ-secretase modulators," *Trends in Pharmacological Sciences*, vol. 31, no. 9, pp. 402–410, 2010.

[13] D. Oehlrich, D. J. C. Berthelot, and H. J. M. Gijsen, "γ-Secretase modulators as potential disease modifying anti-Alzheimer's drugs," *Journal of Medicinal Chemistry*, vol. 54, no. 3, pp. 669–698, 2011.

[14] A. L. Hopkins, C. R. Groom, and A. Alex, "Ligand efficiency: a useful metric for lead selection," *Drug Discovery Today*, vol. 9, no. 10, pp. 430–431, 2004.

[15] F. Bischoff, D. Berthelot, M. De Cleyn et al., "Design and synthesis of a novel series of bicyclic heterocycles as potent gamma;-secretase modulators," *Journal of Medicinal Chemistry*, vol. 55, no. 21, pp. 9089–9106, 2012.

[16] B. Van Broeck, J. M. Chen, G. Tréton et al., "Chronic treatment with a novel γ-secretase modulator, JNJ-40418677, inhibits amyloid plaque formation in a mouse model of Alzheimer's disease," *British Journal of Pharmacology*, vol. 163, no. 2, pp. 375–389, 2011.

[17] H. Borghys, M. Tuefferd, B. Van Broeck et al., "A canine model to evaluate efficacy and safety of γ-secretase inhibitors and modulators," *Journal of Alzheimer's Disease*, vol. 28, no. 4, pp. 809–822, 2012.

[18] B. P. Imbimbo, E. Del Giudice, V. Cenacchi et al., "In vitro and in vivo profiling of CHF5022 and CHF5074. Two β-amyloid1-42 lowering agents," *Pharmacological Research*, vol. 55, no. 4, pp. 318–328, 2007.

[19] H. Peng, T. Talreja, Z. Xin et al., "Discovery of BIIB042, a potent, selective, and orally bioavailable γ-secretase modulator," *ACS Medicinal Chemistry Letters*, vol. 2, no. 10, pp. 786–791, 2011.

[20] A. Hall, R. L. Elliott, G. M. P. Giblin et al., "Piperidine-derived γ-secretase modulators," *Bioorganic and Medicinal Chemistry Letters*, vol. 20, no. 3, pp. 1306–1311, 2010.

[21] M. G. Stanton, J. Hubbs, D. Sloman et al., "Fluorinated piperidine acetic acids as γ-secretase modulators," *Bioorganic and Medicinal Chemistry Letters*, vol. 20, no. 2, pp. 755–758, 2010.

[22] M. Z. Kounnas, A. M. Danks, S. Cheng et al., "Modulation of gamma-secretase reduces beta-amyloid deposition in a transgenic mouse model of Alzheimer's disease," *Neuron*, vol. 67, no. 5, pp. 769–780, 2010.

[23] T. Hashimoto, A. Ishibashi, H. Hagiwara, Y. Murata, O. Takenaka, and T. Miyagawa, "E2012: a novel gamma-secretase modulator; pharmacology part," *Alzheimer's & Dementia*, vol. 6, no. 4, p. S242, 2010.

[24] Z. Wan, A. Hall, Y. Jin et al., "Pyridazine-derived γ-secretase modulators," *Bioorganic and Medicinal Chemistry Letters*, vol. 21, no. 13, pp. 4016–4019, 2011.

[25] J. Qin, W. Zhou, X. Huang et al., "Discovery of a potent pyrazolopyridine series of γ-secretase modulators," *ACS Medicinal Chemistry Letters*, vol. 2, no. 6, pp. 471–476, 2011.

[26] Z.-Y. Sun, T. Asberom, T. Bara et al., "Cyclic hydroxyamidines as amide isosteres: discovery of oxadiazolines and oxadiazines as potent and highly efficacious γ-secretase modulators in vivo," *Journal of Medicinal Chemistry*, vol. 55, no. 1, pp. 489–502, 2012.

[27] T. Lübbers, A. Flohr, S. Jolidon et al., "Aminothiazoles as γ-secretase modulators," *Bioorganic and Medicinal Chemistry Letters*, vol. 21, no. 21, pp. 6554–6558, 2011.

[28] M. Pettersson, D. S. Johnson, C. Subramanyam et al., "Design and synthesis of dihydrobenzofuran amides as orally bioavailable, centrally active γ-secretase modulators," *Bioorganic and Medicinal Chemistry Letters*, vol. 22, no. 8, pp. 2906–2911, 2012.

[29] N. A. Meanwell, "Improving drug candidates by design: a focus on physicochemical properties as a means of improving compound disposition and safety," *Chemical Research in Toxicology*, vol. 24, no. 9, pp. 1420–1456, 2011.

[30] M. M. Hann and G. M. Keseü, "Finding the sweet spot: the role of nature and nurture in medicinal chemistry," *Nature Reviews Drug Discovery*, vol. 11, no. 5, pp. 355–365, 2012.

[31] M. M. Hann, "Molecular obesity, potency and other addictions in drug discovery," *Medicinal Chemistry Communications*, vol. 2, no. 5, pp. 349–355, 2011.

[32] F. Lovering, J. Bikker, and C. Humblet, "Escape from flatland: increasing saturation as an approach to improving clinical success," *Journal of Medicinal Chemistry*, vol. 52, no. 21, pp. 6752–6756, 2009.

[33] P. D. Leeson and B. Springthorpe, "The influence of drug-like concepts on decision-making in medicinal chemistry," *Nature Reviews Drug Discovery*, vol. 6, no. 11, pp. 881–890, 2007.

[34] G. M. Keserü and G. M. Makara, "The influence of lead discovery strategies on the properties of drug candidates," *Nature Reviews Drug Discovery*, vol. 8, no. 3, pp. 203–212, 2009.

[35] A. Tarcsay, K. Nyíri, and G. M. Keserú, "Impact of lipophilic efficiency on compound quality," *Journal of Medicinal Chemistry*, vol. 55, no. 3, pp. 1252–1260, 2012.

[36] R. C. Green, L. S. Schneider, D. A. Amato et al., "Effect of tarenflurbil on cognitive decline and activities of daily living in patients with mild Alzheimer disease: a randomized controlled trial," *Journal of the American Medical Association*, vol. 302, no. 23, pp. 2557–2564, 2009.

[37] H. Wan, M. Rehngren, F. Giordanetto, F. Bergström, and A. Tunek, "High-throughput screening of drug-brain tissue binding and in silico prediction for assessment of central nervous system drug delivery," *Journal of Medicinal Chemistry*, vol. 50, no. 19, pp. 4606–4615, 2007.

[38] E. Karran, M. Mercken, and B. D. Strooper, "The amyloid cascade hypothesis for Alzheimer's disease: an appraisal for the development of therapeutics," *Nature Reviews Drug Discovery*, vol. 10, no. 9, pp. 698–712, 2011.

[39] G. Probst and Y.-Z. Xu, "Small-molecule BACE1 inhibitors: a patent literature review (2006—2011)," *Expert Opinion on Therapeutic Patents*, vol. 22, no. 5, pp. 511–540, 2012.

[40] Y. Ohki, T. Higo, K. Uemura et al., "Phenylpiperidine-type γ-secretase modulators target the transmembrane domain 1 of presenilin 1," *EMBO Journal*, vol. 30, no. 23, pp. 4815–4824, 2011.

[41] T. Jumpertz, A. Rennhack, J. Ness et al., "Presenilin is the molecular target of acidic γ-secretase modulators in living cells," *PLoS ONE*, vol. 7, no. 1, Article ID e30484, 2012.

[42] A. Ebke, T. Luebbers, A. Fukumori et al., "Novel γ-secretase enzyme modulators directly target presenilin protein," *Journal of Biological Chemistry*, vol. 286, no. 43, pp. 37181–37186, 2011.

[43] M. A. Findeis, F. Schroeder, T. D. McKee et al., "Discovery of a novel pharmacological and structural class of gamma secretase modulators derived from the Extract of Actaea racemosa," *ACS Chemical Neuroscience*, vol. 3, no. 11, pp. 941–951, 2012.

[44] J. L. Hubbs, N. O. Fuller, W. F. Austin et al., "Optimization of a natural product-based class of gamma;-secretase modulators," *Journal of Medicinal Chemistry*, vol. 55, no. 21, pp. 9270–9282, 2012.

[45] L. Chévez-Gutiérrez, L. Bammens, I. Benilova et al., "The mechanism of γ-Secretase dysfunction in familial Alzheimer disease," *EMBO Journal*, vol. 31, no. 10, pp. 2261–2274, 2012.

[46] B. De Strooper and W. Annaert, "Novel research horizons for presenilins and γ-secretases in cell biology and disease," *Annual Review of Cell and Developmental Biology*, vol. 26, pp. 235–260, 2010.